CHAPTER

3

Energy Metabolism in the Brain

Gerald A. Dienel

The brain is a complex, heterogeneous organ in which many pathways for its input and output are organized in a somatotopic manner. Activities of neural circuits and networks involved in specific functions govern demand for energy at a local level, e.g., shifts in cellular activities in the pathways in which signaling rises and falls cause parallel changes in the rate of metabolism to generate ATP and rate of blood flow to deliver fuel (*functional activity*, Box 3.1). Brain energy metabolism is a dynamic, highly regulated process that is governed, in large part, by moment-to-moment interactions among brain cells that process information from sensory and cognitive activities and to direct functions of the body. Because cellular energy demands, consumption of oxygen and glucose, and blood flow rise and fall together, these processes are often described as "coupled," and the structures involved in local activity are described in terms of a neurovascular unit, consisting primarily of neurons, astrocytes, and endothelial cells.

Energy budget. Information processing is the hallmark of brain function and, as illustrated in Fig. 3.1, there is a close temporal–spatial relationship between functional activity in brain and rates of glucose utilization and blood flow. The largest component of brain work involves consumption of ATP to pump Na^+ and K^+ across membranes. Energy budgets calculated by Howarth et al. (2012) for subcellular processes in rat cerebral cortical gray matter ascribe ~75% of total ATP turnover to signaling activity. The largest fraction is used for synaptic transmission (~50% for postsynaptic receptors, ~4% for neurotransmitter recycling, and ~5% for Ca^{2+} entry and vesicle cycling), with ~20% for action potentials and ~20% for resting potentials. About 25% of total ATP is consumed over a much longer time scale for so-called "housekeeping" activities. In spite of the pedestrian implications of the name "housekeeping," these energy-requiring processes are essential for brain function and include mRNA, protein, lipid, and organelle turnover, axonal transport, and biosynthetic activities associated with neurotransmitters and other compounds that are synthesized *de novo* in brain. The numerical values assigned to specific functions are likely to be updated further as more is learned about oxidative fluxes at a cellular and subcellular level, neuron–astrocyte interactions, and the contributions of astrocytes, oligodendroglia, inhibitory neurons, and other cell types in different brain regions to overall energetics (also see Harris and Attwell, 2012; Howarth et al., 2012). Defense against oxidative stress arising from generation of reactive oxygen species (ROS) by various enzymes and the electron transport chain involves the glutathione system and consumes NADPH produced by the pentose phosphate shunt pathway (Fig. 3.1). Neuronal signaling events involving fast excitatory action potentials, receptor activation, ion channel opening and closing, and inhibitory transmitter actions take place on a time scale of <10 ms (Korf and Gramsbergen, 2007). Astrocytes surrounding working synapses must also be quickly activated during excitatory transmission because they control glutamate and K^+ levels in extracellular fluid (Hertz et al., 2007). Sensory perception occurs within a time frame of 0.5 to 2 s, similar to that of synaptic vesicle filling. Local rates of cerebral blood flow (CBF) are regulated by many signals, including products of metabolism and glutamate-mediated processes that involve both neurons and astrocytes and their interactions with endothelial cells in blood vessels (Attwell et al., 2010; Paulson et al., 2010). Onset of hemodynamic responses (e.g., blood flow, blood volume, and the blood oxygen-level dependent (BOLD) effect) to activation occurs within ~350–700 ms in anesthetized subjects (Masamoto and Kanno, 2012), and they persist for seconds or longer after a brief stimulus. Notably, the

From Molecules to Networks.
DOI: http://dx.doi.org/10.1016/B978-0-12-397179-1.00003-8

BOX 3.1

CONCEPTS RELATED TO FUNCTIONAL METABOLISM

Functional metabolic activity. Metabolic rate associated with a specific brain function or pathway. In normal brain, metabolic rates rise when functional activity increases (e.g., during sensory or cognitive stimulation) and fall with decrements in activity (e.g., sensory deprivation or anesthesia). Glucose and oxygen consumption may, but need not, change by the same proportion under different conditions. During activation of normal, normoxic subjects, most studies have observed greater increases in blood flow and glucose utilization compared to oxygen consumption.

Resting or baseline activity. Activity of brain cells during conditions in which no specific stimulus is given to the subject. Resting activity and the associated rates of blood flow and metabolism can be difficult to define due to the unknown interactions of the subject with the specific experimental environment (e.g., paying attention to visual, auditory, or other sensory cues or information) and the level of "stress" that a subject may experience.

Brain activation. Responses to a specific stimulus or experimental condition. Brain work involves mainly ion pumping to maintain and restore ionic gradients across cellular membranes and to control the levels of compounds in extracellular fluid. Increased rates of these ATP-requiring processes stimulates metabolism specifically in the activated pathways.

Glucose (Glc) utilization. The cerebral metabolic rate (CMR) of glucose (CMR_{glc}) denotes the overall rate of glucose consumption by all pathways. Under normal steady-state conditions, the rate of any step in the glycolytic pathway equals glucose utilization, whereas the rate of the steps in the TCA cycle are twice those of glycolysis due to formation of 2 pyruvate per glucose. CMR_{glc} is generally assayed at the hexokinase step with radiolabeled deoxyglucose (DG); the rate of phosphorylation of DG is converted to rate of glucose utilization by taking into account the kinetic differences for transport and phosphorylation between DG and glucose; approximately two glucose are utilized per deoxyglucose (Sokoloff et al., 1977).

Oxygen utilization. CMR_{O2} denotes the overall rate of oxygen consumption by all pathways. Most oxygen is consumed via the electron transport chain to generate ATP in mitochondria, but there are a number of other enzymes (e.g., monoamine oxidase, mixed-function oxidases) that utilize oxygen as a substrate and contribute to CMR_{O2}. Global rates of oxygen consumption can be determined by measuring blood flow and arteriovenous differences for oxygen; local CMR_{O2} can be measured by positron emission tomography by determination of metabolism of $^{15}O_2$.

Glycolytic metabolism. Metabolism of glucose or glycogen via the glycolytic pathway to pyruvate by reactions that are not dependent on oxygen consumption. Glycolysis generates a net 2 ATP per glucose converted to 2 pyruvate. Glycolytic flux increases during hypoxic or anoxic conditions, with increased production of lactate from pyruvate in order to regenerate NAD^+ from the $NADH + H^+$ generated by the glyceraldehyde-3-phosphate dehydrogenase reaction.

Oxidative metabolism. Metabolism of pyruvate, keto acids, monocarboxylic acids, fatty acids, and amino acids via the tricarboxylic acid cycle. Oxidative metabolism is linked to the consumption of oxygen and generation of ATP via the electron transport chain. This pathway can be used for generation of energy and for net *de novo* biosynthesis of amino acids from glucose, which also consumes oxygen and generates ATP (see text).

"Coupling" of blood flow and metabolism at a local level. Rates of blood flow and glucose utilization in different structures in the brain are highly correlated and generally change in parallel during different physiological states, leading to the notion of coupling. Regulation of local rates of blood flow by cellular activity and metabolism involves release of substances that regulate vascular diameter and therefore blood flow. Because activities of neurons, astrocytes, and endothelial cells are involved in major aspects of local brain function, metabolism, and blood flow, these cell types together are sometimes collectively referred to as a neurovascular unit.

tissue volume with increased blood flow response is greater than that of activated cells. The highest fraction of energy production is devoted to the fastest processes, and linkage of neuronal and astrocytic signaling to control of blood flow is essential to maintain an adequate and continuous supply of fuel to brain.

Fueling brain work. Glucose and oxygen are the primary and obligatory fuels for brain, and other substrates cannot substitute for the continuous supply of

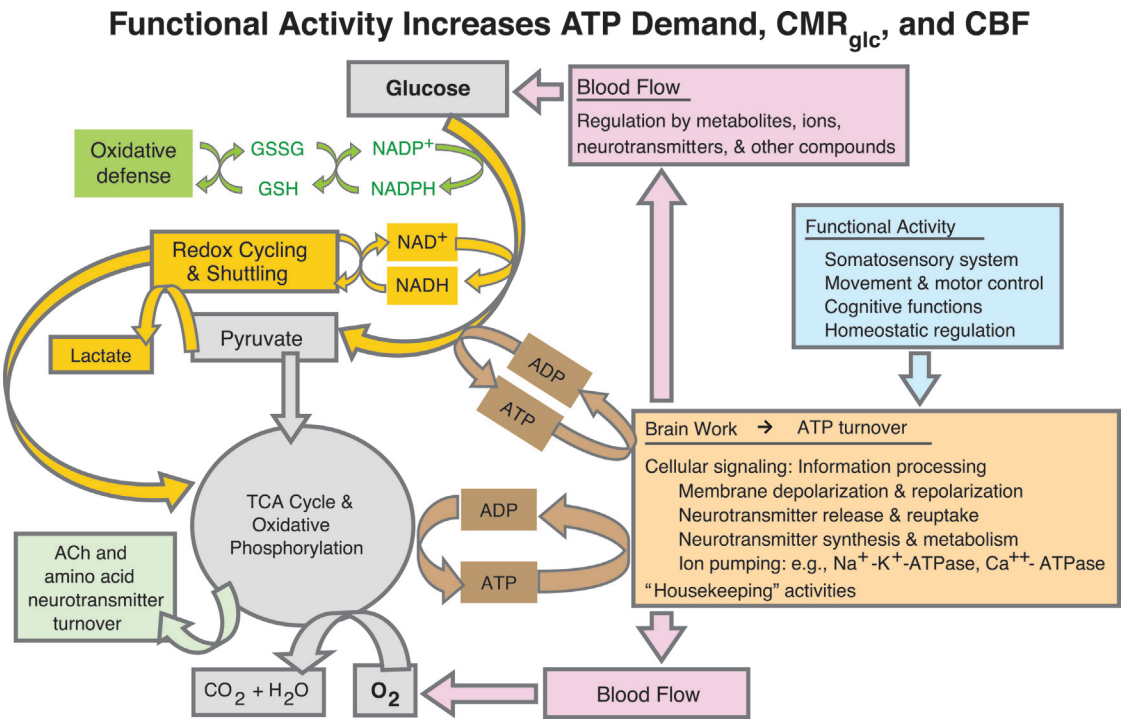

FIGURE 3.1 **Relationships among brain function, metabolism and blood flow.** The predominant energy-requiring brain activities involve restoration of ionic gradients across cellular membranes in conjunction with cellular signaling and information transfer. Compounds derived from cellular activity and metabolism regulate local rates of blood flow to deliver the obligatory fuel, glucose and oxygen to the brain. Glucose is nearly completely oxidized via the glycolytic and oxidative (tricarboxylic acid, TCA, cycle) pathways. Metabolism of glucose generates ATP and precursors for *de novo* synthesis of glucose-derived neurotransmitters, e.g., acetylcholine (Ach), glycine, D-serine, and glutamate, within the brain. Redox (oxidation−reduction) cofactors are also produced and can be used to generate ATP or lactate, defend against oxidative stress, and participate in biosynthetic reactions. GSH and GSSG denote reduced and oxidized forms of glutathione, respectively. *Adapted from Dienel (2002).*

glucose from blood (Dienel, 2012b). Global measurements of arteriovenous differences in early studies in humans and experimental animals provided the first line of evidence for the major substrates taken up into brain and released from brain, leading to identification of major fuel and metabolic by-products. Quantitative cerebral metabolic rates were made possible by the work of Kety and colleagues who developed the first quantitative assays to measure cerebral blood flow by determination of rates of clearance of inert gas (Kety and Schmidt, 1948).

Under *resting conditions* (Box 3.1) the stoichiometry of oxygen to glucose utilization is close to the theoretical maximum of 6.0, which corresponds to the complete oxidation of glucose: 1 glucose + $6O_2 \rightarrow 6CO_2 + 6H_2O$. The ratio of cerebral metabolic rates (CMR) for these two substrates, CMR_{O2}/CMR_{glc} in resting human and animal brain is usually found to be slightly lower than 6.0, e.g., in the range of 5.5−5.8, indicating that some of the glucose carbon is used in nonoxidative biosynthetic reactions and a small amount of lactate is released to cerebral venous blood. Also, some O_2 is consumed by enzymes, such as mixed-function oxidases (e.g., tyrosine and tryptophan hydroxylases that are involved in neurotransmitter synthesis, see Chapter 7), that are not components of the oxidative pathways of glucose metabolism. The *respiratory coefficient* for brain, the ratio of CO_2 released from brain to O_2 taken up, is approximately 1.0, indicating that carbohydrate is the primary brain fuel; oxidation of lipid consumes O_2 in steps that do not result in proportionate CO_2 production. Alternative fuels are used by brain during development or abnormal conditions, such as prolonged starvation, but these compounds are not capable of sustaining brain function in the normal adult (Roberts Jr, 2007).

Typical concentrations of oxygen and glucose in blood of the normal rat are shown in Table 3.1. Note that the concentrations of oxygen and glucose in whole blood are similar but the extraction fraction for oxygen is 4.5 times higher than that of glucose. Nearly half of the oxygen that traverses the brain's microvasculature is extracted and consumed, whereas only 10% of the glucose is removed from the same blood sample by brain. The negative arteriovenous difference for lactate indicates a small net efflux corresponding to about 6% of the glucose taken up into brain, based on two lactate being equivalent to one glucose. Measurement of arteriovenous (A-V) differences across the brain and rates

TABLE 3.1 Blood and brain metabolites and global metabolic rates during rest and brain activation

Variable	Before activation	During sensory stimulation
ARTERIAL BLOOD CONCENTRATION (mmol L^{-1})		
Oxygen	8.15 ± 0.59	7.98 ± 0.73
Glucose	6.81 ± 0.82	7.81 ± 1.32[b]
Lactate	0.50 ± 0.30	1.96 ± 0.43 [b]
ARTERIOVENOUS DIFFERENCE (A-V) (mmol L^{-1})		
$(A\text{-}V)_{O2}$	3.75 ± 0.56	2.97 ± 0.56
Mean O_2 extraction fraction $[(A\text{-}V)_{O2}/A_{O2}]$	0.46	0.37
$(A\text{-}V)_{glucose}$	0.68 ± 0.20	0.60 ± 0.06[b]
Mean Glc extraction fraction $[(A\text{-}V)_{glc}/A_{glc}]$	0.10	0.077
$(A\text{-}V)_{lactate}$	−0.08 ± 0.06	0.02 ± 0.04[b]
Cerebral blood flow (CBF) (mL $\cdot g^{-1} \cdot$ min^{-1})	1.1	1.8
RATIOS OF (A-V) DIFFERENCES (mmol L^{-1}/mmol L^{-1})		
Oxygen/glucose	6.1 ± 1.1	5.0 ± 1.1[b]
Lactate/glucose	−0.14 ± 0.14	0.02 ± 0.08[b]
Mean CMR_{O2} (CBF × $[A\text{-}V]_{O2}$)	4.13	5.35
Mean CMR_{glc} (CBF × $[A\text{-}V]_{glc}$)	0.75	1.08
BRAIN METABOLITE CONCENTRATION (μmol g^{-1})		
Glucose	2.8 ± 0.5	3.1 ± 0.5
Lactate	1.0 ± 0.5	1.9 ± 0.4[a]
Glycogen	6.1 ± 1.4	5.4 ± 1.3

Blood metabolite levels and arteriovenous differences were determined in samples of blood taken from the femoral artery and superior sagittal sinus of normal, nonfasted conscious rats; brain metabolites were determined in cortex from funnel-frozen brain. Values are means ± SD for 39 rats during rest and 8 during activation ([a]$p < 0.05$, [b]$p < 0.01$ compared to resting condition). Activation was initiated by brushing the face, whiskers, paws, and back of the rats with soft paintbrushes. They moved the upper torso, causing lactate release from muscles and an increase in blood lactate level. Blood glucose level also rose somewhat, presumably due to glycogenolysis in liver. Ratios of arteriovenous differences were calculated for each animal, not from means for all animals. Because blood flow was measured in different groups of animals, mean values are calculated for CMR_{glc} and CMR_{O2}. Although the A-V differences for oxygen and glucose were lower during sensory stimulation compared with rest, the increase in blood flow caused the metabolic rates to rise. More glucose was consumed compared with oxygen, causing the oxygen/glucose ratio to fall, indicating a rise in nonoxidative metabolism during activation, consistent with the rise in brain lactate level. The rise in blood lactate caused a slight net influx of lactate into brain during activation, contrasting lactate release during rest.
Data from Madsen et al. (1999).

of cerebral blood flow (CBF) enable calculation of the global cerebral metabolic rate (CMR) using the Fick principle, CMR = CBF(A-V). In the example provided in Table 3.1, CMR_{O2} and CMR_{glc} are 4.13 and 0.75 μmol g^{-1} min^{-1}, respectively, and the ratio of their utilization rates (calculated as the ratio of A-V differences for each substrate; blood flow cancels out) was 6.1. There is no oxygen reservoir in brain, whereas there is a small pool of unmetabolized glucose in brain, along with the reserve glucose stored as glycogen (Table 3.1). The *half life* (Box 3.2) of glucose in resting brain is 1.2−1.6 min (Savaki et al., 1980), and the major carbohydrate pool (glucose + glycogen + 0.5 lactate) is about 9.4 μmol g^{-1}. At the normal rate of glucose utilization of about 0.75 μmol g^{-1} min^{-1} all of this fuel would be consumed within 12.5 min if none were provided from blood. Thus, an insulin overdose that severely reduces blood glucose level or a vascular blockage that reduces or eliminates blood flow to the brain can lead to energy failure, loss of consciousness or function, and perhaps cell death, depending on the severity of decrement, extent of tissue involvement, and duration of the insult.

Stimulation of brain activity. During *brain activation* (Box 3.1) induced by generalized sensory stimulation of the animal by brushing of the body and whiskers with soft paint brushes (Table 3.1), blood glucose and lactate levels rose due to glycogenolysis and muscular activity, respectively. Because plasma lactate rose above that in brain, there was a small net increase in lactate uptake and brain lactate level also increased. Extraction of oxygen and glucose tended to fall

BOX 3.2

SUBSTRATE LEVELS, ENZYMES, AND TRANSPORTERS

Metabolite concentration. The concentration of compound in the intracellular or extracellular fluid or total tissue is the net result of all transport (carrier-mediated and diffusion) and metabolic processes that contribute to its formation and removal. At steady state the overall concentration of a metabolite is stable even though individual molecules are continuously entering and leaving the metabolic pool. Because the sum of all input and output rates determines concentration of a metabolite, concentration itself does not reflect flux of any single pathway and changes in concentration need not be in the same direction as changes in the flux of any specific process.

Metabolite pool. The quantity of a compound in a tissue, cell, or subcellular compartment. *Pool* is sometimes used interchangeably with *concentration* but the concept of a pool often infers localization or compartmentation, since more than one pool can contribute to the cellular content of a compound. For example, (i) the cytoplasmic and mitochondrial NAD/NADH pools are segregated due to the impermeability of the inner mitochondrial membrane to the pyridine nucleotides, and (ii) the glutamate pool that is the precursor for glutamine synthesis is located in astrocytes and is a small fraction of the total glutamate pool, which is mainly neuronal.

Turnover time and half-life. In a simple example of a first-order reaction where $x \rightarrow y$, the turnover time of a metabolite or pool is the reciprocal of the rate constant, k, for a reaction in which the rate of change of compound x is proportional to its concentration, $dx/dt = \mathrm{k}[x]$, and $\mathrm{k} = (dx/dt)/[x]$. This situation applies to enzymatic reactions in which the substrate concentration is much lower than the K_m so that the initial reaction rate varies linearly with substrate concentration (see Fig 3.3C). In this case, turnover time or time constant can be estimated by dividing the metabolite concentration by pathway flux rate. Turnover time is the time required to metabolize the quantity of the intermediate in that pool at a constant rate. Due to the exponential decline of the rate in an irreversible first order reaction, not all molecules in the pool are metabolized even though the pool "turns over." The half-time or half-life is the time required for the concentration to fall by 50%, and the integrated rate equation becomes $kt = 2.3\log[x]_{t=0}/[x]_{t=t}$. Thus, when x is half gone, $kt = 2.3\log(1/0.5) = 0.69$, and the half-life, $t_{1/2} = 0.69/\mathrm{k}$. Thus, at 5 and 6 half-times, 94 and 99% of the pool are consumed, respectively, if there is no substrate replenishment. Note that the expressions for turnover time and half-life are more complex for reversible reactions and second-order reactions involving two substrates.

Labile metabolite. Any metabolite that is rapidly consumed or produced when normal metabolism is disrupted, e.g., when tissue is sampled and extracted for analysis. Labile metabolites include glucose, glycogen, glycolytic and TCA cycle intermediates, pyridine nucleotides, signaling compounds, and high-energy compounds and their metabolites. More stable compounds include most but not all amino acids, proteins, and lipids. Rapid enzyme-inactivation procedures are required for determination of the levels of labile metabolites.

Enzyme or transporter amount or activity. In a simple case when an enzyme catalyzes a one-step reaction with a single substrate and follows Michaelis-Menten kinetics, the rate of the reaction can vary with the amount of enzyme, the substrate concentration, and affinity for the substrate, according to the following relationship: $v = V_{max}\ S/(K_m + S)$, where v is the velocity of the reaction, V_{max} is the maximal velocity, S is substrate concentration, and K_m is the concentration of substrate at which the velocity is half maximal. Note that when the substrate concentration is much higher than K_m, $v = V_{max}$ and the enzyme is "saturated" with substrate; because further increases in S do not alter the rate, the activity is maximal (Fig 3.3C). However, when S is approximately equal to K_m the velocity of the reaction varies as S changes above and below K_m. A similar expression can be derived for transport reactions, $v = T_{max}\ S/(K_t + S)$, where T_{max} is maximal transport capacity and K_t is analogous to K_m. Enzyme activities assayed under optimal conditions in the test tube are proportional to enzyme amount, which is expressed in terms of V_{max} (maximal rate per unit tissue or protein, e.g., $\mu\mathrm{mol}^{-1}\ \mathrm{min}^{-1}$ gram tissue^{-1} or mg $\mathrm{protein}^{-1}$.) *In vitro* assays of enzymatic activity are measures of enzyme amount or capacity when determined under optimal conditions; they do not represent *in vivo* activities or fluxes through that enzymatic step. Histochemical assays based on enzyme reactions, immunostaining of tissue, and Western blots are *representations* of enzyme location, relative amount, or capacity, not actual *in vivo* activity related to pathway flux.

Flux. The overall rate of a specific enzymatic reaction or of a pathway comprised of more than one enzyme. In a multistep pathway the overall flux is governed by the slowest, or rate-limiting, step. Under steady-state conditions the rate of each step in a multistep pathway

BOX 3.2 (*cont'd*)

is equal to the flux through that pathway. Determinants of flux include the amounts and activities of enzymes controlling the nonequilibrium or rate-limiting reactions, metabolite concentrations, transport, and diffusion, concentrations of enzyme regulators (activators and inhibitors), coenzyme availability, and pH. *In vivo reaction rates*, not the concentrations of their pathway constituents, provide information about the *dynamic state* of metabolism.

Steady state. Steady state is the condition under which metabolic rates and metabolite concentrations are constant, and glucose utilization rates (glycolytic and/or TCA cycle) can be linked to overall energy production. In contrast, under non-steady-state conditions, rates may transiently rise or fall to and from the baseline level during activating or depressing conditions, and some of the carbon flowing through a pathway may be used for biosynthetic reactions or some may be produced from other compounds (e.g., glycogen).

Physiological relationships among mRNA level, protein amount, and protein function. Changes in mRNA level are not necessarily reflected by corresponding alterations in protein amount, and variations in protein amount (capacity, amount or *in vitro* activity) need not be reflected by parallel shifts in the *in vivo* activity of the protein or metabolic pathway flux due to regulatory controls. Some examples from the literature included in the "Metabolomics, Transcriptomics, and Proteomics" section illustrate the following points: (i) function-dependent changes in mRNA and protein levels can be discordant and also differ from shifts in pathway activity; (ii) the phenotype of a gene knockout animal may arise, in part, from compensatory changes in the expression of hundreds of genes involved in pathways or processes seemingly unrelated to the gene of interest; and (iii) marked upregulation of enzyme levels by genetic engineering need not alter either pathway flux or levels of metabolites in the pathway. Thus, caution must be applied to interpretation of studies that examine only one aspect of the biological range from gene to mRNA to protein to metabolite to function. Single time points are not sufficient to characterize functional responses to changes in gene expression because induction or suppression of enzymes by various approaches can have effects that vary with response time, duration of response, direction of response, and magnitude of response. In various mammalian species, substrate and enzyme levels are more similar to each other, whereas metabolic rates differ markedly and are scaled to brain (and body) weight. Thus, within normal variations, metabolic fluxes are not indicated by the concentrations of substrates or of the amount of enzymes. Also, enzyme amounts generally enable considerable excess catalytic capacity compared to pathway flux, so large decrements in enzyme amount or activity can be tolerated before biochemical and functional changes become evident (e.g., in genetic diseases such as phenylketonuria).

somewhat, but because blood flow increased considerably, the rates of utilization of both oxygen and glucose increased. The disproportionate rise in glucose compared to oxygen consumption caused the CMR_{O2}/CMR_{glc} *ratio* (Box 3.2) to fall from 6.1 to 5.0 during stimulation. This phenomenon, sometimes called *aerobic glycolysis*, is commonly observed in many (but not all) brain activation studies in humans and experimental animals (e.g., Fox et al., 1988; Madsen et al., 1995; Madsen et al., 1999). The biochemical and cellular basis of utilization of glucose in excess of oxygen in the presence of adequate levels of oxygen in blood and increased rates of delivery of oxygen to the brain is not understood (Quistorff et al., 2008; Dienel, 2012b). The cellular basis of metabolic shifts induced by brain activation is an active research area.

Metabolic flow diagrams (Fig. 3.1) illustrate the flux of glucose through the glycolytic and oxidative pathways to end products, but it is important to recognize that conversion of glucose to CO_2 is not a direct process due to the many side and exchange reactions that mix incoming carbon atoms with those of endogenous metabolite pools. As will become evident later in the chapter, this characteristic of metabolism is important for functional imaging and biochemical and magnetic resonance spectroscopic studies of brain metabolism because label from labeled precursors is trapped by dilution in these endogenous pools. Due to the high yield of ATP from the oxidative phosphorylation reactions in mitochondria, respiration generates most of the ATP in brain cells, with a smaller fraction produced by the glycolytic pathway. The highest energy yield from glucose is obtained when the NADH generated by glycolysis is shuttled from the cytoplasm to the mitochondria for oxidation via the electron transport chain. Nevertheless, specific processes in brain cells may preferentially utilize ATP generated by glycolysis or require compounds generated by nonoxidative metabolism, and overall metabolism of glucose rises disproportionately more than

oxygen consumption during *brain activation* (Table 3.1, Box 3.1). Pathways that branch from the main glycolytic pathway are also important because they participate in defense against oxidative stress (pentose phosphate shunt pathway) and serve as precursors for glucose storage as glycogen and for synthesis of glycoprotein precursors and amino acids, including neuromodulators. Branch pathways linked to the tricarboxylic acid (TCA) cycle are essential for neurotransmitter turnover, and oxidative metabolism is closely linked to turnover of acetylcholine, which is synthesized from glucose via citrate, as well as to excitatory neurotransmission and *de novo* synthesis of glutamate, glutamine, GABA, and aspartate. Because the energy reservoirs in brain are very limited, brain function is dependent on a continuous supply of oxygen and glucose to satisfy local demand for ATP to power brain work, for excitatory and inhibitory neurotransmitter synthesis to signal from cell to cell, and for defense against reactive oxidative species produced by working brain (Fig. 3.1).

To summarize, co-registration of changes in functional activity, metabolism, and blood flow enables the use of markers of metabolism or flow to evaluate brain function as important tools for imaging and quantifying brain function and activity in living subjects under normal and pathophysiological conditions. Understanding the basis for functional imaging signals requires a detailed knowledge of the pathways of brain energy metabolism, cellular specialization that is unique to or critical for brain function, and the involvement of energy metabolism in neurological diseases or disorders. Because metabolic reactions, mechanisms, and their control are common to many tissues, readers are referred to biochemistry texts for details. For greater coverage of many topics presented in this chapter, interested readers are encouraged to consult the reference monographs listed at the end of the chapter. Along with reviews cited in the text, these books provide broad access to the brain energy metabolism literature. For recent, extensive coverage of brain energetics, see Gibson and Dienel (2007).

MAJOR PATHWAYS OF BRAIN ENERGY METABOLISM

The brain requires uninterrupted delivery of glucose and oxygen from blood to generate the energy required to sustain consciousness. Glucose also serves as the carbon source for biosynthesis of essential compounds within brain. Minor substrates that can be metabolized by brain slices and maintain near-normal ATP levels *in vitro* do not enter brain in sufficient quantities to satisfy the energetic or biosynthetic demands of mature brain.

Fuel Delivery to Brain

Blood-brain barrier. As introduced in Chapter 1, tight junctions between adjacent endothelial cells in the cerebral vasculature form the blood–brain barrier (see also monograph by Davson and Siegel (1996)), which restricts entry of water-soluble or aqueous phase compounds into brain from blood. This selective permeability is a critical function, since blood contains many neuroactive compounds such as cations, glutamate, and catecholamines, and intricate control of cell-to-cell signaling in brain would be severely disrupted if material could readily enter the brain. Thus, transporters are required to facilitate movement of essential materials across the blood–brain barrier (Fig. 3.2). Early studies by Oldendorf and colleagues clearly demonstrated that glucose and neutral amino acids had high blood–brain barrier permeability, whereas transit from blood to brain of acidic amino acids, biogenic amines, and short-chain mono- and dicarboxylic acids was highly restricted (Oldendorf, 1981). Although immature brain cells in tissue culture and in slices of adult brain are capable of metabolizing many compounds, these metabolites are not transferred into brain in quantities sufficient to sustain the brain's high energy demands. The consequence of restricted entry into brain of critical amino acids and glucose-derived neurotransmitters is that they must be synthesized from glucose within brain, thereby closely linking energy metabolism with neurotransmitter synthesis and degradation.

Glucose transporters. In adult mammalian brain, only glucose has a sufficiently high number of transporters (GLUT1) to facilitate an adequate flux of carbon fuel into brain from blood (Fig. 3.2), and from extracellular fluid into brain cells. Specific transporter isoforms are preferentially localized in different cell types, e.g., GLUT1 in astrocytes and GLUT3 in neurons (Simpson et al., 2007). Maximal glucose transport capacity (T_{max}) is approximately three times maximal glucose utilization capacity (V_{max}) (Holden et al., 1991) (see Box 3.2, *enzyme activity*). In contrast to glucose and other minor fuels that enter brain in small quantities under normal circumstances, oxygen diffuses across the blood–brain barrier and cellular membranes.

The pathway fluxes for distribution of glucose within brain are poorly understood, and the fraction that enters astrocytic endfeet surrounding capillaries compared to that diffusing through interstitial fluid remains to be established. Diffusion of small molecules through interstitial fluid is restricted by the tortuosity of extracellular fluid space, and cellular membranes are barriers for transcellular movement of aqueous compounds. However, transporters facilitate transmembrane movement, and glucose and lactate transport across the

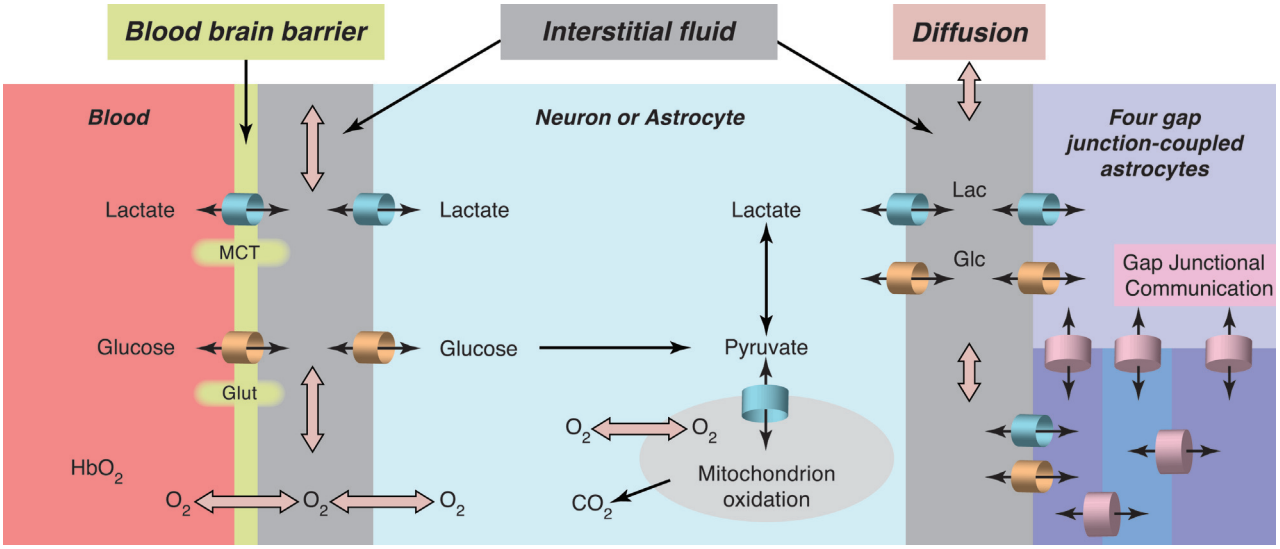

FIGURE 3.2 **Transporters govern passage of hydrophilic compounds across the blood–brain barrier and cellular membranes.** Glucose transporters (GLUTs) are present in high quantities in the endothelial cells in the cerebral microvasculature; the 55kDalton isoform of GLUT1 catalyzes the bidirectional, facilitative transport of glucose (Glc) across the blood–brain barrier, whereas GLUT1 (45kDa isoform) and GLUT3 transport glucose across the plasma membranes of astrocytes and neurons, respectively. Monocarboxylic acid transporters (MCTs) have broad substrate specificity and can transport lactate (Lac), pyruvate, ketone bodies, and short chain fatty acids across membranes. Note that an MCT is required for pyruvate transport into mitochondria. Astrocytes are extensively coupled via gap junctions to form a large syncytium through which many small molecules (<~1kDa) can quickly diffuse, a process called gap-junctional communication. Metabolites can also diffuse throughout brain via the perivascular, interstitial, and cerebrovascular fluids. HbO_2 denotes oxygen bound to hemoglobin (Hb) in blood, and free oxygen can readily diffuse across the blood–brain barrier and cellular membranes.

plasma membrane is much faster than metabolism (Dienel et al., 1991; Holden et al., 1991; Simpson et al., 2007). Astrocytes are extensively coupled via gap junctions (see Chapter 9) to form large intracellular syncytia comprised of thousands of astrocytes in brain *in vivo*, contrasting the low-level (~10–15 cells) coupling of cultured astrocytes (Ball et al., 2007). Thus, compounds taken up into astrocytes can diffuse extensively among coupled cells and along perivascular space through the gap junction-coupled endfeet (Fig. 3.2; Ball et al., 2007). Flow of perivascular fluid within brain is powered by arterial pulsations and is capable of quickly distributing compounds in extracellular space throughout the brain within minutes (Rennels et al., 1985). The *maximal capacity for glucose transport* (T_{max}, Box 3.2) across microvascular membranes is calculated to be much higher than that across neuronal and astrocytic plasma membranes (about 260, 35, and 5 nmol per 10^6 cells per min, respectively), and when kinetic parameters of glucose transporters and number of transport cycles per transporter per s (k_{cat}) are taken into account, neurons are calculated to have a 9-fold higher capacity for glucose transport than astrocytes at 5 mM glucose (Simpson et al., 2007).

Glucose transporters are facilitative, and glucose moves down its concentration gradient from arterial plasma to interstitial fluid to intracellular fluid. Thus, brain glucose level passively follows changes in plasma (Fig. 3.3A). Normal rats have a brain-to-plasma ratio for glucose of approximately 0.22 for arterial plasma glucose levels within the normal to hyperglycemic range (~8–25 mM). Within this wide range brain glucose level rises and falls in proportion to that in plasma and the brain-to-plasma ratio is stable (Figs. 3.3A and 3.3B). However, when the steady-state level of glucose in plasma is reduced below ~8 mM in a graded manner, the brain-to-plasma distribution ratio progressively falls because glucose delivery is increasingly unable to match demand (Fig. 3.3B). Brain hexokinase has a K_m for glucose of ~0.05 mM and the enzyme is saturated with substrate in normoglycemic conditions; its rate is maximal and independent of substrate concentration (inset, Fig. 3.3C). However, during hypoglycemia, hexokinase becomes progressively more unsaturated as brain glucose level falls below ~0.5 mM, causing the rate of glucose phosphorylation to fall (Fig. 3.3C). Glucose concentration is normally relatively uniform throughout the brain, as shown by autoradiographic studies using the radiolabeled, non-metabolizable glucose analog, 3-O-methylglucose. Local changes in brain glucose level during activation or during depression of brain metabolism can be detected with labeled methylglucose, but the changes are relatively small (see later, Fig. 3.13). To summarize, glucose supply is not limiting for brain metabolism. Supply matches demand in activated brain when glucose utilization rates are

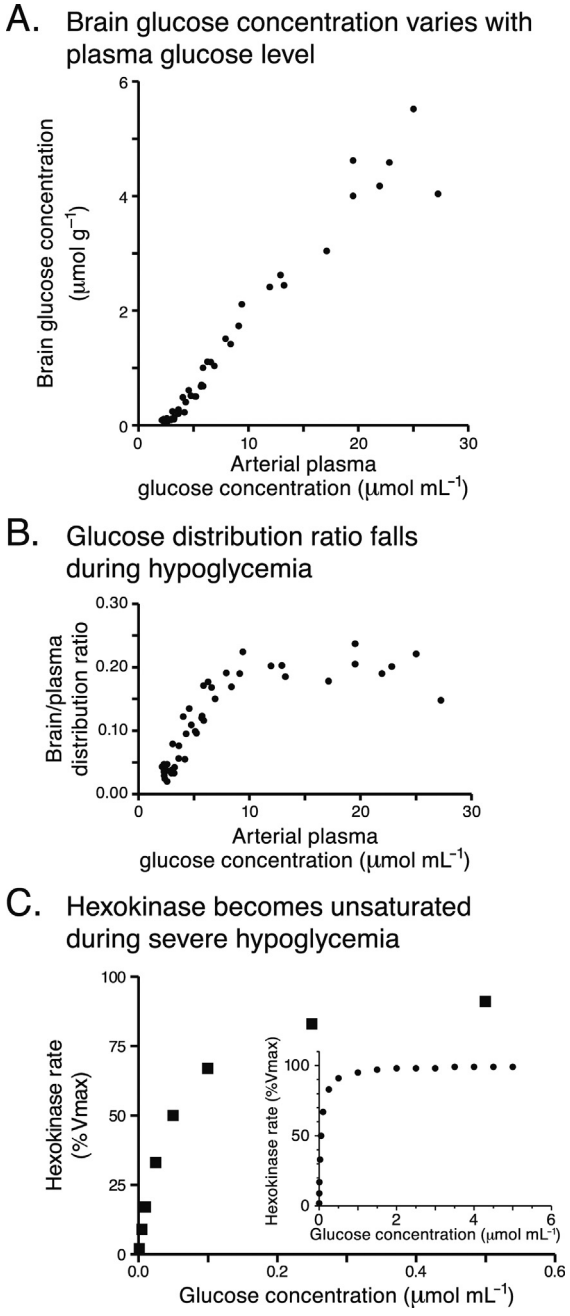

FIGURE 3.3 **Brain glucose concentration during hyperglycemic, normoglycemic, and hypoglycemic conditions.** Steady-state concentration of brain glucose (A) and brain-to-plasma glucose concentration ratio (B) as functions of arterial plasma glucose level (Panels A and B are plotted from data of Dienel et al. (1991)). Under normal and hyperglycemic conditions (plasma glucose range ~8–25 μmol mL^{-1}) the mean glucose brain-to-plasma distribution ratio is about 0.22, but this ratio falls as plasma glucose is clamped at progressively lower levels because glucose delivery does not match the metabolic demand for glucose. Brain hexokinase has a K_m for glucose of ~0.05 mM. Hexokinase is saturated with substrate under normal conditions (brain glucose level >1 mM) (inset, panel C), but the velocity of the hexokinase reaction, calculated using simple Michaelis-Menten kinetics ($v = V_{max}\ S/[K_m + S]$, where v is the reaction velocity, V_{max} = maximal velocity, S = substrate concentration, and K_m is the value for S at which $v = 0.5\ V_{max}$), falls progressively as intracellular glucose concentration falls below 0.5 mM (C).

stimulated by several-fold, although there may be brief transients at the onset of stimuli before compensatory processes respond to change in demand.

Monocarboxylic acid transporters (MCT). MCTs are facilitative transporters with broad substrate specificity that co-transport one H^+ ion along with each monocarboxylic acid (e.g., lactate and pyruvate; reviewed by Halestrap and Price (1999)). In the adult rodent (postnatal day 60 and older), different MCT isoforms are preferentially, but not exclusively, enriched in brain cell types; MCT 1 is present in endothelial cells, MCT1 and MCT4 are mainly in astrocytes, whereas MCT2 is mainly in neurons. The K_m's of these isoforms for lactate are in the range of about 0.7 mM, 3–5 mM, and 15–30 mM for MCT 2, 1, and 4, respectively (Halestrap and Price, 1999; Hertz and Dienel, 2005; Simpson et al., 2007; and references cited in these reviews), indicating that the neuronal isoform can be close to saturation under normal physiological levels of lactate (Table 3.1). In contrast, lactate fluxes across the endothelial and astrocytic membranes will rise and fall with lactate level within the normal physiological range. An important finding is that the substrate specificity for astrocytic MCT isoform(s) is the basis for preferential uptake of acetate into astrocytes, not neurons (Waniewski and Martin, 1998). The cell-type specificity of acetate uptake and metabolism enables its use as an astrocyte "reporter molecule" to study astrocytic oxidative metabolism, glutamate–glutamine cycling between astrocytes and neurons (Lebon et al., 2002), and astrocytic responses to brain activation and pathology (Dienel et al., 2001a; Dienel et al., 2001b; Cruz et al., 2005; Dienel et al., 2007b). Metabolic compartmentation and cellular aspects of metabolism are discussed in more detail in the following text related to Fig. 3.17.

Blood-borne lactate, acetate, and ketone bodies are minor fuels for normal adult brain due to low metabolite levels in normal arterial plasma and low monocarboxylic acid transporter levels in the microvasculature of adult brain. However, in the suckling mammal, the level of the MCT1 isoform at the blood–brain barrier is about 10-fold higher than in the adult to facilitate utilization of ketone bodies (β-hydroxybutyrate and acetoacetate) and lactate; after weaning, the capacity for monocarboxylic acid transport across the blood–brain barrier falls markedly (Cremer, 1982). The level of MCT1 in the microvasculature can adapt to pathophysiological conditions, and during prolonged starvation or feeding of a ketotic diet to help control seizures the MCT levels increase, thereby enabling greater use by the brain of ketone bodies in blood (Nehlig, 1996; Veech, 2004; Yudkoff et al., 2007; Prins, 2008). Studies in exercising humans have shown that intense muscular activity generates increased amounts of lactate, causing blood lactate level to rise from <1 mM to

7−15 mM, greatly exceeding brain lactate concentration which ranges from ~0.5−1 μmol g wet weight $^{-1}$ during rest to ~2 during activation) (reviewed by Dalsgaard, 2006; Quistorff et al., 2008). Higher blood-to-brain lactate levels drive inward facilitative transport of lactate from blood into brain where it is oxidized as a supplementary fuel (van Hall et al., 2009) and contributes to reducing the calculated ratio of $CMR_{O2}/CMR_{glucose+lactate}$. In normal adult rats, labeled lactate and glucose inserted into the interstitial fluid via microdialysis probes are oxidized by both neurons and astrocytes in substantial amounts (Zielke et al., 2009). Use of endogenously generated lactate as fuel is controversial and is discussed in more detail in following text.

Glycolytic Pathway: Generation of Pyruvate from Glucose

Glycolysis is a highly regulated series of reactions that convert the six-carbon glucose (Glc) to pyruvate, a triose, by steps that do not require oxygen (Fig. 3.4). The first irreversible step of the pathway is catalyzed by hexokinase and consumes 1 ATP to generate glucose-6-phosphate (Glc-6-P), which traps the glucose molecule inside of the cell. Glc-6-P regulates hexokinase activity by feedback inhibition, and ATP also inhibits the reaction. Glc-6-P is in equilibrium with Glc-1-P via the phosphoglucomutase reaction and with fructose-6-P (Fru-6-P) via the phosphoglucoisomerase reaction. These three compounds are readily interconvertible and constitute a pool that can be considered as a major *branch point*. Thus, Glc-6-P has three major fates: continuation down the glycolytic pathway, entry into the pentose phosphate shunt pathway, and storage as glycogen via Glc-1-P and UDP-glucose (Fig. 3.4). Glycogen is the major energy reserve in brain and is located mainly, but not exclusively, in astrocytes; it is actively used during normal physiological activity. The pentose shunt pathway is present in all brain cells and is regulated mainly by availability of NADP; this pathway generates NADPH for biosynthetic reactions and oxidative defense plus 5-carbon precursors for nucleic acid biosynthesis, particularly in dividing cells. Fru-6-P is also the precursor for synthesis of monosaccharides and complex carbohydrates that are key components of glycoproteins and glycolipids, including mannose, glucosamine, and sialic acid.

Synthesis of fructose-1,6-bisphosphate (Fru-1,6-P_2) by phosphofructo-1-kinase (PFK) consumes a second ATP and is the committed step for glycolysis. PFK is a very highly regulated enzyme, with many activators and inhibitors that together convey to the enzyme information about the cellular energy demand and the "status" of downstream pathways (Passonneau and Lowry, 1964). Cleavage of Fru-1,6-P_2 by aldolase generates two trioses, dihydroxyacetone-P and glyceraldehyde-3-P, and these three compounds form another readily interchangeable pool.

Oxidation of glyceraldehyde-3-P to 1,3-diphosphoglycerate by glyceraldehyde-3-P dehydrogenase (GAPDH) requires the cofactor NAD^+ and generates $NADH + H^+$. The next enzymatic step catalyzed by 2-P-glycerate kinase generates 1 ATP for each of the two 3-carbon molecules formed from glucose, and energy required to "activate" the hexose is now "replaced." 3-P-Glycerate is then converted via 2-P-glycerate to phosphoenolpyruvate (PEP). 3-P-Glycerate is also the precursor for 3-P-hydroxypyruvate, from which L serine is synthesized (Fig. 3.4). L-serine is then the precursor for glycine and the one-carbon pool that is essential for the methyl-transfer reactions. L-serine is also the precursor for D-serine, a neuromodulator. PEP is converted to pyruvate by the action of pyruvate kinase to produce 1 ATP per PEP. Thus, the net ATP yield for direct conversion of glucose to two pyruvate via glycolytic pathway is 2 ATP, with the generation of 2 NADH which must be oxidized to NAD^+ for glycolytic flux to continue. Pyruvate also has alternative metabolic fates (Fig. 3.4). If NADH is not oxidized via a redox shuttle system (see following and Fig. 3.5) as fast as it is generated, lactate dehydrogenase (LDH) converts pyruvate to lactate and regenerates NAD^+. Pyruvate can also be transaminated to form alanine or decarboxylated by the pyruvate dehydrogenase complex to form acetyl CoA that is oxidized in the TCA cycle. In astrocytes, pyruvate is a substrate for pyruvate carboxylase, the enzyme required for CO_2 fixation and anaplerotic reactions. Under normal resting conditions when the ratio of oxygen to glucose utilization is close to 6, nearly all pyruvate is oxidized.

The concentration of each of the glycolytic intermediates in brain is very low, and taken together, the total amount of all intermediates, approximately 0.4 μmol g^{-1}, is in the range of 15−25% of the brain glucose level (Table 3.2). Due to the small pool sizes of these compounds and the high glucose utilization rate (~0.7 μmol g^{-1} min^{-1}, Table 3.1), the *turnover times* (e.g., divide metabolite concentration by pathway flux rate; Box 3.2) of glycolytic intermediates are much higher than those of brain glucose. The total concentration of $NAD^+ + NADH$ is also low and oxidation-reduction (redox) cycling of these cofactors must be rapid to sustain a high glycolytic rate, e.g., it must be twice CMR_{glc}, or 1.4 μmol g^{-1} min^{-1}, since two trioses are formed per glucose consumed. The calculated cytoplasmic $[NAD^+]/[NADH_2]$ and $[NADP^+]/NADPH_2]$ ratios in rapidly frozen brains are about 670 and 0.12, respectively, and the ratio of $[ATP]/[ADP][HPO_4^{2-}]$ in

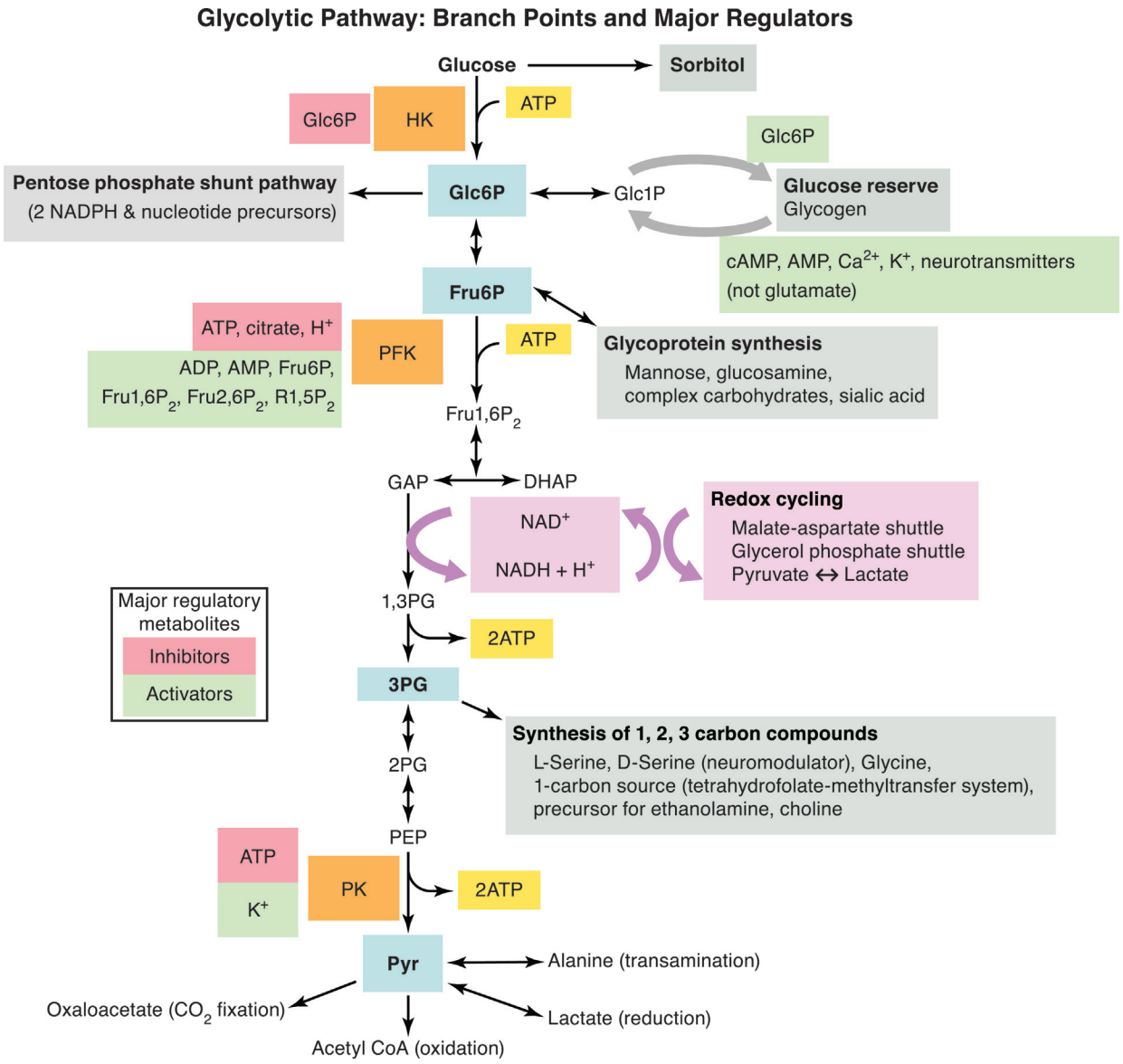

FIGURE 3.4 **Conversion of glucose to pyruvate and use of glucose carbon for storage and biosynthetic reactions.** Glucose is the obligatory carbon source for brain, and most is converted to pyruvate during normal resting conditions. However, glucose also supplies precursors for a number of other critical pathways with diverse and essential roles in brain structure and function. The metabolites in the blue boxes can be regarded as "branch-point" metabolites because carbon can be diverted from the glycolytic pathway to other pathways. Regulation of the glycolytic pathway involves feedback inhibition and allosteric modulation by metabolites involved in different pathways, thereby integrating control with overall metabolic, biosynthetic, and redox economies of the cell. Major inhibitors or activators of key glycolytic enzymes are indicated in red or green boxes, respectively, adjacent to the enzymes. Abbreviations: Glc6P, glucose-6-phosphate (P); HK, hexokinase; Glc1P, glucose-1-P; Fru6P, fructose-6-P; Fru1,6P_2, fructose-1,6-bisphosphate; Fru2,6P_2, fructose-2,6-bisphosphate; R1,5P_2, ribose-1,5-bisphosphate; PFK, phosphofructo-1-kinase; DHAP, dihydroxyacetone-P; GAP, glyceraldehyde-3-P; 1,3PG, 1,3-diphosphoglycerate; 3PG, 3-phosphoglycerate; 2PG, 2-phosphoglycerate; PEP, phosphoenolpyruvate; Pyr, pyruvate.

cytoplasm is 370 M^{-1} indicating a high phosphorylation state in brain (Veech et al., 1973). NADH and NADPH are fluorescent and are commonly used to evaluate changes in redox state (expressed as change in fluorescence divided by baseline fluorescence, e.g., $\Delta F/F$) under various conditions (Shuttleworth, 2010). However, interpretation of changes must be made with caution because NADH levels are very low (<0.1 μmol g^{-1}, Table 3.2) and ΔF is typically in the range of 5–10%. This means that the very small changes in NADH level (<0.01 μmol/g), are unlikely to represent fluxes; they indicate net changes in redox state. For comparison, the turnover times for brain glucose (assume 2 μmol g^{-1}, Table 3.2, divided by 0.7 μmol g^{-1} min^{-1}) and for NADH (0.1 μmol g^{-1} divided by 1.4 μmol g^{-1} min^{-1}) are 2.9 min and

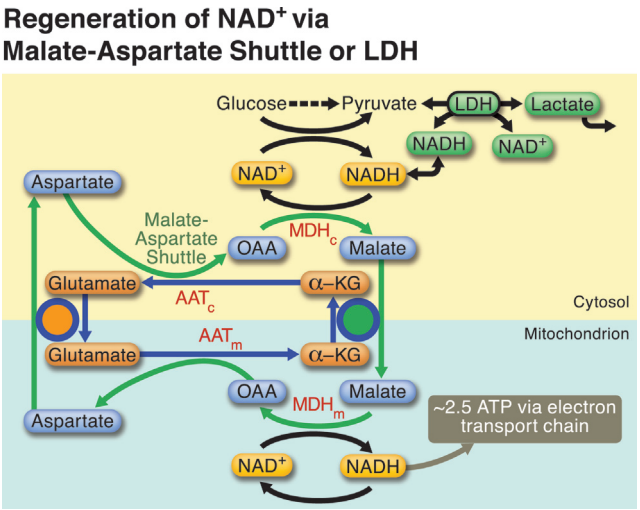

FIGURE 3.5 **Redox shuttle systems transfer reducing equivalents from cytosol to mitochondrial electron transport chain.** NAD^+ can be regenerated by conversion of pyruvate to lactate or the malate–aspartate shuttle (MAS), which is the major redox shuttle system in brain (McKenna et al., 2006; LaNoue et al., 2007). Note the different ATP yields from the two processes. Lactate formation removes pyruvate from the metabolic pathway of the cell and NADH oxidation yields no energy but allows glycolysis to continue by regeneration of NAD^+. The MAS produces the highest yield of ATP due to generation of pyruvate that is oxidized and generates ATP and entry of "shuttled NADH" into the electron transport chain at complex I. The carrier proteins involved in the MAS are the aspartate–glutamate carrier, which is an electrogenic process due to co-transport of H^+ with glutamate, and the malate-α-ketoglutarate carrier. *Reproduced from Dienel and Cruz (2004), with permission of Elsevier.* Note that the mixing of carbon between the mitochondrial to cytosolic pools via the malate–aspartate shuttle serves another function that is critical for metabolic studies of brain. Oxidative metabolism of labeled glucose causes labeling of the tricarboxylic acid (TCA) cycle intermediates, including oxaloacetate and α-ketoglutarate. By means of transaminase-mediated exchange reactions, label is transferred to the mitochondrial glutamate and aspartate amino acid pools. A key aspect of dilution of label in the large cytoplasmic amino acid pools is shuttling of keto and amino acids across the mitochondrial membrane. Without this shuttling, label would be more rapidly lost via the decarboxylation reactions in the TCA cycle. Abbreviations: OAA, oxaloacetate; αKG, α-ketoglutarate; LDH, lactate dehydrogenase; MDH, malate dehydrogenase; AAT, aspartate aminotransferase. The subscripts c and m denote the cytosolic and mitochondrial enzymes, respectively.

0.07 min, respectively. In other words, turnover of NADH (e.g., an oxidation-reduction cycle) is about 40 times that of glucose.

Gluconeogenesis. Reversal of the glycolytic pathway to synthesize glucose or glycogen from triose precursors (Fig. 3.4) can occur in brain but it is considered to be a minor pathway. Thus, label from ^{14}C-*labeled* (radiolabeled tracers, Box 3.3) lactate, alanine, aspartate, and glutamate can be incorporated into glycogen in cultured astrocytes (Hamprecht and Dringen, 1995). This process involves pyruvate carboxylase to carry out the ATP-requiring, CO_2-fixation step to convert pyruvate to oxaloacetate, followed by decarboxylation to generate phosphoenolpyruvate (PEP), then the actions of PEP carboxykinase and fructose-1,6-phosphatase to generate Glc-1-P that can be incorporated into glycogen. A net of 6 ATP is required to convert two molecules of lactate to Glc-6-P, and one more is needed to incorporate the Glc-6-P into glycogen.

Redox Shuttling and Recycling Mechanisms: Oxidation of Pyruvate or Conversion to Lactate

NADH generated in the cytosol cannot directly cross the inner mitochondrial membrane to be oxidized via the electron transport chain (see following), and alternative processes must be used to regenerate NAD^+. When the CMR_{O2}/CMR_{glc} ratio is close to 6, almost all of the glucose is oxidized and reducing equivalents are nearly quantitatively transferred into the mitochondria, mainly by the malate-aspartate shuttle (MAS). The first step of the MAS (Fig. 3.5) is reduction of oxaloacetate to generate malate, which enters the mitochondrial matrix in exchange for α-ketoglutarate. Malate is oxidized in mitochondria to form NADH, which enters the electron transport chain at complex I (see Fig. 3.8), with the subsequent generation of ATP. Oxaloacetate is transaminated to form aspartate that leaves the mitochondrion via the aspartate–glutamate carrier, an electrogenic process driven by co-transport of H^+ with glutamate; oxaloacetate is then regenerated in the cytosol by transamination (LaNoue et al., 2007). Another redox shuttle, the glycerol–phosphate shuttle, is thought to be minor in brain (McKenna et al., 2006). This shuttle involves cycling of dihydroxyacetone phosphate and glycerol-P across the inner membrane and transfer of reducing equivalents to Coenzyme Q, with a lower ATP yield than the MAS (Fig. 3.8). Another potential mechanism for redox shuttling proposed by Cerdan and colleagues (2006) involves transcellular metabolite transfer in which lactate moves from one cell to another where it is converted to pyruvate, which is then shuttled back to the originating cell and oxidized; this mechanism can bypass the requirement for an intracellular redox shuttle in one cell type.

Early studies demonstrated the predominance of the malate–aspartate shuttle compared to glycerol–phosphate shuttle system in brain (Siesjö, 1978), but more recent reports raised the possibility of large differences in MAS capacities in neurons and astrocytes. This is a very important issue related to understanding metabolic labeling in these cell types and their contributions to oxidative metabolism and brain energetics. The finding that the aspartate–glutamate

TABLE 3.2 Approximate concentrations of metabolites in rodent brain

Glycolytic pathway[a]		TCA cycle intermediates[a]		Amino acids[b]		Energy reserves and high energy metabolites [a,c]	
Metabolite	**Concentration (μmol g^{-1})**	**Metabolite**	**Concentration (μmol g^{-1})**	**Metabolite**	**Concentration (μmol g^{-1})**	**Metabolite**	**Concentration (μmol g^{-1})**
Glucose (Glc)	1.5–2.5	Acetyl CoA	0.001–0.005	Glutamate	11.6	Glucose-1-P	0.004–0.01
		CoA	0.003	Taurine	6.6	UDP-Glc	0.1
Glucose-6-P	0.06–0.2	Citrate	0.25–0.35	N-Acetylaspartate	5.6	Glycogen	1.5–12
Fructose-6-P	0.01–0.02	Isocitrate	0.02	Glutamine	4.5		
Fructose-1,6-P_2	0.01–0.1	α-Ketoglutarate	0.15–0.2	Aspartate	2.6	Creatine-P	4.7–4.9
Dihydroxyacetone-P	0.01–0.03	Succinate	0.45–0.7	GABA	2.3	Creatine	5.6–6.1
3-P-Glycerate	0.04–0.05	Fumarate	0.07	Glycine	0.68		
Phosphoenolpyruvate	0.004–0.005	Malate	0.35–0.45	Alanine	0.65	ATP	2.5–3
Pyruvate	0.05–0.2	Oxaloacetate	0.004–0.007	Serine	0.98	ADP	0.4–0.6
Total (Glc-6-P to Pyr)	**~0.4**	**Total**	**~1.5**	Threonine	0.66	AMP	0.03–0.07
				Lysine	0.21	P_i	2.0–2.7
Lactate	0.5–1.5			Arginine	0.11		
				Histidine	0.05		
NAD	0.20–0.3			Leucine	0.05		
NADH	0.03–0.1			Isoleucine	0.02		
NADP	0.005–0.02			Valine	0.07		
NADPH	0.003–0.02			Phenylalanine	0.05		
				Tyrosine	0.07		
				Proline	0.08		
				Methionine	0.04		
				Ornithine	0.02		
				Tryptophan	0.003		
				Glutathione	2.6		
				Total	**~40**		
				Total (Glu + Gln + Asp + GABA)	**~21**		

[a]*Data from Siesjö (1978), Veech (1980), McIlwain and Bachelard (1985).*
[b]*From the mean values of many studies that were compiled by Clarke et al. (1989).*
[c]*Data from Duffy et al. (1975), Siesjö (1978), McIlwain and Bachelard (1985), Cruz and Dienel (2002).*
Metabolite levels are approximate ranges of values from rat, mouse, or guinea pig brain taken from cited sources. Note that rat brain glucose level varies with arterial plasma glucose level and the normal brain:plasma ratio for glucose is about 0.2 over the normo- and hyperglycemic range. Concentrations of some metabolites vary with animal handling and history (e.g., glycogen) have a large range. Estimates of the total tissue concentrations in each category were calculated using the mean values of the indicated ranges.

BOX 3.3

USE OF RADIOLABELED TRACERS IN BIOLOGY

Nuclide. Atom characterized by atomic number (number of protons in nucleus) and atomic mass (number of protons plus neutrons).

Isotope. Nuclide with same number of protons but different number of neutrons. The chemical properties are the same but the mass is different; a preceding superscript indicates mass.

Radioactive and stable isotopes. A radioactive atom undergoes spontaneous disintegration with emission of radiation, e.g., ^{14}C. A stable isotope does not decay to generate another compound, e.g., ^{13}C. Autoradiographic and positron emission tomographic (PET) studies use many different radiolabeled compounds, whereas magnetic resonance spectroscopic (MRS) studies use stable isotopes.

Activity. Number of nuclear disintegrations per unit time; the standard international unit is the Becquerel (Bq) = 1 disintegration per s (dps). A commonly used unit of activity is the Curie (Ci), which equals 2.22×10^{12} disintegrations per min (dpm); 1 μCi = 2.22×10^6 dpm.

Specific activity. Ratio of activity to molar quantity (e.g., dpm/mole or nCi/μmol). Knowledge of specific activity of a precursor and counts in a compound derived from the precursor allows calculation of the amount of a labeled compound (e.g., dpm in unknown x mole/dpm of precursor = moles unknown). A similar expression, isotopic enrichment, is used in MRS studies to describe relative proportion of an isotope (see Fig. 3.17B).

Precursor-product relationships. The specific activity or isotopic enrichment of a precursor in a metabolic pathway is always higher than that of the product due to dilution of the label by the quantity of unlabeled material in each of the successive metabolic pools through which a compound is metabolized. For example: (1) If the specific activity of glutamate is 1 mCi/mmol and if 1 mmol glutamate is converted to glutamine in a reaction mixture that contains 1 mmol glutamine, the specific activity of glutamine will be 0.5, i.e., 1 mCi in glutamine/(1mmol unlabeled glutamate + 1 mmol unlabeled glutamine). (2) If [1-^{14}C]glucose is converted to lactate, the maximal specific activity of [^{14}C]lactate is half that of glucose because only one of the two lactate formed from glucose will be labeled (see Fig. 3.17A).

Interpretation of radiolabeling studies is often complicated by metabolic compartmentation and insufficient knowledge of the specific activities of important but small precursor pools. For example, an apparent decrease in a pathway flux can be caused by dilution of the precursor specific activity even if there is no flux change. Thus, if unlabeled lactate were added to a tissue along with labeled glucose, the equilibrative steps of lactate−pyruvate interconversion would quickly reduce the specific activity of pyruvate, thereby reducing the amount of labeled pyruvate entering the TCA cycle. In this example, reduced label accumulation into TCA cycle-derived amino acids (e.g., glutamate) might be incorrectly interpreted as lower oxidative metabolism of glucose when in fact the apparent labeling was due to dilution of the pyruvate specific activity (that was not measured and appropriately taken into account). Increased glycogenolysis could also cause dilution of labeled downstream labeled metabolites derived from labeled glucose, thereby reducing the apparent label incorporation into astrocytic amino acid pools.

Integrated specific activity. Integral of specific activity over time (time-activity integral), or the area under the curve when specific activity is plotted as function of time

Beta-emitter. Decay releases an electron (beta particle). For example, ^{14}C decays to produce electron plus nitrogen. Beta emitters commonly used in biological studies include ^{3}H, ^{14}C, ^{35}S, ^{32}P, ^{45}Ca. These compounds can be assayed by detection of the electron by liquid scintillation counting or autoradiography using X-ray film or imaging plates.

Positron emitter. Decay releases a positron that travels a short distance then annihilates with an electron to produce simultaneously two photons emitted at a 180° angle; these events are assayed with pairs of coincidence detectors. Examples include ^{18}F, ^{11}C, ^{15}O, which are commonly used in labeled compounds in positron-emission tomographic (PET) studies.

Physical half-life. The time for half of the atoms to decay. For example, ^{14}C, 5730 years; ^{3}H, 12.3 years; ^{18}F, 109 min; ^{11}C, 20 min; ^{15}O, 2 min. Isotopes used in PET assays generally have short half-lives, thereby reducing exposure of the subject to radiation. In contrast, the relative stability of ^{14}C and ^{3}H facilitates broad utilization of these isotopes in biological and biochemical studies.

Biological half-life. The time for half of the dose to be eliminated; biological half-life depends on the compound and its metabolic and excretory fates.

Tracer amount or quantity. The dose of a radiolabeled compound is usually so small that it does not change the concentration of the endogenous compound and does not alter fluxes; the higher the specific activity, the lower the molar amount of the tracer to achieve the same labeling sensitivity. Introduction of tracer amounts of a radiolabeled compound allows specific enzymatic steps, pathways, and fluxes to be studied *in vitro*, in cultured cells, and *in vivo*.

carrier (Fig. 3.5) is poorly detectable by immunocytochemical procedures in astrocytes compared to neurons in tissue sections from adult brain implies low MAS activity (Ramos et al., 2003; LaNoue et al., 2007). This was unexpected because magnetic resonance spectroscopic (MRS) studies have shown substantial oxidative metabolism of glucose in astrocytes in adult brain *in vivo*. Entry of glucose-derived pyruvate into the TCA cycle would not occur without a working redox shuttle mechanism; e.g., if there were no shuttle, all pyruvate must be converted to lactate to maintain glycolysis (Figs. 3.4, 3.5). Also, astrocytes contain pyruvate carboxylase, which confers to them the anaplerotic capability for net synthesis of glutamate and aspartate via the oxidative pathway in the TCA cycle, and CO_2 fixation by pyruvate carboxylase increases with brain activity (Yu et al., 1983; Shank et al., 1985; Öz et al., 2004). Direct evidence for oxidative metabolism of glucose in mature astrocytes acutely isolated from adult mice comes from ^{13}C-labeling patterns of TCA cycle-derived metabolites after incubation with [U-^{13}C]glucose (Lovatt et al., 2007), and high aspartate−glutamate carrier mRNA and protein levels are found in astrocytes isolated from adult brain (Li et al., 2012). The quantitative contribution of astrocytic oxidative metabolism to brain energetics is unresolved, and emerging data suggest that the contribution of astrocytes to overall brain energy metabolism is greater than previously recognized.

When the rate of glycolysis exceeds the redox shuttle capacity, pyruvate is converted to lactate by lactate dehydrogenase (LDH), with release of lactate from the cell (Fig. 3.5). This reaction also enables the glycolytic pathway to operate under hypoxic or anaerobic conditions. Coupling of glycolysis to LDH activity has the advantage of sustaining a high flux rate at the cost of release of oxidative fuel. Because (i) glucose is rarely rate-limiting under normal conditions and (ii) glucose and lactate transport are facilitative (e.g., driven by concentration gradients and not energy-requiring), the energetic cost of lactate release from brain for use by other body tissues is negligible. However, as discussed below, lactate efflux has consequences for metabolic imaging and spectroscopy using labeled glucose as a tracer. Lactate carries all of the labeled carbon atoms of glucose (except that lost via decarboxylation reactions in the pentose shunt pathway) and release of labeled lactate causes underestimation of product formation and metabolic rate.

Glycogen—Glucose Storage and Mobilization During Brain Activation and Energy Crisis

Incorporation of glucose into a macromolecule minimizes cellular osmotic changes, and glycogen, along with the enzymes involved in its synthesis and degradation, is widely distributed throughout the brain. Glycogen is mainly localized in the soma, perivascular endfeet, and fine processes of astrocytes but glycogen granules are also present in some large neurons in the brain stem and spinal cord. The concentration of glycogen in brain has historically been found to be rather low, in the range of $\sim 1-3\ \mu mol$ glucosyl units g^{-1} (note: tissue glycogen concentration actually refers to the glucose equivalents [i.e., glucosyl units] released from glycogen when it is assayed in tissue extracts by enzymatic degradation), and glycogen had been considered to be a minor energy store since its level was similar to that of glucose (Table 3.2). However, assays using carefully handled animals and tissue fixation and extraction methods that prevent enzymatic degradation of *labile metabolites* (Box 3.2) found much higher glycogen levels in unstimulated rat brain, ranging from 5 to 12 μmol glucosyl units g^{-1} (Cruz and Dienel, 2002). Glycogen utilization during whisker stimulation of the rat (Swanson et al., 1992) and large compensatory increases in utilization of blood-borne glucose during whisker stimulation when glycogenolysis is blocked (Dienel et al., 2007a) indicate that both net consumption of glycogen and glycogen turnover increase during normal physiological activity of astrocytes. A novel finding is that glycogen is involved in taste-aversion learning and memory formation in the newborn chick (Hertz and Gibbs, 2009). Two studies have linked glycogenolysis to memory formation and lactate shuttling (Newman et al., 2011; Suzuki et al., 2011), but direct evidence for lactate transfer to neurons remains to be obtained, and it is possible that lactate serves as a redox signaling compound. Increased glycogen turnover under normoglycemic conditions indicates that activity-evoked glycogenolysis is not due to generalized hypoglycemia in brain and suggests that glycogen turnover plays an important role at a local level. Because glycogen phosphorylase is located throughout the subcellular compartments of astrocytes (Hamprecht et al., 2004), glycogen probably serves as a fuel "buffer" for specific *metabolic pools* (Box 3.2) during times of abrupt increases in energy demand associated with excitatory neurotransmission. For example, glycogenolysis is predicted to support astrocytic energetics of removal of K^+ from extracellular space and simultaneously raise the level of glucose-6-phosphate in astrocytes, thereby inhibiting hexokinase and freeing-up blood-borne glucose for utilization by neurons during brain activation (DiNuzzo et al., 2010b; DiNuzzo et al., 2011; Dinuzzo et al., 2012). Increased levels of extracellular potassium and catecholamine neurotransmitters (e.g., adrenaline, serotonin, histamine), but *not* extracellular *glutamate* (Sorg and Magistretti, 1991), are capable of stimulating

glycogenolysis (Fig. 3.4) in cultured cells and brain slices, thereby linking astrocyte glycogen turnover to synaptic activity (Hertz et al., 2007). High levels of glutamate cause glycogen levels to rise in cultured astrocytes, ^{13}C-MRS studies have shown that glutamate can be converted to lactate, and ^{14}C labeling studies have shown incorporation of label from lactate into glycogen, so it is conceivable that some glutamate can be converted to glycogen under specific conditions.

The reactions involved in glycogen synthesis and degradation are tightly regulated (Obel et al., 2012), and transfer of glucosyl groups to and from glycogen interfaces with the glycolytic pathway at the glucose-6-P step (Fig. 3.4). The phosphoglucomutase reaction brings glucose-6-P into equilibrium with glucose-1-P, which is about 7% of the level of glucose-6-P. Glucose-1-P is next converted to uridine diphosphoglucose (UDP-glucose) with the release of pyrophosphate. The glucosyl moiety of UDP-glucose is then added to glycogen in an α-1,4-glycosydic linkage to a growing amylose chain by glycogen synthase, a highly regulated enzyme. Epimerization of UDP-glucose forms UDP-galactose, which is an important precursor for complex carbohydrates. The phosphorylated form of glycogen synthetase is dependent (D form) on glucose-6-P as an activator, whereas the unphosphorylated form is independent (I form) of glucose-6-P. 3′,5′-cyclic AMP (cAMP) stimulates the phosphorylation of the I form to the D form. Glycogen phosphorylase is also very highly regulated and exists in the a (active) and b (inactive) forms; interconversion of these forms is governed by phosphorylase b kinase and phosphorylase a phosphatase. Phosphorylase b is activated by AMP and inorganic phosphate (Pi) (i.e., during low energy conditions) and inhibited by ATP and glucose-6-P (i.e., when energy levels are adequate). cAMP stimulates a protein kinase to phosphorylate the phosphorylase b kinase, which is also activated by Ca^{2+}; these steps generate phosphorylase a and stimulate glycogenolysis to form glucose-1-P. Regulation of glycogen turnover is fine-tuned by intracellular metabolic regulators and coordinated with (i) local neuronal activity by K^+ uptake from extracellular fluid and (ii) local and global neuronal activity via neurotransmitter receptors. The noradrenergic system from the locus coeruleus has widespread innervation throughout the brain and β-adrenergic receptors on astrocytic membranes are potent stimulators of glycogenolysis. Astrocytic glycogenolysis is also regulated by oxidative stress, and increased demand for NADPH via the pentose phosphate shunt pathway is triggered by exposure of cultured astrocytes to reactive oxygen species and hydrogen peroxide, causing rapid degradation of glycogen (Dringen et al., 2007).

Cultured astrocytes degrade glycogen to pyruvate, which is converted to lactate and released to the tissue culture medium, contrasting the liver, which converts glycogen to glucose-6-P that is dephosphorylated and released to blood (Hamprecht and Dringen, 1995). There are reports of glucose-6-phosphatase activity in brain cells, but its physiological significance is not established. A number of studies of glucose-6-phosphatase in brain *in vivo* and in cultured astrocytes by the Sokoloff laboratory failed to detect significant phosphatase activity, consistent with the release of lactate instead of glucose from astrocytes. Thus, a major difference between the fate of glycogen in brain compared to liver is astrocytic metabolism of glycogen to generate pyruvate and lactate, whereas liver glycogen is used for whole body glucose homeostasis. The ultimate fate of the pyruvate and lactate generated from glycogen remains to be established, and it probably varies with physiological condition; it may be oxidized or released.

Under *"resting" conditions* (Box 3.1), the rate of glycogenolysis in brain *in vivo* is low, on the order of 0.01 $\mu mol\ g^{-1}\ min^{-1}$, and the glycogen molecule is relatively stable. However, during physiological stimulation, glycogenolysis rises by a factor of 6−50 to 0.06−0.5 $\mu mol\ g^{-1}\ min^{-1}$, and increases even more (to 0.2−2.6 $\mu mol\ g^{-1}\ min^{-1}$) during pathophysiological conditions with very high ATP demand, e.g., seizures, anoxia, or ischemia (Dienel and Cruz, 2006). Note that the highest rates of glycogenolysis are more than three times the resting rate of utilization of blood-borne glucose (Table 3.1). Thus, rapid activation of glycogenolysis by physiological activity, stressful handling conditions, and actions of neurotransmitters probably caused the low levels of brain glycogen found in many studies because sensory stimulation and handling prior to tissue sampling are sufficient to stimulate rapid degradation of this labile metabolite.

The glycolytic energy yield from glycogen can be higher or lower than that from glucose, depending on how the calculation is made. Conversion of one glucosyl-unit from *preformed glycogen* to two pyruvate *yields 3 ATP* because glycogen phosphorylase is a phosphoryl transferase that forms glucose-1-P from glycogen, thereby bypassing the initial ATP required by the hexokinase reaction. Thus, metabolism of preformed glycogen has a 50% higher ATP yield than glycolysis of blood-borne glucose (Fig. 3.4). On the other hand, if one takes the viewpoint that there is *turnover of glycogen*, the accounting must include the hexokinase and UDP-glucose steps for synthesis of glycogen from glucose. Two ATP are consumed for conversion of glucose to glycogen to glucose-6-P and another ATP is needed to form fructose-1-6-P_2, for a net consumption of 3 ATP per glucose cycled through glycogen.

Because glycolysis has a net yield of 4 ATP, the overall gain of shunting glucose through glycogen is only one ATP per glucose. The advantage of this process is the glycogen can be stored when fuel is readily available and rapidly degraded upon demand, without requiring the initial input of ATP.

In summary, the finding of high levels of glycogen in brain and increased glycogen turnover during brain activation has stimulated considerable interest in the contributions of glycogen to astrocytic energetics. The specific physiological functions of glycogen during brain activation and the fate of the carbon derived from glycogen during normal brain activity remain to be experimentally established, but during a hypoglycemic or ischemic energy crisis glycogen clearly helps prolong the duration of brain and nerve function and minimize cellular damage.

Pentose Phosphate Shunt Pathway: Oxidative Defense and Biosynthesis

The pentose phosphate shunt pathway (Fig. 3.6) has two major roles: provision of NADPH that is utilized in biosynthetic reactions and oxidative defense, and generation of 5-carbon intermediates that are precursors for nucleic acids (Dringen et al., 2007). Both of these functions are particularly important in developing brain when lipid biosynthesis and cell division are most active. In adult brain the flux through the pentose shunt pathway is approximately 5% of the rate of glucose utilization, but brain tissue has a huge excess capacity that is revealed by incubation of brain slices with an artificial electron acceptor, phenazine methosulfate, which stimulates the pathway by 20–50-fold. Flux through the pentose shunt pathway is also

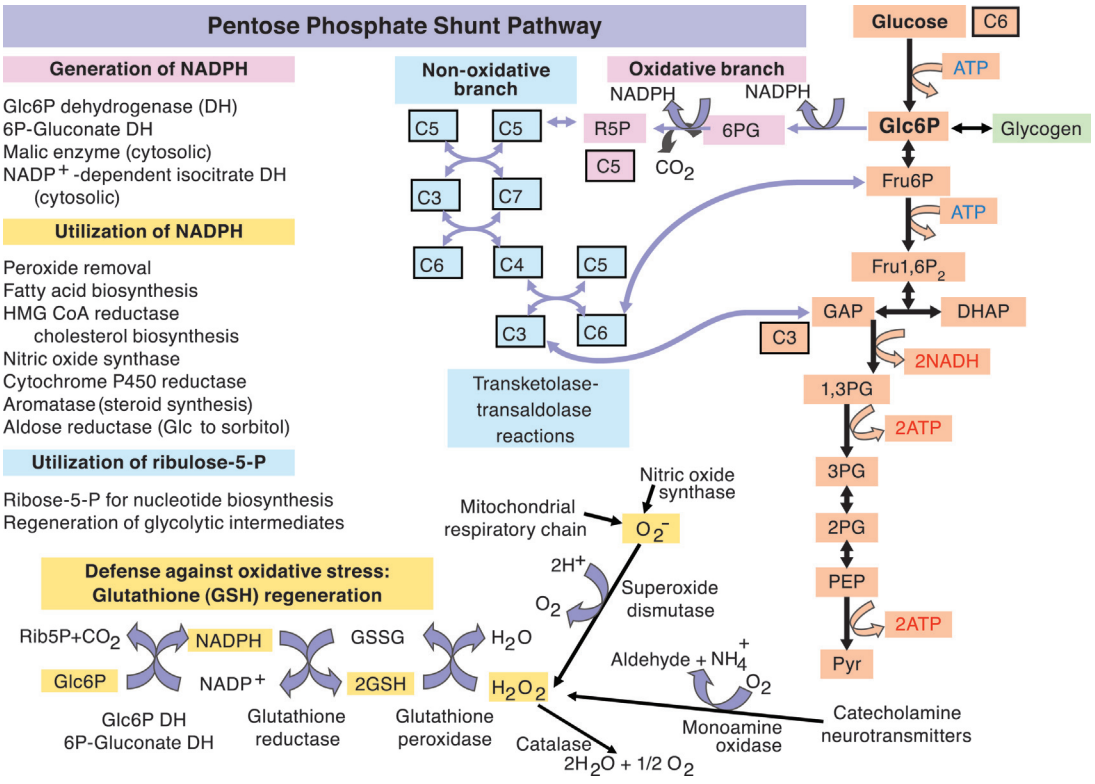

FIGURE 3.6 **The pentose phosphate shunt pathway provides substrates for oxidative defense, biosynthetic reactions, and nucleotide biosynthesis.** The oxidative component of the pathway generates 2NADPH + 2 H^+ in successive oxidation reactions starting with glucose-6-P and forming 6-P-gluconate (6PG), then ribulose-5-P (R5P) + CO_2. The 6-carbon glucose (denoted as C6 in a box next to glucose) is converted to a C5 intermediate, which by means of interconversions catalyzed by transketolases and transaldolases, can regenerate C6 and C3 glycolytic intermediates. The pentose shunt pathway is not the only source of NADPH, but it is likely to be the major supplier due to its activation by oxidative stress and exposure to peroxides. NADPH is necessary for a variety of biosynthetic reactions, some of which are highly active during brain growth and maturation (e.g., lipid biosynthesis) and some that are involved biosynthesis of neuroactive compounds, e.g., nitric oxide synthase, as well as in degradation of catecholamine neurotransmitters (monoamine oxidase). An important function of the NADPH is its role as a cofactor in the glutathione reductase and peroxidase systems to eliminate hydrogen peroxide that is produced by various cellular reactions. Note that glucose-6-P can be derived from blood-borne glucose and from glycogen in astrocytes. Abbreviations for compounds in the glycolytic pathway are as in Fig. 3.4; GSH, reduced glutathione; GSSG, oxidized glutathione.

stimulated by addition of catecholamine neurotransmitters to brain slices, presumably due to formation of H_2O_2 by monoamine oxidase, as well as by exposure of cells to H_2O_2 or other peroxides that are substrates for glutathione peroxidases (Fig. 3.6). Thus, the predominant function of this pathway is likely to serve different purposes in developing compared to adult brain.

There are two divisions of the pentose shunt pathway, the oxidative branch and nonoxidative branch (Fig. 3.6). The oxidative branch consists of two sequential steps that convert glucose-6-P to ribulose-5-P. The first, catalyzed by glucose-6-P dehydrogenase (glc-6-P DH), is the flux-regulating step and forms NADPH plus an unstable intermediate, 6-phosphogluconolactone, that spontaneously hydrolyzes to form 6-P-gluconate. The concentrations of glucose-6-P, $NADP^+$, and NADPH in brain tissue are low (Table 3.2), and the $NADP^+$/NADPH ratio is ~0.01 (Veech et al., 1973). NADPH is a competitive inhibitor of glucose-6-P DH, indicating that consumption of NADPH and formation of $NADP^+$ provides the required substrate for the reaction which is dependent on continuous supply of glucose-6-P that can be derived from blood-borne glucose or glycogen. 6-P-Gluconate and $NADP^+$ are the substrates for the second step, oxidative decarboxylation, that releases carbon 1 of glucose as CO_2. This reaction forms the basis for the most widely used assay for pentose shunt activity, comparison of the rate of formation of $^{14}CO_2$ from [1-^{14}C]glucose compared to [6-^{14}C]glucose. The nonoxidative branch of the pentose shunt pathway involves interconversion of intermediates via transketolase and transaldolase reactions that can regenerate fructose-6-P and glyceraldehyde-3-P. Thus, for every 6 glucose molecules that enter this pathway, one molecule (17%) is lost as CO_2, and the carbon that is not used for nucleic acid biosynthesis is returned to the glycolytic pathway as fructose-6-P or glyceraldehyde-3-P (Fig. 3.6). Transketolase is a thiamine pyrophosphate (vitamin B_1)-dependent enzyme, and, along with pyruvate dehydrogenase and α-ketoglutarate dehydrogenase of the tricarboxylic acid cycle, the enzyme is affected by thiamin deficiency (beriberi). Severe thiamin deficiency affects selective areas of the central nervous system even though all of the enzymes affected are present in all cell types. Conversion by phosphopentose isomerase of ribulose-5-P to ribose-6-P forms the precursor for 5-phosphoribosyl-1-pyrophosphate (PRPP), which is the starting point for *de novo* synthesis of purine ribonucleotides.

In summary, the overall reaction glucose-6-P plus 2 $NADP^+$ generates ribulose-5-P + CO_2 + 2 NADPH + 2 H^+. Rearrangement of the 5-carbon intermediates that are not utilized for biosynthesis via the non-oxidative reactions returns carbon to the glycolytic pathway. In astrocytes, the pentose phosphate shunt pathway is fueled by glucose and glycogen, whereas neurons are dependent on glucose.

The Tricarboxylic Acid (TCA) Cycle: ATP Production and Biosynthetic Activity

Energy generation. The tricarboxylic acid (TCA) cycle has two major functions: generation of energy and biosynthesis of amino acids and other compounds. After entry into mitochondria via a monocarboxylic acid transporter, pyruvate is converted to acetyl coenzyme A (CoA) by pyruvate dehydrogenase (PDH), a multienzyme complex, that causes oxidative decarboxylation of carbons 3 and 4 of glucose and their release as CO_2. PDH is a highly regulated enzyme, with a K_m for pyruvate of ~0.05 mM, which approximates the concentration of pyruvate in brain tissue. Two products, acetyl CoA and NADH, are competitive inhibitors of the PDH reaction. PDH exists in an inactive, phosphorylated form and an active, dephosphorylated form; the protein kinase that renders PDH inactive is inhibited by ADP, pyruvate, CoASH and NAD^+, whereas it is activated by acetyl CoA and NADH. The protein phosphatase is activated by Mg^{2+} and Ca^{2+}.

Condensation of acetyl CoA with oxaloacetate to generate citrate (Fig. 3.7) is catalyzed by citrate synthase, a regulated enzyme that is inhibited by ATP, NADH, and succinyl CoA and stimulated by ADP. Citrate is converted to isocitrate by aconitase, and the first oxidative decarboxylation step in the cycle is carried out by isocitrate dehydrogenase to generate NADH + H^+ and α-ketoglutarate. This enzyme requires Mg^{2+} or Mn^{2+} and is stimulated by ADP and Ca^{2+}. α-Ketoglutarate dehydrogenase then converts α-ketoglutarate to succinyl CoA in a thiamine-dependent reaction, releasing the second CO_2 in the pathway and generating NADH + H^+; this enzyme can be inhibited by ATP, GTP, NADH, and succinyl CoA. The next step, succinyl CoA synthetase, forms succinate, releases CoASH, and generates GTP. Succinate dehydrogenase oxidizes succinate to fumarate, with conversion of FAD to $FADH_2$. Because FAD is fluorescent, this step can be used to monitor mitochondrial redox status by fluorescence microscopy during brain activation, and this application is discussed below in more detail (see Fig. 3.12). Succinate dehydrogenase is inhibited by malonate, a 3-carbon dicarboxylic acid that has been a useful compound for studies of the TCA cycle. Fumarase adds water to fumarate to form L-malate, which is a substrate to regenerate oxaloacetate with formation of the third NADH + H^+ of the cycle per acetyl CoA. The activities of TCA cycle dehydrogenases can be stimulated by

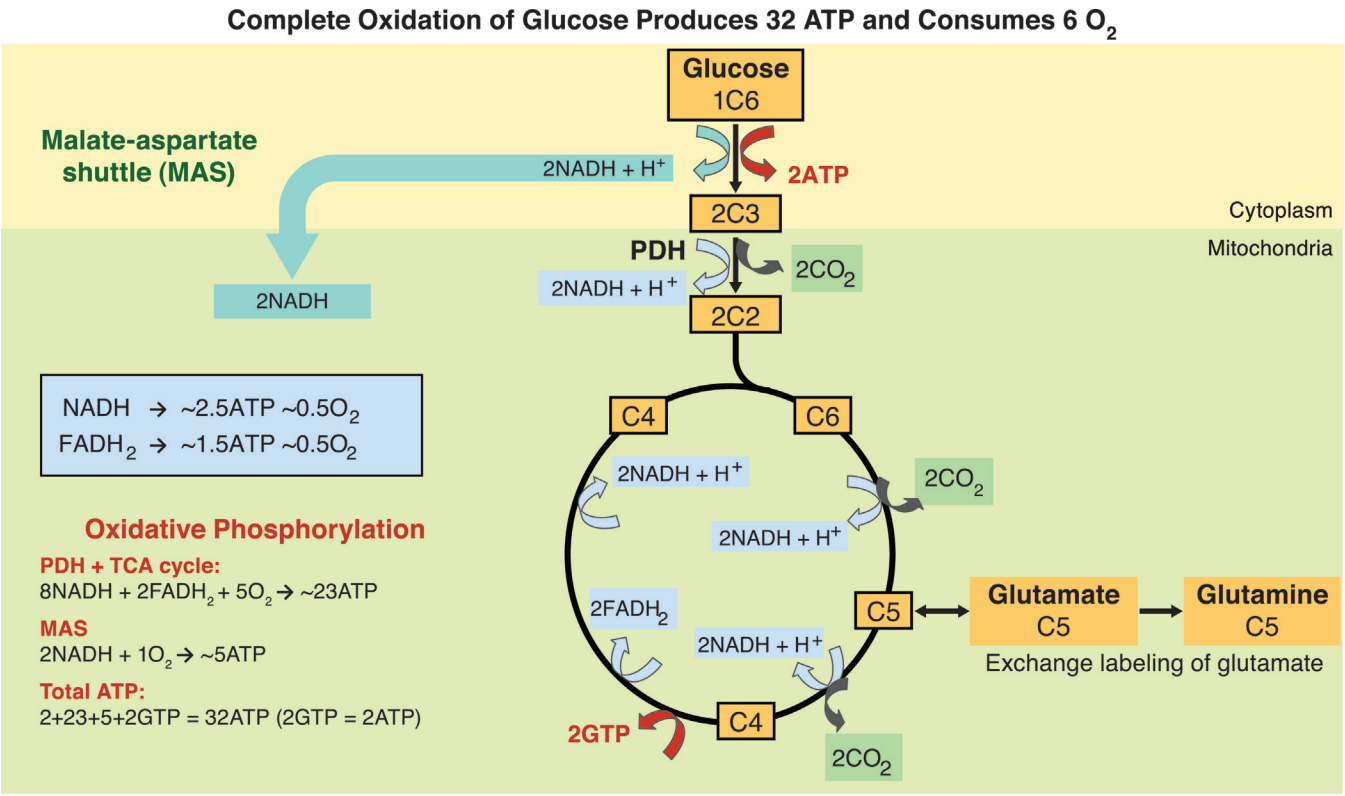

FIGURE 3.7 **Oxidation of pyruvate via the tricarboxylic acid cycle.** Pyruvate is transported from the cytosol to mitochondria along with H^+ by a monocarboxylic acid transporter. Oxidative decarboxylation of pyruvate by the pyruvate dehydrogenase complex generates acetyl coenzyme A (CoA) and releases CO_2 corresponding to the 3 and 4 positions of glucose. This 2-carbon compound (denoted C2 in a box) condenses with oxaloacetate, a 4-carbon (C4) catalytic component of the TCA cycle by the action of citrate synthase. Complete oxidation of acetyl CoA releases CO_2 via the isocitrate dehydrogenase (C6→C5 step) and α-ketoglutarate dehydrogenase (C5→C4 step) reactions; since two acetyl CoA are generated from glucose, a total of 4 CO_2 are produced by the TCA cycle. Note that for each turn of the cycle, a two-carbon compound enters and two 1-carbon compounds are released; there is no net synthesis of any intermediate. Exchange-mediated labeling of the glutamate, glutamine, GABA, and aspartate pools occurs by transamination reactions that shuttle compounds to and from the TCA cycle, thereby leading to label dilution and pool labeling. (Note: The transamination reaction involving oxaloacetate (C4) and aspartate (C4) is not shown in the figure.) This characteristic of intermediary metabolism slows the release of CO_2 from labeled glucose, since the route to the decarboxylation reactions is not direct. A total of 8 NADH, 2 $FADH_2$ and 2 GTP are also generated from one glucose via the TCA cycle, for a net energy yield equivalent to about 32 ATP. Note that the lower yield of ATP compared to previous estimates of 36 in the earlier literature is due to adjustments made for H^+ leakage across the inner mitochondrial membrane and the electrogenic cost of transport of glutamate via the malate–aspartate shuttle and pyruvate via the MCT. *Reproduced from Hertz et al. (2007), with permission of Nature Publishing Group.*

changes in Ca^{2+} levels that are evoked by altered functional activity.

In summary, the TCA cycle is a highly regulated "regenerative" process in which two carbons enter the cycle as acetyl CoA and two carbons are released as CO_2; there is no net gain or loss of carbon with each full turn of the cycle (Fig. 3.7). The carbon atoms entering the cycle corresponding to carbons 2 and 5 of glucose are lost on the second turn of the cycle, whereas carbons 1 and 6 of glucose are released on the third turn of the cycle. Note that transaminase exchange reactions at the α-ketoglutarate and oxaloacetate steps can transfer label from TCA cycle intermediates to the large glutamate and aspartate pools (Table 3.2). These reactions, along with glutamine synthetase in astrocytes and glutamate decarboxylase in neurons, delay release of labeled carbon atoms as CO_2. The total concentration of all TCA cycle intermediates is low, about 1.5 μmol g^{-1}, whereas the sum of glutamate + glutamine + aspartate + γ-aminobutyric acid (GABA) is about 21 μmol g^{-1} (Table 3.2). Thus, the turnover times of TCA cycle intermediates are low due to their low levels and high flux through the cycle. Under normal resting conditions, the overall rate of the cycle is twice that of glycolysis due to formation of two pyruvate molecules from each glucose. Incorporation of label from glucose into TCA cycle-derived amino acids is the basis for magnetic resonance spectroscopic analysis of metabolic fluxes in brain (Rothman et al., 2011) (see later, Fig. 3.17).

Electron transport chain and oxidative phosphorylation. Only one high-energy compound is formed per turn of

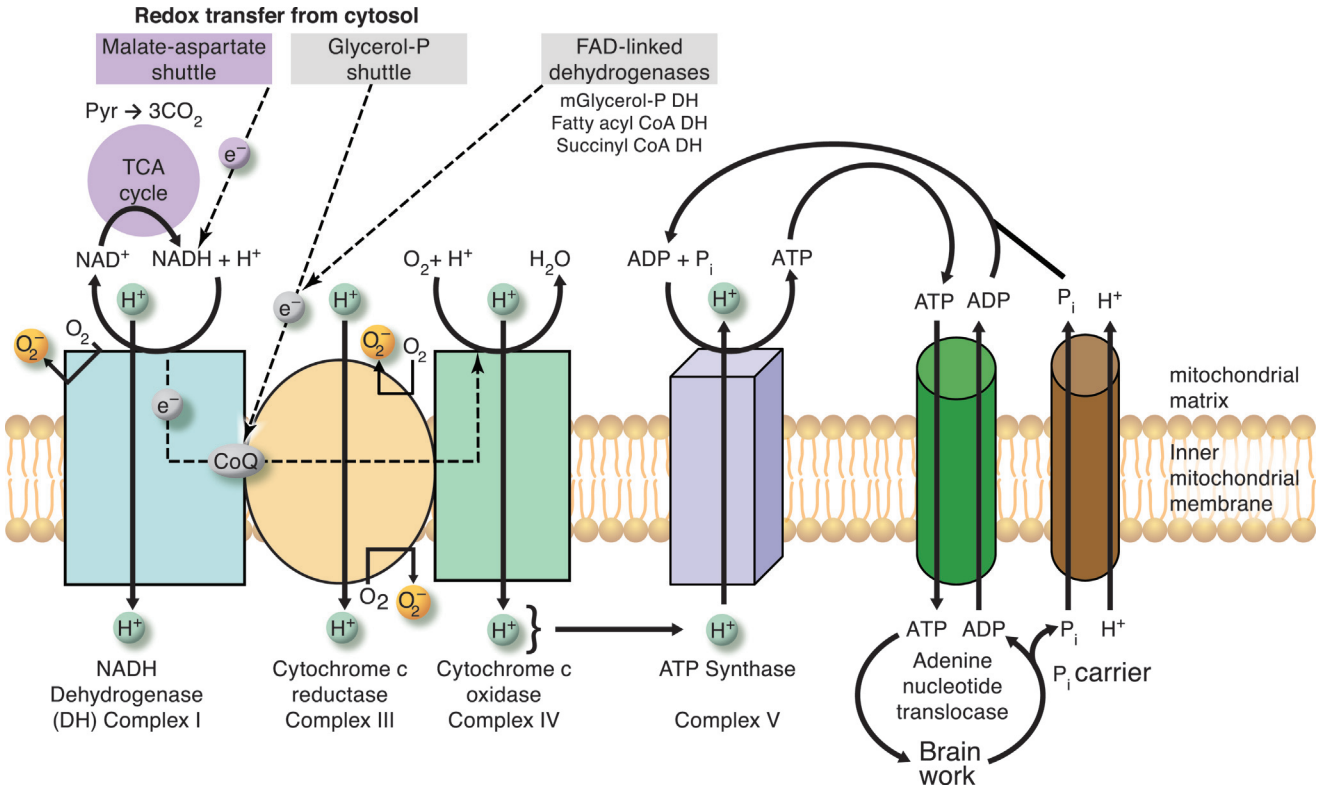

FIGURE 3.8 **Electron transport chain and oxidative phosphorylation.** NADH generated via the malate−aspartate shuttle and from the NAD-linked oxidative reactions in the TCA cycle enters the electron transport chain at Complex I, whereas the FAD-linked reactions enter at the Coenzyme Q (CoQ) step, with a lower net ATP yield. Translocation of H^+ from the mitochondrial matrix at three steps, Complex I, Complex III, and Complex IV, produces a proton gradient that is coupled to ATP synthesis by ATP synthase (Complex V). The adenine nucleotide translocase and phosphate carrier are necessary to transfer ADP and inorganic phosphate (P_i) into the mitochondrial matrix and transfer ATP from the matrix to cytoplasm. A continuous supply of ADP is necessary for maximal ATP synthesis. Respiration in the presence of ADP (state 3) is much higher than in the absence of ADP (state 4). *Adapted from Papa et al. (2007), with the kind permission of Springer Science and Business Media.*

the TCA cycle, i.e., the substrate-level phosphorylation of GDP to form GTP at the succinyl CoA synthetase step (Fig. 3.7). Most of the ATP generated via glucose oxidation reactions is recovered from oxidation of the three NADH and one $FADH_2$ generated per turn of the cycle. Electrons are transferred from NADH and $FADH_2$ to O_2, the terminal acceptor, via a series of enzyme complexes that constitute the electron transport chain. Protons are pumped from the mitochondrial matrix across the inner mitochondrial membrane to generate an electrochemical potential across the membrane; the proton gradient is used to drive ATP synthesis (Papa et al., 2007; Fig. 3.8). The NADH-linked dehydrogenase has a higher energy yield than FAD-linked dehydrogenases due to the additional protons pumped across the membrane by Complex I compared to Complex II (FAD-linked succinate dehydrogenase that delivers electrons to Coenzyme Q). The active state of respiration requires a continuous supply of oxygen, ADP, and P_i and the rate is much higher than the "resting" respiratory rate. If all of the cytoplasmic NADH is transferred to the electron transport chain by the malate−aspartate shuttle, an estimated 32 ATP are generated by the combined action of the TCA cycle, electron transport chain, and oxidative phosphorylation reactions (Fig. 3.7). This value is somewhat lower than early estimates of 36 ATP per glucose due to proton leakage across the mitochondrial membrane (Brand and Nicholls, 2011). Note that ADP is a required substrate for respiration, and generation of ADP from ATP by brain work provides the "catalytic link" (i.e., ATP turnover) between cellular activities and respiration because phosphorylation is coupled to oxidation.

Biosynthetic roles of the TCA cycle—generation of neurotransmitters. Glucose provides the carbon for synthesis of numerous compounds required for brain structure and function, and various biosynthetic reactions branch from the glycolytic pathway (Fig. 3.4), as well as in the TCA cycle (Fig. 3.9A). The TCA cycle-derived biosynthetic reactions directly link oxidative energy generation with neurotransmitter turnover in cholinergic and

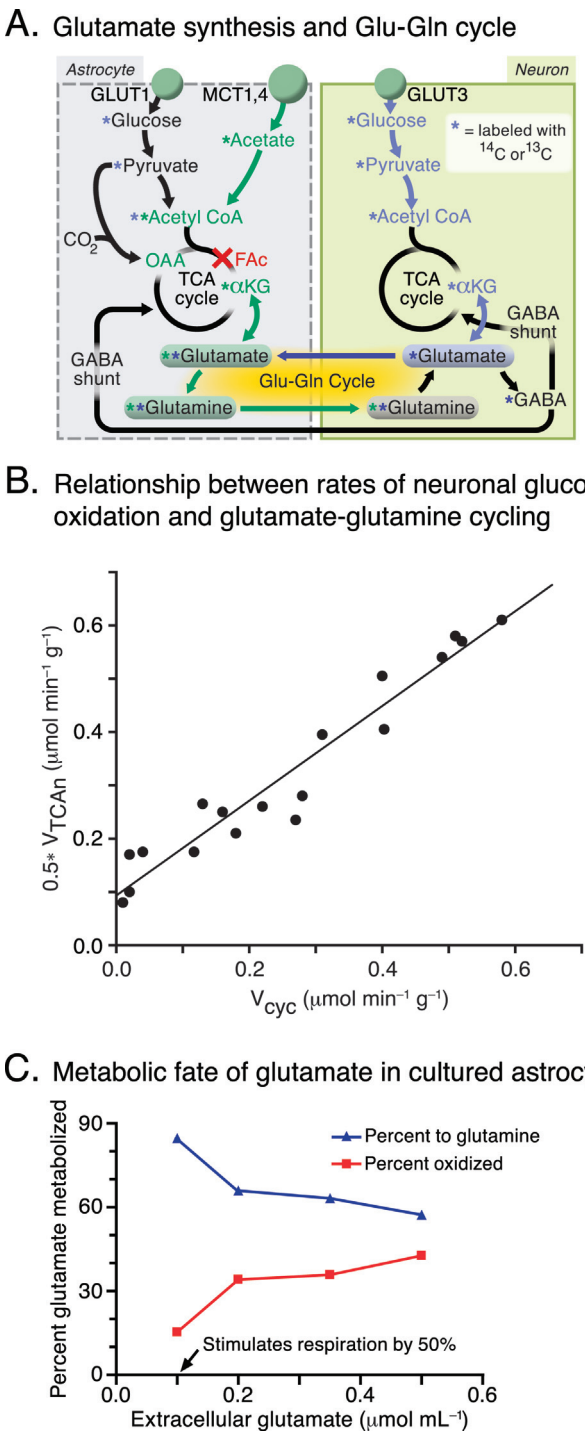

FIGURE 3.9 Anaplerotic reactions are required for net synthesis of glutamate, glutamine, and aspartate and for normal synaptic transmission. (A) Net synthesis of TCA cycle-derived amino acids requires the ATP-dependent CO_2 fixation reaction catalyzed by pyruvate carboxylase to generate oxaloacetate (OAA) from pyruvate. Condensation of the OAA with acetyl CoA from a second molecule of pyruvate forms a "new" molecule of citrate, a 6-carbon compound that, after decarboxylation, can generate a "new" molecule of glutamate, glutamine, aspartate, or GABA. Pyruvate carboxylase is located in astrocytes thereby conferring this cell type with the capacity for generation of important TCA cycle-derived amino acids within the brain. Because the astrocytic monocarboxylic acid transporters (MCTs) have a substrate specificity for transport of acetate, labeled acetate preferentially labels the glutamine pool in brain, whereas metabolic labeling by glucose preferentially labels the large glutamate pool that is located in neurons (see text and Fig. 3.17). When given at low doses, fluoroacetate (FAc), like acetate, is preferentially transported into astrocytes where it is metabolized via the TCA cycle to generate fluorocitrate, an inhibitor of aconitase that blocks the astrocytic TCA cycle by preventing conversion of citrate to isocitrate. The GABA shunt is the pathway by which GABA is returned to the TCA cycle following transamination to succinate semialdehyde and oxidation by succinate semialdehyde dehydrogenase; this can take place in neurons and astrocytes. See text for discussion of the glutamate (Glu)–glutamine (Gln) cycle between astrocytes and neurons. *Modified from Hertz et al. (2007), with permission of Nature Publishing Group.* (B) The rate of glucose oxidation in neurons ($0.5V_{TCAn}$) is approximately directly proportional to the rate of glutamate–glutamine cycling (V_{cyc}) or excitatory glutamatergic neurotransmission in rat cerebral cortex. Because two molecules of acetyl CoA are generated from each glucose, the rate of the tricarboxylic acid (TCA) cycle is twice that of total glycolytic glucose utilization (ignoring the flux into the pentose phosphate shunt pathway and lactate release), and the rate of glucose oxidation is half that of the TCA cycle. Neuronal glucose oxidation rate increases about 6-fold from the isoelectric state (flat EEG, $V_{cyc} = 0$) to the awake state, i.e., from $\sim 0.09\ \mu mol\ g^{-1}\ min^{-1}$ to $>0.6\ \mu mol\ g^{-1}\ min^{-1}$, respectively. *Reproduced from Rothman et al. (2011), with permission of John Wiley & Sons, Ltd. The figure was kindly provided by Douglas Rothman and Henk De Feyter, Department of Diagnostic Radiology, Magnetic Resonance Research Center, Yale University School of Medicine, New Haven, CT.* (C) Glutamate has two major metabolic fates, conversion to glutamine, which is exclusively an astrocytic process due to the cellular localization of glutamine synthetase in astrocytes, and oxidation via the TCA cycle after transamination or oxidative deamidation. Astrocytes metabolize glutamate by both pathways in a glutamate concentration-dependent manner; the higher the extracellular glutamate the smaller the fraction converted to glutamine and the greater the fraction oxidized via the TCA cycle *(plotted from data of McKenna et al., 1996); modified from Dienel and Cruz (2006), with permission from Elsevier.* The 50% stimulation of oxygen consumption by glutamate ($0.1\ \mu mol\ mL^{-1}$) in cultured astrocytes that can be blocked by ouabain (plotted from data from (Eriksson et al., 1995) is consistent with stimulation of glutamate oxidation and respiration to help dispose of excess glutamate and to generate ATP to fuel Na^+,K^+-ATPase activity. To completely oxidize glutamate to CO_2, a 4-carbon molecule, malate, must exit from the TCA cycle, then be converted to pyruvate, then re-enter the cycle. This process is called pyruvate re-cycling (see text) and is a consequence of the catalytic nature of the TCA cycle (Fig. 3.7)

amino acid transmitter pathways. For example, synthesis of acetylcholine from glucose requires the action of the mitochondrial pyruvate dehydrogenase in neurons; the acetyl CoA is transferred from mitochondria to the cytosol where choline and choline acetyltransferase are localized, but the pathways of the transfer process remain to be established (Joseph and Gibson, 2007). Synthesis of acetylcholine is closely linked to glucose metabolism, and, even though less than 1% of the glucose is used for synthesis of acetylcholine, the cholinergic pathway is especially sensitive to mild hypoglycemia and mild hypoxia, both of which are

associated with reduced acetylcholine turnover and decrements in acetylcholine levels (see later, Fig. 3.19).

The neuroactive amino acids are highly restricted from passage across the blood–brain barrier (Oldendorf and Szabo, 1976), yet their concentrations in brain are substantial (Table 3.2). The high brain-to-plasma concentration ratios for GABA (300), aspartate (300), glutamate (~150), and glutamine (10) (McIlwain and Bachelard, 1985) indicate considerable net synthesis of these amino acids within the brain. Because the TCA cycle cannot support net synthesis of 4- or 5-carbon compounds from acetyl CoA, another reaction, CO_2 fixation, is required to generate oxaloacetate that forms a "new" 4-carbon backbone from pyruvate. This anaplerotic reaction is carried out by pyruvate carboxylase and is predominantly localized in astrocytes (Yu et al., 1983; Shank et al., 1985). Thus, astrocytes carry out *de novo* synthesis of the molecules that are used as precursors for excitatory and inhibitory amino acid neurotransmitters (Fig. 3.9A). Oxaloacetate can undergo a transamination reaction to form a "new" molecule of aspartate, or it can condense with acetyl CoA derived from a second pyruvate to produce citrate, which continues through the TCA cycle to generate α-ketoglutarate. A transamination reaction "withdraws" this new 5-carbon compound from the TCA cycle as glutamate. In astrocytes, the glutamate is converted to glutamine by the action of glutamine synthetase, an astrocyte-specific, ATP-dependent enzyme (Martinez-Hernandez et al., 1977; Norenberg and Martinez-Hernandez, 1979). Glutamine can then be released to extracellular fluid and taken up by neurons, where it is converted to glutamate by glutaminase. The pyruvate carboxylase reaction consumes one ATP and is stimulated by K^+, which is taken up from the synaptic cleft by astrocytes during neuronal activation thereby linking the anaplerotic reactions and the astrocytic TCA cycle flux with neuronal signaling activity (Hertz et al., 2007). In vivo studies show that CO_2 fixation increases with brain activity (Öz et al., 2004). If all of the reducing equivalents produced from glucose are transferred to the electron transport chain via redox shuttle systems, then synthesis of glutamate from glucose is an energy-producing process, with a net yield of 11 ATP and consumption of 2 O_2. This yield contrasts with production of 32 ATP and consumption of 6 O_2 by complete oxidative metabolism of glucose. Under steady state conditions, glutamate level is constant, rates of *de novo* synthesis and oxidative degradation of glutamate are equal, and glutamate oxidation generates ATP.

Glutamate–glutamine cycle and GABA shunt. In excitatory neurons, the glutamate is packaged into synaptic vesicles, released as a neurotransmitter, taken up into astrocytes via sodium-dependent glutamate transporters, and either oxidized or converted to glutamine (see also Chapter 7). This cyclic process involving shuttling of glutamine and glutamate among astrocytes and neurons is called the *glutamate–glutamine cycle* (Fig. 3.9A). Glutamatergic signaling increases demand for ATP that is predominantly satisfied by oxidative metabolism, and the calculated rate of the TCA cycle in neurons is approximately proportional to the rate of cycling of glutamate and glutamine (Fig. 3.9B) under different conditions in animal and human brain (Rothman et al., 2011). When glutamate–glutamine cycling is zero (isoelectric EEG), there is still oxidative metabolism to support basal activities. Oxidative and Glu–Gln cycling rates rise in parallel with increasing level of consciousness from the deeply anesthetized to conscious resting state (Fig. 3.9B).

Glutamine is also a good precursor of GABA, an inhibitory neurotransmitter. Inhibitory neurons take up and convert glutamine to glutamate, which is then converted to GABA by glutamate decarboxylase (Fig. 3.9A). After its release to the synaptic cleft, GABA can be taken up by neurons and astrocytes, undergo a transamination reaction by GABA transaminase to generate succinate semialdehyde. Next, oxidation by succinate semialdehyde dehydrogenase forms succinate that is oxidized in the TCA cycle. Because the flux from α-ketoglutarate to glutamate to GABA to succinate bypasses some of the TCA cycle reactions, this pathway is referred to as the *GABA shunt* (Fig. 3.9A).

The gliotoxin fluoroacetate, when given in low doses, is preferentially transported via a monocarboxylic acid transporter (MCT) into astrocytes where it is metabolized by their TCA cycle to generate fluorocitrate, a potent inhibitor of aconitase (Fonnum et al., 1997) (Fig. 3.9A). Fluorocitrate blocks astrocytic TCA cycle flux, interferes with synaptic transmission, and reduces glial but not synaptosomal ATP levels (Keyser and Pellmar, 1994; Keyser and Pellmar, 1997). Blockade of the TCA cycle by fluoroacetate is circumvented by providing the downstream metabolite, isocitrate, that restores evoked potentials and ATP levels. These findings illustrate the importance of astrocytic oxidative metabolism for neuronal function. Note that glutamate cannot be synthesized *de novo* from glucose unless glucose-derived pyruvate enters the astrocytic TCA cycle by two pathways, pyruvate carboxylation to generate oxaloacetate and pyruvate dehydrogenase to generate acetyl CoA.

Glutamate oxidation vs. its conversion to glutamine. Glutamate released by excitatory neurons and taken up into astrocytes has two major fates, conversion to glutamine and oxidation via the TCA cycle. Fig. 3.9A illustrates cycling of one molecule between an astrocyte and neuron as glutamate and glutamine, but it is important to recognize that some of the glutamate is

oxidized after its uptake, some is converted to glutamine, and mixing of molecules in different cellular pools will occur due to diffusion of glutamine (and probably also glutamate) among astrocytes via gap junctional channels (Ball et al., 2007; Cruz et al., 2007; Gandhi et al., 2009). The higher the extracellular glutamate level the greater the fraction of glutamate oxidized, and, at 0.5 mM glutamate, cultured astrocytes metabolize similar proportions by these two pathways (McKenna et al., 1996; Fig. 3.9C). Glutamate concentrations in the synaptic cleft reach several millimolar (Bergles et al., 1999), suggesting that a significant fraction of the released glutamate may be oxidized during excitatory neurotransmission. The oxidized glutamate can be replaced by deamidation of glutamine, by *de novo* synthesis in astrocytes, and by diffusion of glutamine through interstitial fluid and through astrocytic gap junctional channels.

Extracellular glutamate (0.1 mM) stimulates respiration in cultured astrocytes by 50% (Fig. 3.9C) and this rise in oxygen consumption is blocked by ouabain, directly linking Na^+,K^+-ATPase activity to astrocytic oxidative metabolism (Eriksson et al., 1995). Extracellular glutamate also inhibits glucose utilization in cultured astrocytes (by 20% at 0.5 mM (Qu et al., 2001), and 50% at 1 mM (Swanson et al., 1990)), consistent with the oxidation of some glutamate by astrocytes to supply some of the ATP for Na^+ extrusion and glutamine synthesis after glutamate uptake from extracellular fluid (Peng et al., 2001). In support of this conclusion, later studies have shown that (i) astrocytic perisynaptic processes contain mitochondria (Lovatt et al., 2007; Lavialle et al., 2011; Pardo et al., 2011), and (ii) the astrocytic glutamate transporter, GLAST, forms macromolecular complexes with mitochondria, Na^+-K^+-ATPase, and glycolytic enzymes so that some of the glutamate taken up is oxidized (Genda et al., 2011; Bauer et al., 2012). Glutamate is continuously synthesized and degraded in astrocytes (Hertz et al., 2007; Hertz, 2011), but the amount of glutamate oxidized by perisynaptic processes during excitatory neurotransmission *in vivo* remains to be established. The notion of glutamate oxidation to support astrocytic energetics appears to contradict the observation that total glutamate levels actually increase somewhat during activation in rat (Dienel et al., 2002) and human (Mangia et al., 2007; Lin et al., 2012) brain, probably due to increased anaplerotic activity via the pyruvate carboxylase reaction (Öz et al., 2004). This apparent discordance may reflect a greater overall biosynthetic activity compared with localized oxidation of small quantities of transmitter glutamate in perisynaptic processes, i.e., compartmentation of the two processes in different regions of the astrocyte, i.e., soma and filopodia, respectively. For example, K^+ taken up by astrocytes stimulates pyruvate carboxylase activity (Kaufman and Driscoll, 1992). In addition, more widespread activation of the anaplerotic pathway throughout the astrocytic syncytium in association with K^+ uptake from extracellular space and gap junction-mediated spreading during synaptic signaling may exceed perisynaptic oxidation of glutamate. This is an exciting, emerging research area that will help clarify the energetics of neuron−astrocyte interactions.

The metabolic effects of glutamate on cultured astrocytes have been controversial for decades. Glutamate has been found to stimulate glucose utilization and lactate release in some astrocyte preparations (Pellerin and Magistretti, 1994; Takahashi et al., 1995), whereas other laboratories find unchanged or reduced glucose utilization and no rise in lactate production, indicating that glutamate-stimulated glycolysis is not a robust phenotype of all cultured astrocytes (Dienel and Cruz, 2004; Dienel and Cruz, 2006; Dienel, 2012a; Dienel, 2012b). The basis for these discrepant results remains to be established, but culture conditions and developmental plasticity influence astrocytic oxidative capability (Abe et al., 2006; Takahashi et al., 2012). To sum up, the quantitative contributions of different pathways that supply ATP to astrocytes and neurons during glutamate−glutamine cycling (e.g., glycolysis, glucose or lactate oxidation, glutamate oxidation, glycogenolysis) and the direction and magnitude of cell-to-cell lactate shuttling during brain activation are not yet established (see below, lactate shuttle). These important aspects of neuroenergetics are under active investigation (Dienel, 2013).

Pyruvate recycling. Glutamate, glutamine, GABA, and aspartate are continuously degraded via the TCA cycle after entry of the carbon skeleton into the cycle at the α-ketoglutarate, succinyl CoA, or oxaloacetate steps. However, the TCA cycle is a catalytic process and only two carbons are removed by decarboxylation reactions per turn of the cycle. Thus, oxidative metabolism of the 4-carbon backbone of these amino acids requires its exit from the cycle and re-entry of pyruvate into the TCA cycle followed by its oxidative metabolism, i.e., recycling of pyruvate carbon skeleton that was used for anaplerosis (Cerdan et al., 1990). Complete oxidative degradation of the amino acids occurs when malate leaves the mitochondria and undergoes oxidative decarboxylation by the cytosolic malic enzyme to produce NADPH, CO_2, and cytosolic pyruvate. Some of this pyruvate can be converted to lactate and released from the cell. Re-entry of pyruvate into mitochondria generates 3 CO_2 and results in a distinct labeling pattern of TCA cycle-derived amino acids that can be detected by ^{13}C-magnetic resonance spectroscopy. Complete oxidation of glutamate generates 20 ATP and consumes 4 O_2, and, in conjunction

with synthesis of glutamate from glucose, the net yield (31 ATP) of glutamate turnover (synthesis and degradation) is calculated to be similar to oxidation of glucose (32 ATP) (Hertz et al., 2007).

Oxidation of other compounds via the TCA cycle. A variety of compounds that are taken up from blood or turn over in brain are metabolized via the TCA cycle, including ketone bodies, fatty acids, and amino acids, but in adult brain these compounds are not important energy sources compared to glucose, which is continually supplied to brain from the blood. Suckling mammals have high capacity to oxidize the ketone bodies acetoacetate and β-hydroxybutyrate (in addition to glucose) due to high levels of monocarboxylic acid transporters at the blood–brain barrier and the necessary metabolic enzymes (e.g., β-hydroxybutyrate dehydrogenase); after weaning both transport of and metabolic capacity to use ketone bodies are markedly downregulated, but the transporters and oxidative enzymes can be induced by prolonged starvation (Cremer, 1982; Nehlig, 2004). Fatty acid oxidation is high in cultured astrocytes, whereas it is very low in cultured neurons (Edmond, 1992). Beta-oxidation of fatty acids generates acetyl CoA plus NADH, which feeds into the electron transport chain at complex I (Fig. 3.8), thereby producing ATP and consuming oxygen without generating equivalent amounts of CO_2. Complete oxidation of carbohydrates, such as glucose, consumes 6 O_2 and produces 6 CO_2, yielding a *respiratory quotient (ratio of CO_2 produced to O_2 consumed)* of one; the respiratory quotient for fatty acid and ketone body oxidation is less than one. Assays of arteriovenous differences across the brain for oxygen and CO_2 demonstrate that the respiratory quotient for brain is close to one, indicating that carbohydrate is the primary fuel for normal brain. Thus, fatty acids, amino acids, and ketone bodies taken up from blood into normal adult brain are not significant substrates for brain energy metabolism. However, during development or prolonged starvation ketone bodies are consumed in much higher amounts, and the respiratory quotient is less than one. During severe hypoglycemia endogenous compounds, including glycolytic and TCA cycle intermediates, amino acids (e.g., glutamate, glutamine, GABA, alanine), and lipids are oxidized to help maintain ATP levels until energy failure occurs (Siesjö, 1978). Consumption of brain constituents during severe, transient hypoglycemia implies that recovery will not be complete until normal levels of these compounds are restored.

Neutral amino acids are readily taken up into brain via amino acid carriers (Oldendorf and Szabo, 1976) and oxidized. The branched-chain essential amino acids (valine, isoleucine, leucine) have similar degradative pathways, involving transamination to form a keto acid, followed by oxidation reactions that feed into the TCA cycle at different points. Valine produces propionyl CoA which enters the TCA cycle at the succinyl CoA step after a CO_2 fixation reaction, and isoleucine generates acetyl CoA plus propionyl CoA. In contrast, degradation of leucine generates acetyl CoA plus acetoacetate. Due to their participation in transamination reactions, branched chain amino acids may serve as ammonia carriers in transcellular shuttle systems that are required to sustain the glutamate–glutamine cycle (Rothman et al., 2012).

Summary

Glucose carbon enters the energy and biosynthetic pathways via the hexokinase step, where phosphorylation traps the molecule in the cell where it was initially metabolized. The glycolytic pathway is regulated at three major sites—hexokinase, phosphofructokinase, and pyruvate kinase—and fluxes from the major branch point metabolites are tightly controlled. Glycogen turnover is governed by second messengers and phosphorylation reactions, and flux into the pentose shunt pathway governed mainly by NADP availability. Pyruvate dehydrogenase and key enzymes comprising the TCA cycle are regulated by [Ca^{2+}] and metabolites related to the energy status of the cell. Regulatory mechanisms have an "integrative" effect to coordinate and satisfy the overall demands for the cell for energy production, biosynthetic activity, and neurotransmitter turnover. Because glycolysis can be rapidly upregulated the lactate dehydrogenase reaction serves as a "release valve" by which pyruvate can be converted to lactate to regenerate NAD^+ so that glycolysis can continue. Because lactate formation and transport are equilibrative processes and because glucose is rarely limiting in normal brain, partial metabolism of glucose to lactate may be preferentially used to support specific processes, even though the energy yield is much lower than that of the TCA cycle and electron transport chain.

SUBSTRATES, ENZYMES, PATHWAY FLUXES, AND COMPARTMENTATION

The metabolic machinery of brain and its components are very heterogeneous in terms of distribution, composition, and capacity at the regional, cellular, and subcellular level. The *steady state concentration* of any metabolite, mRNA, or protein (Box 3.2, Table 3.2) is the net result of all processes that generate and remove the compound. Enzyme activity assayed *in vitro* under optimal conditions represents the *capacity* for catalytic activity (i.e., *enzyme activity* is proportional to *enzyme*

amount, Box 3.2), but activities of many enzymes are generally in great excess of the *in vivo* fluxes through the steps catalyzed by the enzymes (McIlwain and Bachelard, 1985). For example, the *in vitro* activities of many glycolytic and TCA cycle enzymes exceed *in vivo* glucose utilization rate by 10–100-fold, whereas others are present in lower amounts; energy demand and regulatory processes govern actual flux rates. Excess capacity is extremely important so that metabolic fluxes can change according to local demand, and are not limited by enzyme amount. Immunohistochemical staining of enzymes and transporters provides a representation of the detectable amounts of these proteins and their locations, but not their actual activities in living brain. Thus, determination of *concentrations*, *amounts*, or *in vitro activities* of biological compounds represents a *"static" description* of brain function, indicative of capacity. On the other hand, assays of *in vivo fluxes* or *pathway rates* under different conditions represent *dynamic activities* of cells. Thus, changes in amount with development, aging, and disease reflect altered capacity but do not necessarily indicate changes in flux or the actual magnitude of flux changes. There are many examples in which enzyme amounts are reduced by 90% or more under pathophysiological conditions, with no adverse physiological effects; conversely increasing enzyme amounts may, but need not, be reflected by altered rates due to metabolic regulation of key steps in the pathways (Fell, 1996). However, if the catalyzed process is substrate concentration-driven, increased capacity can reflect proportionate changes in flux, depending on the substrate level in the system of interest. For example, changes in enzyme or transporter level will reflect differences in reaction or transport rate if the enzyme or transporter is not saturated, but not if the substrate level is well above the K_m. Thus, it is essential to understand the relationships among concentrations, activities, and fluxes, particularly under pathophysiological conditions when levels of biomarkers are frequently used as diagnostic indicators. Elucidation of function–metabolism relationships has been driven by technological advances to assay processes of interest *in vitro* and *in vivo*.

Metabolite Concentrations: Net Result of Fluxes to and from the Metabolite Pool

Oliver Lowry's laboratory pioneered the field of "enzyme histochemistry" and metabolite analysis by (i) devising precise, sensitive, and quantitative microanalytical techniques with which the maximal activities of as many as nine enzymes and many metabolites could be measured in an extract of a single dissected neuron, (ii) developing quantitative fluorescent assays and cycling reactions that enabled accurate determination of 10^{-15} to 10^{-17} moles of specific compounds, and (iii) evaluating changes in metabolic flux from changes in metabolite levels in a "closed system" under different experimental conditions (Lowry, 1990; Passonneau and Lowry, 1993). These studies showed that many compounds of interest are very *labile* (Box 3.2) because they are consumed within seconds of the initial postmortem ischemic interval (Lowry et al., 1964; see following later, Fig. 3.21). Thus, inadequate procedures to inactivate enzymes yield low levels for glycogen, glucose, glycolytic and TCA cycle intermediates, and high energy phosphates. Advances in analysis of labile metabolites required development of techniques to quickly stop metabolism, e.g., freeze-blowing (Veech et al., 1973), funnel-freezing (Ponten et al., 1973), and microwave fixation (Stavinoha et al., 1973; Medina et al., 1975) as well as appropriate procedures for tissue extraction and animal handling. Because metabolism is closely integrated with neurotransmitter activity, changes with behavioral state, sensory stimulation, stress due to handling, placement in an apparatus for tissue sampling, anesthesia, and other factors can substantially influence the concentrations of metabolites of interest. For example, glycogenolysis can be stimulated by activation of β-adrenergic receptors on astrocytes and the adrenergic innervation of the brain from the locus coeruleus, a structure involved in attention and orienting responses, is extensive. Stimuli that disrupt ongoing behavior or activity and generate reorienting behavior elicit strong responses from locus coeruleus neurons and activation of this pathway may reduce glycogen levels throughout the brain. Also, glycogen phosphorylase is quickly activated in response to postmortem ischemia, even during decapitation and freezing in liquid nitrogen. Slow inactivation of enzymes in frozen tissue powders during extraction can lead to substantial loss of glycogen and other compounds, with increases in the level of lactate (Cruz and Dienel, 2002). Thus, metabolic activity in situ (pre- and postmortem) and *in vitro* can affect the measured levels of labile metabolites and signaling compounds. Interpretation of results needs to take into account the physiological and biochemical procedures employed with tissue sampling.

Enzyme Levels: Metabolic Capacity or Potential

Maximal activity (V_{max}) of an enzyme assayed under optimal conditions *in vitro* is proportional to enzyme amount and therefore reflects catalytic capacity or potential. The maximal activities of enzymes in the glycolytic and oxidative pathways of glucose metabolism assayed *in vitro* are generally much higher

than the overall *in vivo* rate of brain glucose utilization (i.e., $\sim 0.7\ \mu mol\ g^{-1}\ min^{-1}$), indicating that *metabolic capacities* of the enzymes (Box 3.2) greatly exceed the usual fluxes through the steps they catalyze. For example, only about 5% of the maximal hexokinase activity is sufficient to sustain the overall resting rate of glucose utilization in brain *in vivo*; the enzyme is inhibited by about 95% by glucose-6-phosphate, and this inhibition is relieved by activation of downstream fluxes, i.e., at the phosphofructokinase step (Lowry and Passonneau, 1964; Lowry et al., 1964). Thus, the brain has a large reserve to meet demands of extreme conditions that is evident during bicuculline-induced seizures where glucose and oxygen utilization rates increase 2–4-fold (Siesjö, 1978). Relative amounts of enzymes in different brain structures, cells, and subcellular organelles are often assessed by immunological and histochemical assays in tissue slices and Western blots; these types of assays report the relative capacity of an enzyme to carry out its function, but do not describe the actual rates catalyzed by the enzyme in the living tissue. Nevertheless, enzyme assays are very useful to identify compensatory responses to altered physiological demand and abnormal conditions, as well as the processes that regulate pathways and their interactions.

The large excess capacity of glycolytic compared to TCA cycle enzymes suggests that substantial decrements in the anaerobic metabolic capacity are less likely to have an impact on normal metabolic fluxes than deficits in mitochondrial enzymes, which correlate with deficits in energy metabolism, biosynthetic activity, and cognition in disease states (Gibson and Shi, 2010). In human and rodent brain, the maximal activity of the α-ketoglutarate dehydrogenase complex is one of the lowest of the enzymes of energy metabolism in brain and it is considered to be one of the especially vulnerable enzymes. This enzyme complex is particularly sensitive to damage by reactive oxygen species (ROS), and deficiencies in its activity occur in many neurodegenerative diseases, including Alzheimer's disease (Gibson et al., 2010).

Levels of Metabolites vs. Pathway Fluxes: Magnitude or Direction of Change

Substrates of the enzymes in the major energy-producing pathways are present in low concentrations, and, with the exception of glycogen, there is no significant energy reserve in brain (Table 3.2). Although substrate concentrations can change during different physiological states, they need not reflect the magnitude or direction of change in pathway fluxes. In fact, large flux changes can occur while metabolite levels are relatively constant or change in directions that, in the absence of sufficient information about the system, appear to contradict the flux change. For example, sensory stimulation of the normal awake rat by brushing of the body and whiskers causes arterial plasma glucose and lactate levels to rise because the animals move around in response to the brushing (Table 3.1). Brain glucose levels at the end of a 10-min stimulation interval rise in proportion to that in plasma (as expected from equilibrative transport), demonstrating that glucose influx across the blood–brain barrier matched the overall increase in metabolic demand during brain activation (Dienel et al., 2007a). Whisker stimulation also increased local rates of glucose utilization (CMR_{glc}) in the somatosensory cortex by about 30%, and brain tissue lactate level rose two-fold, from about 1 to 2 $\mu mol\ g^{-1}$ (Fig. 3.10). Although the *percentage increase* in lactate concentration is *high*, the *net change* (1 $\mu mol\ g^{-1}$) in the *quantity* of glucose-derived carbon in the enlarged lactate pool is *small*, corresponding to *<5% of the flux* from glucose to pyruvate

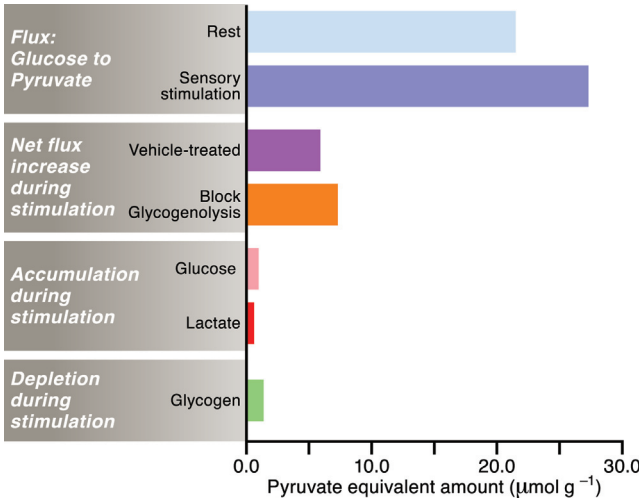

FIGURE 3.10 **Metabolite concentrations do not provide information about pathway flux.** The amount of glucose converted to pyruvate during rest and generalized sensory stimulation of the conscious rat was calculated from *in vivo* assays of the rate of glucose utilization and expressed in pyruvate equivalents (2 pyruvate = 1 glucose or 1 glucosyl unit of glycogen). The net increase in pyruvate formed in somatosensory (whisker barrel) cortex was enhanced by prior inhibition of glycogenolysis, indicating a role for rapid glycogen turnover *in vivo* during sensory stimulation of normal, normoglycemic rats. Because rats moved during stimulation (gentle brushing of the body and whiskers), the plasma glucose and lactate levels rose; the increase in brain glucose concentration was in proportion to that in plasma. Although brain lactate level doubled, the net increase was a tiny fraction of the glucose consumed during the same time interval. Lactate accumulation was also considerably smaller than net depletion of brain glycogen. Thus, the changes in brain glucose and lactate concentration do not reflect the magnitude or direction of the change in rate of glucose utilization during sensory stimulation. *Plotted from data of Dienel et al. (2007a).*

during the stimulus interval (Fig. 3.10). The sensory stimulation procedure also caused net consumption of glycogen even though overall brain glucose levels were normal, consistent with a role of glycogen in normal physiological activity, not just as an emergency energy reserve (Fig. 3.10). An intriguing finding was that inhibition of glycogenolysis prior to and during the whisker stimulation increased glucose utilization by an additional 25–50% in sensory and parietal cortex, suggesting that as much as half of the additional glucose consumed in somatosensory cortex is involved in glycogen turnover in astrocytes (Dienel et al., 2007a).

In the studies described previously, the net increase in lactate concentration was much smaller than the stimulus-increased rise in pyruvate formation, the net consumption of glycogen, and the net rise in glucose utilization evoked by glycogenolysis blockade (Fig. 3.10). If only glucose and lactate concentrations were measured, one might incorrectly conclude that glucose utilization was reduced causing brain glucose levels to rise, and that the tissue became "glycolytic," even though there was only a very small net change in lactate level that could arise from various pathways. *Changes in tissue concentration do not identify the origin or fate of the metabolite*, and lactate level might be explained by contributions from the rise in plasma lactate, increased glycogenolysis, and perhaps a rise in pyruvate level that is reflected by higher lactate level due to mass action and the lactate dehydrogenase equilibrium. Comparisons of *percentage changes* in levels of different metabolites (e.g., lactate and glucose) *can also be very misleading* because percentages do not account for the actual concentration differences or the fluxes through the metabolite pools (see Tables 7 and 8 in Dienel, 2012a, and related discussion). As emphasized by Veech (1980), changes in levels of specific glycolytic and TCA cycle intermediates cannot, except under unusual circumstances, be equated with changes in flux through the pathway; it is necessary to consider contributions of many conditions that affect the level of the metabolite.

The combination of tissue low levels of metabolic intermediates and high glucose utilization rate means that there must be fast turnover of the glycolytic and TCA cycle intermediates. In the simplest case, using the mean overall rate of glucose utilization of 0.7 μmol g^{-1} min^{-1} (Table 3.1) and the tissue concentration of a hypothetical intermediate of 0.1 μmol g^{-1} (compare to Table 3.2) the *turnover time* (Box 3.2) can be estimated by dividing the metabolite concentration by pathway flux rate, or 0.1/0.7 = 0.14 min or 8 s. Note that a triose (a 3-carbon intermediate in the glycolytic pathway), NADH, or TCA cycle metabolite with a concentration of 0.1 μmol g^{-1} would have a turnover time of 4 s because two triose and two acetyl CoA molecules are generated from each glucose. *Turnover of pools* or molecules is often expressed as *half time or half life*, the time required for half of the pool to be replaced (Box 3.2).

Under steady-state conditions the concentrations of all metabolites in a pathway are constant and the rate of each step in the pathway is equal to the flux through the entire pathway. In contrast, under non-steady-state conditions, part of the flux may be used to establish new levels of intermediates by pool filling or depletion. Steady state is critical for the conduct of *in vivo* metabolic assays to measure fluxes because the steady state assumption enables simpler solutions of rate equations, i.e., rates of change of levels of metabolic intermediates can be set equal to zero. The high flux and low pool size also facilitate rapid changes in the concentrations of the various pathway intermediates compared to the large pools of amino acids; the shorter the half-life, the faster the rate of change to the new level (Riggs, 1970). Labeling of the large TCA cycle amino acid pools with radioactive or stable isotopes is used to calculate rates of oxidative metabolism and trafficking of intermediates between different metabolic pools located in different cell types, as for example cycling of glutamate and glutamine between neurons and astrocytes (Rodrigues and Cerdan, 2007; Rothman et al., 2011; Fig. 3.9).

Heterogeneity and Compartmentation: Glutamate Metabolism as an Illustrative Example

Mitochondrial heterogeneity. Isolation of crude mitochondrial fractions in the late 1960s by the Whittaker and De Robertis laboratories provided a means to separate "free" mitochondria (derived from the soma of all brain cells) from synaptosomes, which are pinched-off nerve endings that contain cytosol and mitochondria. Ultracentrifugation studies using continuous and discontinuous gradients to separate mitochondria in conjunction with analysis of their enzyme composition and substrate-supported respiration clearly demonstrated differences between synaptic and nonsynaptic mitochondria, among synaptic mitochondria, and among mitochondria isolated from different brain regions (Clark and Lai, 1989; Lai and Clark, 1989). In addition to the biochemical and functional heterogeneity of mitochondria, these organelles also differ morphologically as well as functionally, and their subcellular localization involves specialized binding to the cytoskeletal network (Perkins and Ellisman, 2007; Dubinsky, 2009; Perkins et al., 2010; Keil et al., 2011). Mitochondrial functions differ during development,

with preferential expression of specific mitochondrial enzymes compared with mature brain. For example, β-hydroxybutyrate dehydrogenase activity peaks prior to weaning when ketone bodies are an important brain fuel, and it falls rapidly thereafter (along with the monocarboxylic acid transporter levels in the brain's vasculature), whereas other metabolic enzyme activities rise during maturation (Leong and Clark, 1984b; Leong and Clark, 1984a).

Radiolabeling studies identify "large and small" glutamate pools. Brain metabolism studies during the 1960s and 1970s examined the fate of radiolabeled substrates and developed the concept of metabolic compartmentation involving at least two different functional TCA cycles in brain that do not directly communicate with each other (see monographs Balázs and Cremer, 1972; Berl et al., 1975). Metabolic compartmentation was first firmly established for glutamate metabolism on the basis of differences in labeling of glutamate and glutamine from various labeled precursors. In brief, when [^{14}C]glucose was injected intravenously or intraperitoneally and brain amino acids purified and counted to determine their extent of ^{14}C-labeling, the *specific activity* (Box 3.3) of glutamate was higher than the specific activity of its product, glutamine (Fig. 3.9A). This is the expected *precursor–product relationship* because the ^{14}C derived from tracer amounts of [^{14}C]glucose sequentially traverses the glycolytic and TCA cycle pathways, then enters the glutamate pool and finally the glutamine pool. The label is continuously diluted with unlabeled carbon as it flows into successive metabolic pools, and the specific activity of the true precursor is always higher than that of the product.

On the other hand, when [^{14}C]acetate was used as the precursor, the specific activity of glutamine was unexpectedly higher than that of its obligatory precursor. This finding was explained by the existence of two "independent" TCA cycles, one associated with a "large" glutamate pool that is predominantly labeled by glucose, the other associated with a "small" glutamate pool, the true precursor for glutamine, that is preferentially labeled by acetate and other compounds. The large and small glutamate pools are segregated *in vivo*, but when the tissue is homogenized and amino acids are extracted, all of the labeled and unlabeled glutamate in the various tissue pools is combined, thereby reducing the apparent specific activity of the true glutamate precursor pool for glutamine; this pool would, in fact, have a higher specific activity than glutamine *in vivo*. Subsequent studies in many laboratories using different experimental approaches clearly demonstrated that the "small" glutamate pool is located in astrocytes and the "large" pool is neuronal. Note that glucose is also oxidized in astrocytes but trapping of the label is achieved by dilution in glutamate, which is mainly neuronal. The basis for the preferential uptake of acetate into astrocytes was found to be transport (Waniewski and Martin, 1998), and acetate and its toxic analog, fluoroacetate, are important tools to study oxidative and biosynthetic metabolism in astrocytes, glutamate–glutamine cycling, and astrocyte–neuron interactions.

Biosynthetic capability and ammonia detoxification. Studies of cellular specialization have revealed high enrichment or exclusive localization of specific enzymes in different cell types in brain, as would be expected with the specialized functions of the major classes of brain cells (Wiesinger, 1995). Neurons are endowed with the capability to synthesize and package various neurotransmitters, including acetylcholine from glucose. Phosphate-activated glutaminase is also enriched in neurons, serving to convert glutamine derived from astrocytes into glutamate prior to its entry into the neurotransmitter pool. Inhibitory neurons contain glutamate decarboxylase for the synthesis of GABA from glutamate. Astrocytes are highly enriched in the capability to synthesize the neuromodulator D-serine from glucose (Fig. 3.4), as well as the capability for *de novo* synthesis of glutamate and aspartate (Fig. 3.9) due to their enrichment with pyruvate carboxylase. Glutamine synthetase also enables astrocytes to detoxify ammonia entering brain from blood by conversion of glutamate to glutamine (Cooper and Plum, 1987; Cooper, 2012). Ammonia and ammonium ion are rapidly interchangeable, and free ammonia readily diffuses across lipid membranes into brain. In patients with liver disease, removal of ammonia produced by gut bacteria by the liver is severely impaired and blood ammonia levels rise, contributing to the progression of hepatic encephalopathy which is characterized, in part, by very high brain glutamine levels (Butterworth, 2006). In addition to inhibitors of reactions in the glutamate–glutamine and TCA cycles, methionine sulfoximine, an inhibitor of glutamine synthetase, is an important tool for studies of astrocyte–neuron interactions (Sonnewald et al., 2007).

Summary

The brain is a complex, heterogeneous organ that is very difficult to study due to cellular and subcellular specialization of major functions and metabolic activities. Early studies of brain function and metabolism relied on global methods (e.g., arteriovenous differences and CBF), and these approaches provided valuable information by identifying glucose and oxygen as the major brain fuel, compounds that enter brain from blood, and metabolites released from brain. However, changes in local rates of functional activity are not

detectable unless high-resolution methods are used. Microanalytical and cell culture methods enabled analysis of the composition and capabilities of different cell types *in vivo* and *in vitro*, and radiolabeling studies set the stage for development of *in vivo* methods to study brain function in living subjects. Magnetic resonance spectroscopy and use of stable isotopes facilitate dynamic *in vivo* studies of transport and metabolism of specific carbon atoms via different pathways. Glutamate metabolism is an important, instructive example of complexities of compartmentation of functional metabolism and integration of neurotransmitter turnover with generation of energy.

IMAGING OF FUNCTIONAL METABOLIC ACTIVITY IN LIVING BRAIN AND IN VIVO ASSAYS OF PATHWAY FLUXES

Functional activity in brain involves electrical and molecular events that transmit signals from cell to cell within specific networks and anatomical pathways. The current understanding of functional metabolism in brain has been advanced by development of quantitative local methods to measure blood flow, blood oxygen levels, oxygen consumption, glucose utilization, the fate of specific atoms in labeled precursors, and metabolite levels. Noninvasive technologies employing different approaches (nuclear, optical, magnetic resonance, fluorescence, thermal, and acoustic imaging) and various tracers (inert gases, radiolabeled compounds, compounds labeled with stable isotopes, voltage-sensitive dyes, bioluminescence, and endogenous compounds) have been particularly important for a wide variety of *in vivo* brain imaging studies of molecular, metabolic, physiologic, and cognitive processes in normal and disease states (Dienel, 2006).

Determination of Local Rates of Blood Flow and Metabolism in Brain

Blood flow. Quantitative autoradiographic determination of local rates of blood flow and glucose utilization using *radioactive tracers* (Box 3.3) provided high sensitivity and appropriate spatial resolution to measure flow and metabolism in all brain regions. Kety and colleagues (Landau et al., 1955), used a radioactive gas, trifluoromethane, to establish activity-dependent changes in blood flow in the cat, and Sokoloff's group developed the use of a less volatile tracer with high blood–brain barrier permeability (Sakurada et al., 1978). In brief, the experimental procedure involves a pulse intravenous injection of the tracer, collection of timed samples of arterial blood from which the *time-activity integral* (i.e., the area under the curve; Box 3.3) in blood is calculated, the brain tissue is sampled, cut into thin sections, exposed to x-ray film along with calibrated radioactivity standards, local optical densities measured and converted to tissue concentration by use of the standard curve for that film, then blood flow rates are calculated. Blood flow assays measuring unidirectional uptake of a labeled tracer must be of short duration to prevent efflux of significant amounts tracer from tissue to blood during the assay interval, and the tracer must have high lipid permeability so that its accumulation in brain tissue is blood flow-dependent. The advantage of these *in vivo* procedures is that the tracers label all regions of the brain simultaneously and assay of local tissue levels of the tracer enables comparisons between activated and nonactivated pathways in the same brain. Development of the use of calibrated ^{14}C standards along with each x-ray film by Sokoloff and colleagues transformed qualitative pictures and relative changes (e.g., structures of interest normalized to one other structure) to fully quantitative autoradiographic assays, a procedure that had a high impact on many fields that used autoradiographic detection methods. Blood flow is often used to identify activated brain structures, particularly in brief experiments, but blood flow and the oxygen content of blood in the brain's microvasculature are not measures of metabolism, and flow and metabolism do not always change proportionately. Dynamic, calibrated functional magnetic resonance imaging (fMRI) takes advantage of changes in the magnetic resonance signal of deoxyhemoglobin (i.e., the blood oxygen level dependent (BOLD) fMRI signals (Ogawa et al., 1990; Kim and Ogawa, 2012)), and, in combination with modeling, can be used to calculate changes in oxygen utilization during brain activation (Buxton, 2010; Hyder et al., 2010; Buxton, 2012).

Glucose utilization—radiotracer techniques. Early studies of glucose utilization rates in brain *in vivo* used labeled glucose as a precursor but were limited by the loss of labeled products at various stages of metabolism of glucose at rates that vary with the position of the label and the state of the subject. For example, label is released from the one position via the pentose phosphate shunt pathway, from carbons 3 and 4 at the pyruvate dehydrogenase step, from positions 2 and 5 during the second turn of the TCA cycle, and from positions 1 and 6 during the third turn of the TCA cycle; label is also lost when lactate is released from brain (Fig. 3.11). Due to difficulties associated with complete accounting of precursor and products of labeled glucose in brain *in vivo*, radiolabeled glucose has been most useful for assessment of specific aspects of glucose transport and metabolism *in vitro* using cultured cells, brain slices, and preparations of whole

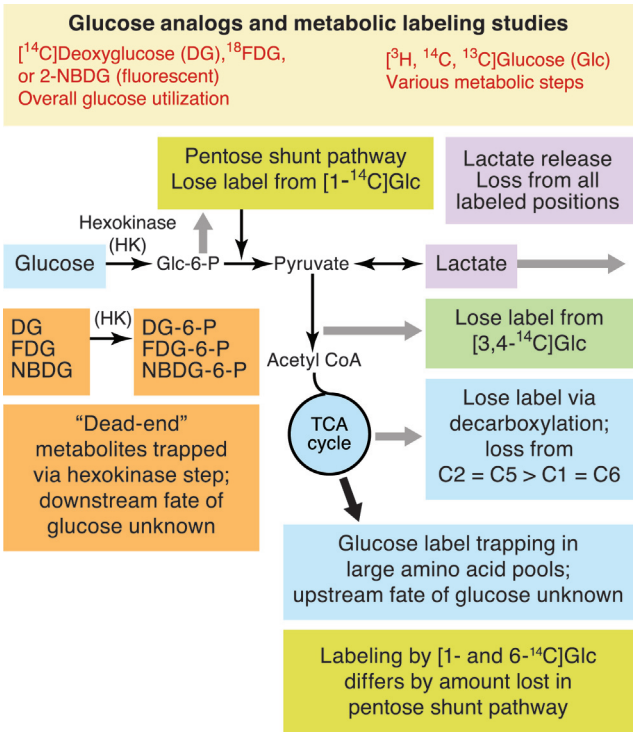

FIGURE 3.11 **Metabolic imaging and spectroscopy using labeled glucose and its analogs.** Various steps of glucose metabolism can be measured in different preparations by using differentially labeled glucose; these assays can take advantage of loss of label from glucose at different steps, and overall glucose utilization assays must account for label loss. In contrast, the glucose analogs 2-deoxy-D-glucose (DG) and 2-fluoro-2-deoxy-D-glucose (FDG) compete with glucose for transport and for metabolism by hexokinase. Their major metabolites, DG-6-P and FDG-6-P, respectively, are trapped intracellularly; hexokinase activity and glucose utilization rates can be calculated from labeled product accumulation (see text and (Sokoloff et al., 1977)). 2-NBDG is a fluorescent derivative of DG that is phosphorylated by hexokinase and trapped as 2-NBDG-6-P. 6-NBDG is a non-metabolizable fluorescent analog that would behave like methylglucose and track glucose concentration. However the kinetic properties of NBDG competition with glucose for transport and phosphorylation are not sufficiently well established for its use in quantitative assays of glucose utilization or comparative rates in different cell types. *Modified from Dienel and Cruz (2008), with permission of Wiley-Blackwell Publishers.*

homogenates and subcellular fractions derived from brain. As discussed below, determination of rates of incorporation of ^{13}C from [^{13}C]glucose into amino acids is used to calculate rates of oxidative metabolism of glucose in animal and human brain.

A major advance in metabolic assays was development of the use of 2-deoxy-D-[^{14}C]glucose (DG), a glucose analog, as a tracer to determine local rates of glucose utilization in brain *in vivo* (Sokoloff et al., 1977). Sokoloff recognized that because (i) DG competes with glucose for transport across the blood–brain barrier and into brain cells and for phosphorylation by hexokinase and (ii) DG is not metabolized via glycolysis beyond the hexokinase step (i.e., it is a "dead-end" metabolite, Fig. 3.11), [^{14}C]DG can be given in *tracer doses* (Box 3.3) and used to measure a single reaction, the hexokinase step, in all regions of the living brain simultaneously (Figs. 3.11 and 3.12). Based on the kinetic differences between glucose and DG for transport and phosphorylation, approximately two molecules of glucose are phosphorylated for each molecule of [^{14}C]DG phosphorylated. Thus, [^{14}C]DG-6-P (and its derivatives—there is some incorporation into other phosphorylated compounds and macromolecules) is trapped in the cells where it is phosphorylated and quantitatively retained for a reasonable amount of time (30–60 min). Accumulation of labeled products of [^{14}C]DG serves as a "meter" to register the amount of glucose consumed at a local level.

Shortly after development of the autoradiographic [^{14}C]DG method, the procedure was extended for use in human and primate brain by synthesis of a positron-emitting analog [^{18}F]2-fluoro-2-deoxy-D-glucose ([^{18}F]FDG) (Phelps et al., 1979). This tracer has had broad application in positron emission tomographic (PET) studies of brain, particularly in metabolic studies of the progression and efficacy of treatment of human neurodegenerative diseases. [^{18}F]FDG is also widely used for detection and localization of brain tumors, as well as tumors throughout the body, which are readily detected as metabolic "hot spots" due to their high glycolytic metabolism compared to surrounding normal tissue. Interested readers are referred to reviews by Sokoloff (Sokoloff, 1986; Sokoloff, 1996a) for details of the DG method and its broad application to many fields, including physiology, pharmacology, cognition, psychology, behavior, and pathophysiology and to the autobiographical perspectives of Seymour Kety (Kety, 1996) and Louis Sokoloff (Sokoloff, 1996b). Since these pioneering studies that devised local quantitative methods to measure blood flow and glucose utilization, a wide variety of compounds labeled with positron-emitting isotopes have been developed for *in vivo* studies of gene expression, protein, phospholipid, and neurotransmitter turnover, receptor assays, transporters, and other processes (see monographs: Phelps et al., 1986; Phelps, 2004).

Tracking of carbon atoms through metabolic pathways—stable isotopes and magnetic resonance spectroscopy. Assays of the hexokinase step with deoxyglucose quantify the amount of glucose consumed by brain but do not provide any information regarding the downstream fate of glucose carbon (Figs. 3.11 and 3.12). The complexities of compartmentation of metabolism were established by tracer labeling studies using ^{14}C- and

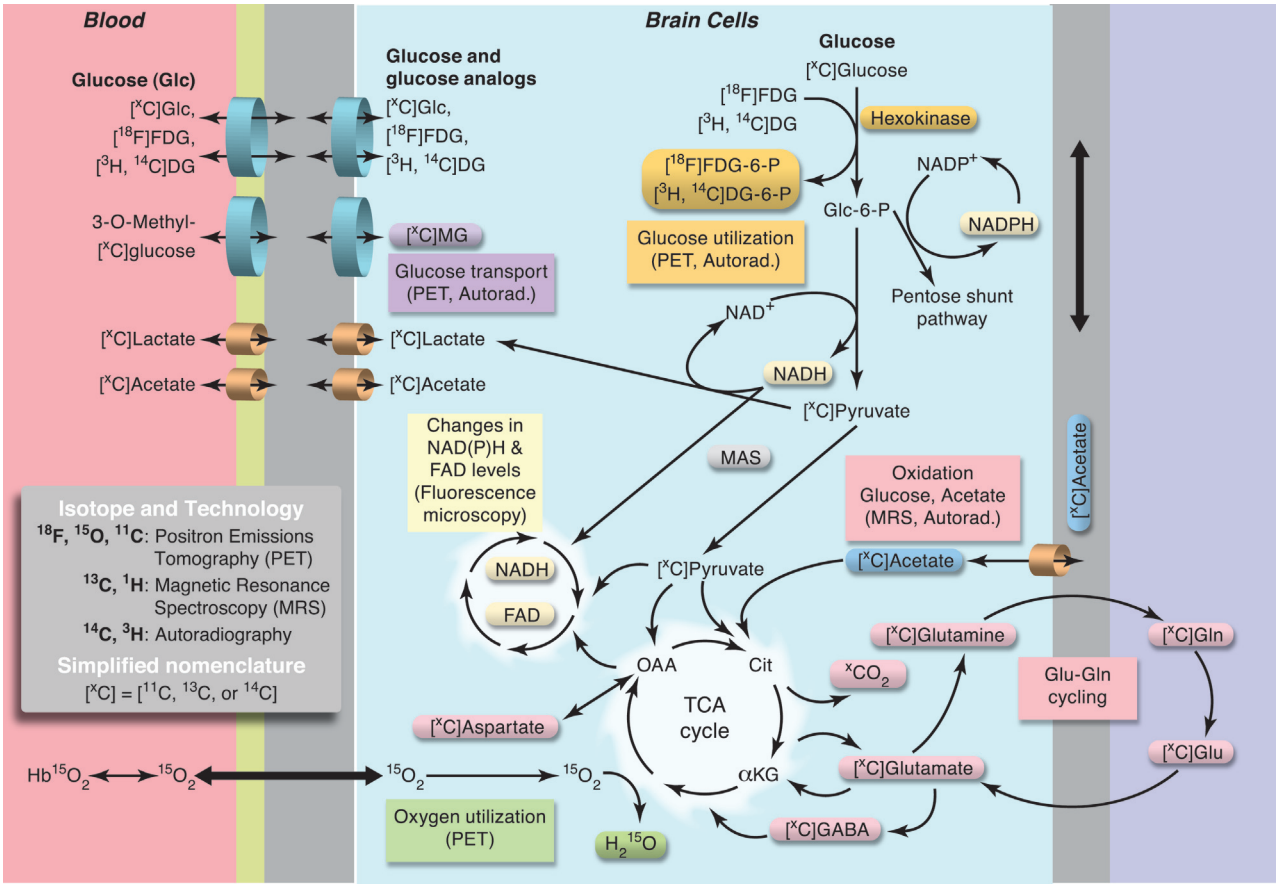

FIGURE 3.12 **Metabolic brain imaging and spectroscopic assays take advantage of transport and metabolism of specific labeled precursors.** By use of appropriate precursors labeled with beta- or positron-emitting radioactive or stable isotopes (see Box 3.3), transport, hexokinase activity, pentose phosphate shunt activity, glycolytic and oxidative metabolism, and redox state can be assayed in living brain under various experimental conditions using different technologies, positron emission tomography (PET), magnetic resonance spectroscopy (MRS), autoradiography (Autorad.), and fluorescence microscopy. For example, the nonmetabolizable glucose analog, methylglucose, is used to assay blood–brain barrier and cellular membrane transport and the steady-state glucose concentration. The glucose analogs DG and FDG are used to assay hexokinase activity and calculate glucose utilization rates. Glucose, lactate, and acetate labeled with radioactive or stable isotopes are used to assess rates of oxidative pathways in neurons and astrocytes, decarboxylation reactions (e.g., pentose shunt or pyruvate dehydrogenase, see Fig. 3.11), or glutamate–glutamine cycling. Labeled oxygen is used for *in vivo* assays of cerebral respiration, and labeled water is used to assay cerebral blood flow. Changes in the redox state of endogenous compounds (NAD(P)H and FAD) are assayed by fluorescence microscopy. For simplicity, isotopes of carbon are sometimes denoted by the superscript x to collectively represent ^{11}C-, ^{13}C-, and ^{14}C-labeled compounds that can be used to evaluate similar pathways using different technologies (see text and previous figures for details and abbreviations).

^{3}H-labeled precursors, but the analytical procedures are time-consuming and labor-intensive and only one time point can be obtained from each subject; many reviews describing the history of this field are in the monographs edited by Balázs and Cremer (1972) and Berl et al. (1975). The next major advance was the use of stable isotopes, magnetic resonance spectroscopy (MRS), and metabolic modeling to evaluate fluxes in metabolic pathways of interest in diverse preparations, ranging from cell cultures to human brain. MRS has the advantages of no radiation exposure, determination of time courses in each subject, and longitudinal studies in the same subject; disadvantages are lower sensitivity compared to radiolabeling studies and immobilization of the brain during the assay procedure, which requires use of anesthesia in experimental animals.

Pioneering work in the Shulman laboratory demonstrated the high potential for MRS with ^{31}P and ^{13}C studies in animal brain (reviewed by Pritchard and Shulman (1986) and Hyder and Rothman (2012)), and initial applications of this *in vivo* approach to human brain included determination of brain glucose levels (Gruetter et al., 1992) and assays of incorporation of ^{13}C from glucose into C4 of glutamate (Rothman et al., 1992). ^{13}C- and ^{15}N-Labeled tracers were also used in other laboratories to explore the complexity of brain energy metabolism, metabolite

trafficking, astrocyte–neuron interactions, and metabolic compartmentation (Badar-Goffer et al., 1990; Cerdan et al., 1990; Kanamori et al., 1991; Brand et al., 1992; Bachelard and Badar-Goffer, 1993), and numerous subsequent MRS studies have greatly expanded these research areas (Rodrigues and Cerdan, 2007; Zwingman and Leibfritz, 2007); see Figs. 3.16 and 3.17, following later). Metabolic modeling of brain metabolic activity and energy transfer within cells are very important research areas that are continually evolving to accommodate new data, refined mathematical approaches, and revised concepts describing cell–cell interactions.

Changes in redox state—fluorescence microscopy. Optical signals are generated by activity-dependent electrolyte- and metabolism-driven changes in properties of intrinsic molecules, and these signals can be used to probe real-time changes in tissue metabolic activity (Villringer and Chance, 1997). For example, reduction of NAD and NADP generates the respective fluorescent compounds, NADH and NADPH (often denoted as NAD(P)H because the absorption and fluorescence spectra are similar), whereas oxidation of the mitochondrial flavoprotein, $FADH_2$, yields a fluorescent product FAD (Chance et al., 1962). Thus, spatial-temporal changes in cytoplasmic and mitochondrial oxidation state can be assayed by fluorescence microscopy (Fig. 3.12) under a variety of experimental conditions using biological samples of varying complexity, ranging from isolated mitochondria to the intact animal. The pioneering studies by Chance and colleagues demonstrated the capability of real-time, continuous fluorescent assays of redox changes in living cells and brain tissue during anoxia and other conditions (i.e., Chance and Thorell, 1959; Chance et al., 1962), and early work in other laboratories assessed NAD(P)H fluorescence changes in isolated brain mitochondria, brain slices, and intact cerebral cortex (i) to evaluate effects of oxygen and ADP levels on mitochondrial redox state, (ii) to reveal biphasic responses to electrical stimulation (i.e., rapid oxidation followed by a slower reduction phase with an overshoot above the initial baseline level) that were related to changes in ions and signaling molecules, and (iii) to characterize responses of intact brain tissue to electrical stimulation and seizure activity (e.g., Jöbsis et al., 1971; Lipton, 1973).

An advantage of functional studies that combine electrophysiological and fluorescence techniques is that various fluorescent indicators can be loaded into tissue samples and interactions among cellular activity, energy metabolism, ion concentration changes, and mitochondrial function evoked by different electrical stimuli or pharmacological challenge can be simultaneously evaluated. For example, in hippocampal slices from mature brain the electrical stimulus-induced biphasic response of NAD(P)H fluorescence was shown to be an "inverted match" of the FAD fluorescence that did not reflect mitochondrial Ca^{2+} dynamics; both components of the biphasic NAD(P)H response were abolished by blockade of ionotropic glutamate receptors and were therefore attributed mainly to postsynaptic neuronal activity compared with presynaptic neuronal activity or astrocytic glutamate uptake (Shuttleworth, 2010). Similar conclusions were drawn by Hall et al. (2012), who showed that the NADH overshoot occurs concomitant with increased oxygen consumption and that oxidative consumption was enhanced even when lactate dehydrogenase activity was blocked, consistent with predominant postsynaptic neuronal oxidative activity, with little, if any, astrocyte-to-neuron lactate shuttling. Flavoprotein fluorescence imaging is also a useful tool to evaluate dynamic, local changes in mitochondrial activity in brain slices and *in vivo* during electrical and physiological stimulation. For example, forepaw or hindpaw stimulation elicits FAD autofluorescence changes in somatosensory cortex that correlate with evoked changes in field potentials in the tissue, and transcranial imaging through the intact skull of anesthetized mice enabled tonotopic mapping of cortical responses to acoustic stimuli of different frequencies (Shibuki et al., 2007).

In summary, autofluorescence responses of NAD(P)H and FAD reveal major contributions of postsynaptic activity to stimulus-evoked metabolism in various brain regions. Interpretation of changes in concentrations of redox compounds requires assessment of the relevant fluxes that underlie the redox changes and the effects of tissue preparation (e.g., deafferentation, ischemia, substrate supply by diffusion from medium, and mechanical damage). The high spatial and temporal resolution of fluorescence imaging, in conjunction with electrophysiological, pharmacological, and metabolic assays opens the door for new approaches to studies of the cellular basis of images generated by functional metabolism (Fig. 3.12). However, because the relative changes in NADH or FAD fluorescence (i.e., $\Delta F/F$) are generally within the range of 5–10%, the net concentration and redox state changes are very small (i.e., $10\% \times 0.1\ \mu mol\ g^{-1}$ (Table 3.2) = $0.01\ \mu mol\ g^{-1}$), while at the same time CMR_{glc} is $0.3–0.5\ \mu mol\ g^{-1}\ min^{-1}$ in brain slices (it would be higher in stimulated slices; CMR_{glc} in brain slices is about half that *in vivo* due to deafferentation). Thus, NADH and FAD turnover is very high and caution must be applied when interpreting $\Delta F/F$ in terms of pathway fluxes because small concentration changes are not equivalent to fluxes; they only represent the net result of input and output to the pool.

Function–Metabolism Relationships

Carbohydrates, amino acids, carboxylic acids, alcohols, aldehydes, ketones, lipids, nucleic acids, steroids, and other compounds labeled with *beta-emitting isotopes* (Box 3.3), especially ^{14}C and ^{3}H, as well as ^{35}S, ^{32}P and ^{33}P, have been used for over 50 years to study metabolic reactions and pathways in biochemical and autoradiographic studies. *Positron-emitting isotopes* (^{18}F, ^{15}O, ^{11}C, and ^{13}N) have been incorporated into a wide variety of tracers used for PET studies, whereas *stable isotopes* (e.g., ^{1}H, ^{13}C, ^{31}P, ^{15}N) are used in MRS studies. Some of the specific aspects of blood–brain barrier transport and brain metabolism that can be evaluated by means of these technologies are illustrated in Fig. 3.12. Assays can be designed to determine quantitatively uptake across the blood–brain barrier, metabolism, or concentrations of endogenous compounds or of exogenous compounds labeled with radioactive or stable isotopes. For example, the nonmetabolizable glucose analog, 3-O-methylglucose, is useful for biochemical, autoradiographic, and PET assays of unidirectional glucose transport across the blood–brain barrier and into cultured cells. Because the steady-state brain-to-plasma ratio for methylglucose is proportional to brain glucose concentration, methylglucose can also be used to measure local tissue glucose concentration in brain. DG and FDG are metabolized to the hexose-6-P step and procedures are established for quantitative assays of rates of the first (irreversible) step of glucose utilization in living brain. Fluorescent glucose analogs, 2-NBDG and 6-NBDG, are used to assay glucose phosphorylation and transport, respectively, but the kinetics of their competition with glucose is not sufficiently developed for their use in quantitative, comparative studies in astrocytes and neurons (Dienel, 2012b). Metabolism of $^{15}O_2$ or $^{17}O_2$ measures the terminal step of the electron transport chain, and $[^{15}O]H_2O$ is useful for PET assays of blood flow in humans. ^{13}C-Labeled glucose and acetate are incorporated into metabolites generated by the TCA cycle, and these precursors are particularly useful to measure oxidative metabolism, metabolite cycling, neurotransmitter trafficking, and compartmentation by MRS. Finally, fluorescence microscopy can be used to detect changes in the fluorescence intensity of NADH and FAD with brain function, and evaluate changes in redox status generated during activating or pathophysiological conditions (Fig. 3.12). Taken together, autoradiographic, PET, MRS, and fluorescence studies of metabolism are complementary technologies, each with its strengths and weaknesses, that can be used to investigate complex issues in brain function and disease.

Glucose concentration and utilization. Local rates of glucose utilization (CMR_{glc}) are very heterogeneous whereas brain glucose concentration is fairly uniform, indicating that under steady-state conditions glucose delivery matches its rate of utilization at a local level. CMR_{glc} is highest in gray matter (range: 0.50–1.20 $\mu mol\ g^{-1}\ min^{-1}$) and lowest in white matter (range: 0.15–0.25 $\mu mol\ g^{-1}\ min^{-1}$), and rates in various gray matter structures in different anatomical pathways can differ by >2-fold (Sokoloff et al., 1977). CMR_{glc} varies throughout the cerebral cortex, as well as in stations in the same pathway (e.g., auditory pathway, Table 3.3). Unilateral acoustic stimulation of awake rats increases CMR_{glc} and astrocytic acetate utilization in selected regions of the auditory pathway but not in other brain structures (Table 3.3). Regional and laminar differences are readily detectable in $[^{14}C]$DG autoradiographs of the cerebral cortex, hippocampus, caudate-putamen, and thalamus (Figs. 3.13A, B; top panels). In contrast, $[^{14}C]$methylglucose autoradiographs (Fig 3.13, A, B; lower panels) have relatively uniform optical densities, reflecting similar glucose levels throughout the brain. Note the relatively small glucose concentration differences among gray and white matter structures, contrasting the much larger differences in metabolic rate (compare top and bottom panels in Figs. 3.13A, B). Focal activation of metabolism by a penicillin-induced seizure doubles cortical CMR_{glc} at the application site but only slightly depresses local glucose level (i.e., glucose supply nearly matches the two-fold rise in demand), whereas focal suppression of brain activity by barbital depresses CMR_{glc} by 50% at the application sites and causes a small increase in local glucose content (i.e., the excess glucose delivered returns to blood). Thus, specific, focal changes in metabolism throughout the brain due to altered physiological activity or pharmacological treatment are readily detected and quantifiable. At the level of autoradiographic resolution (100–200 μm), glucose supply and demand are closely matched over a four-fold range of CMR_{glc}.

The cellular basis of autoradiographic images of glucose utilization has been of intense interest for more than 30 years because the major brain cell types are likely to have different metabolic requirements and routine ^{14}C-autoradiographic assays do not have cellular resolution. Studies to identify metabolically labeled cells have been hindered by serious technical difficulties, particularly the quantitative retention of labeled metabolites in cells and tissue during histological processing to identify cell type; membrane damage results in efflux of the labeled metabolites. Label losses during tissue processing can be as high as 90%, and even in the study with the best label retention (~50%) (Nehlig

TABLE 3.3 Regional metabolic responses to unilateral broadband click stimulus

Region of interest	Activated (right) Hemisphere	Contralateral (left) Hemisphere	Right/left ratio
	Glucose utilization (μmol 100 g^{-1} min^{-1})		
Auditory structures			
Superior olive	87.3 ± 23.6	80.2 ± 25.4	1.11 ± 0.17
Lateral lemniscus	92.0 ± 29.4[a]	63.6 ± 13.6	1.41 ± 0.25
Inferior colliculus	119.8 ± 36.9[a]	70.8 ± 10.2	1.66 ± 0.34
Medial geniculate	63.9 ± 12.0	57.9 ± 9.5	1.11 ± 0.13
Auditory cortex	67.9 ± 5.0	65.0 ± 4.3	1.05 ± 0.08
Other structures			
Visual cortex	51.5 ± 7.6	52.4 ± 7.5	0.98 ± 0.04
Sensory cortex	71.7 ± 2.0	71.6 ± 4.6	1.00 ± 0.05
Sensorimotor cortex	70.5 ± 5.2	71.7 ± 3.9	0.98 ± 0.03
Thalamus	62.4 ± 6.1	63.1 ± 5.3	0.99 ± 0.02
Caudate	69.7 ± 5.3	71.9 ± 4.7	0.97 ± 0.03
Genu corpus callosum[c]	17.0 ± 7.0	16.4 ± 6.9	1.04
Cerebellar white matter[c]	24.2 ± 7.2	24.2 ± 4.9	1.0
	[2-^{14}C]Acetate minimal net uptake coefficient (mL 100 g^{-1} min^{-1})		
Auditory structures			
Superior olive	5.9 ± 1.5	5.7 ± 1.5	1.04 ± 0.05
Lateral lemniscus	6.0 ± 1.3[b]	5.1 ± 1.4	1.18 ± 0.10
Inferior colliculus	6.1 ± 1.2[b]	5.3 ± 1.0	1.15 ± 0.03
Medial geniculate	5.5 ± 1.9[a]	5.3 ± 1.8	1.03 ± 0.01
Auditory cortex	5.6 ± 1.4	5.5 ± 1.5	1.02 ± 0.04
Other structures			
Visual cortex	5.3 ± 2.1	5.4 ± 2.1	0.99 ± 0.02
Sensory cortex	5.4 ± 1.1	5.4 ± 1.2	1.01 ± 0.02
Sensorimotor cortex	5.6 ± 1.3	5.6 ± 1.4	1.00 ± 0.03
Thalamus	4.9 ± 2.3	4.8 ± 2.3	1.03 ± 0.02
Caudate	4.9 ± 2.6	4.9 ± 2.7	0.99 ± 0.01
Genu corpus callosum[c]	2.1 ± 0.3	2.2 ± 0.3	0.95
Cerebellar white matter[c]	2.1 ± 0.5	2.1 ± 0.5	1.0

The acoustic stimulus (~88 dB) was initiated 10 min prior to intravenous [^{14}C]tracer injection into conscious rats kept in a sound-insulated environment. Glucose utilization was assayed with the routine [^{14}C]deoxyglucose method. The net acetate uptake coefficient were assayed during a 5-min experimental interval and were calculated by dividing the ^{14}C level in the region of interest by the time-activity integral for total ^{14}C in arterial plasma. Plasma acetate levels in a parallel group of rats averaged 0.9 μmol/ml, and net acetate uptake coefficients can be converted to μmol 100 g^{-1} min^{-1} by multiplying by 0.9. Note that CMR_{glc} reflects activity in all brain cells, whereas acetate oxidation is astrocytic. Values are mean ± SD (n = 5); statistically significant right-left differences were identified by the paired t test ([a]$P < 0.05$, [b]$P < 0.01$). The right/left ratios are means of values calculated for each structure in each rat, not ratios of the mean values for structures in each hemisphere.
Data from Cruz et al. (2005) except for the values for two white matter structures from normal unstimulated rats from [c]Cetin et al. (2003).

et al., 2004), the estimates suggest that CMR_{glc} is similar in astrocytes and neurons under resting conditions. Specific subsets of neurons and astrocytes are, however, known to be more metabolically active than others during resting conditions and accumulate high levels of [^{3}H]DG compared to other cells (Duncan et al., 1987a; Duncan et al., 1987b; Duncan et al., 1990). During swimming or rotation paradigms increased

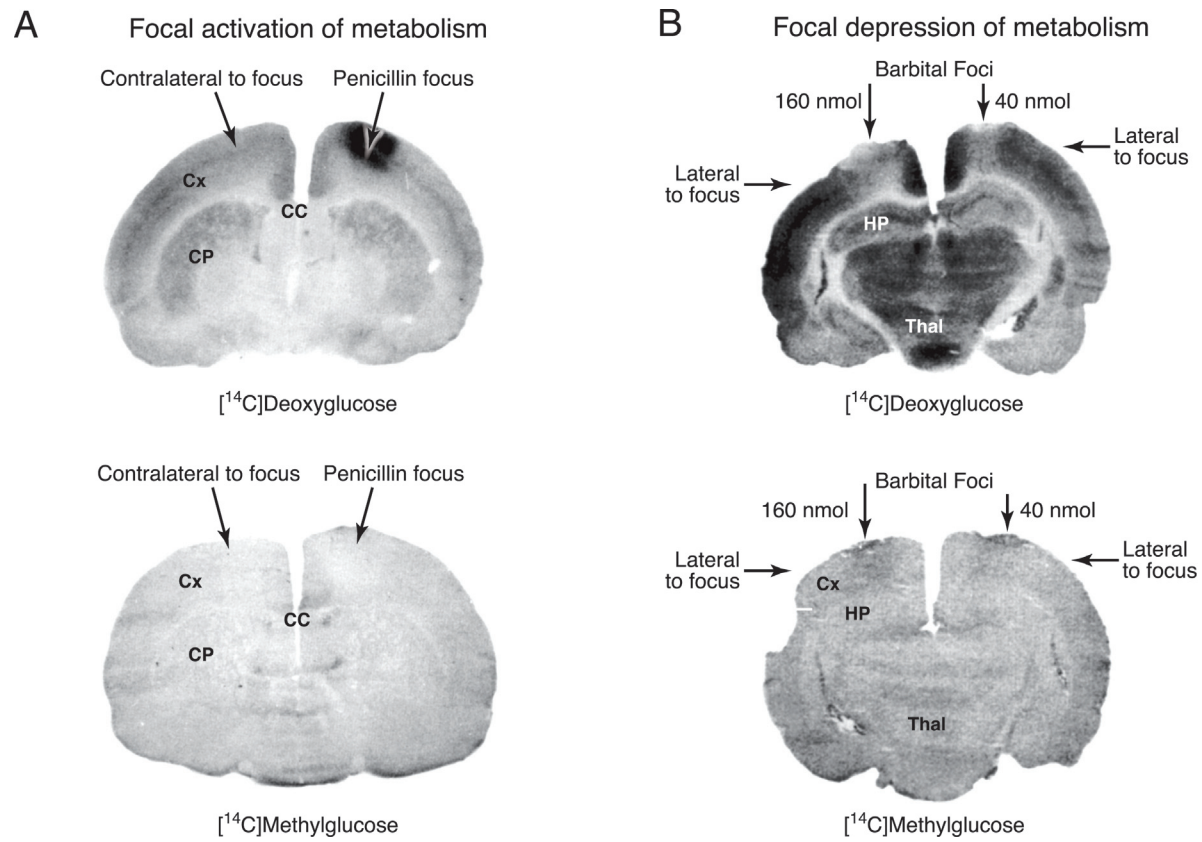

FIGURE 3.13 **Autoradiographic assays of local rates of glucose utilization and glucose concentration.** A focal seizure was induced by topical application of penicillin to the cerebral cortex (A) and focal anesthesia resulted from topical application of 40 or 160 nmol of barbital (B). Local rates of glucose utilization (CMR_{glc}) were assayed with [^{14}C]deoxyglucose (top panels) and local glucose concentration assayed with [^{14}C]methylglucose (bottom panels). In brief, a pulse intravenous bolus of [^{14}C]deoxyglucose is given to the animal; 45 min later the brain is sampled, frozen, cut into serial coronal 20 μm-thick sections, and exposed to X-ray film along with calibrated ^{14}C standards; the darker the region, the higher the ^{14}C concentration and the higher the metabolic rate or glucose level. Similar procedures were used for the [^{14}C]methylglucose assays except that a programmed infusion was used to establish steady-state conditions for the tracer. Note that in the untreated tissue CMR_{glc} is very heterogeneous whereas glucose concentrations are relatively uniform throughout the brain. CMR_{glc} increased two-fold at the site of the seizure (dark spot in the cerebral cortex in the upper figure in panel A) and barbital anesthesia reduced CMR_{glc} (light spots in cerebral cortex the upper figure in panel B) by 36% and 52% at the 40 and 160 nmol barbital sites, respectively. The steady-state brain-to-plasma ratio for [^{14}C]methylglucose, which varies with brain glucose concentration, fell 13% at the seizure focus and rose 14–19% in the barbital foci. Abbreviations: Cx, cerebral cortex; CC, corpus callosum (white matter); CP, caudate-putamen; Hip, hippocampus; Thal, thalamus. *Reproduced from Nakanishi et al. (1996), with permission of Nature Publishing Group.*

neuronal trapping of labeled DG occurs in activated brain structures (Sharp, 1976a; Sharp, 1976b). Increased neuronal glucose utilization during *in vivo* activation is consistent with the large excess capacity of synaptosomes to carry out glycolysis and respiration; synaptosomal glycolytic rate increased 10-fold for at least 30 min and respiration rose 6-fold after treatment of synaptosomes with FCCP to uncouple respiration and ATP synthesis (Kauppinen and Nicholls, 1986; Choi et al., 2009; Choi et al., 2011). In spite of many attempts to improve the cellular resolution of *in vivo* autoradiographic studies, the available data cannot determine the metabolic contributions of major cell types. Label accumulation in the cell bodies of astrocytes and neurons is most readily identified and tallied according to cell type, but neuronal perikarya are likely to have lower CMR_{glc} than the active synaptic-rich regions of neuropil. The energetic contributions of neuronal pre- and postsynaptic processes and the fine filopodia of astrocytes remain to be established, particularly during activation, but increased glucose utilization and oxidation in pre- and postsynaptic neuronal elements are evident when assayed in synaptosomes and brain slices.

Imaging focal activation with different metabolic tracers. Presentation of an acoustic stimulus to a subject activates the auditory pathway in a tonotopic manner, and

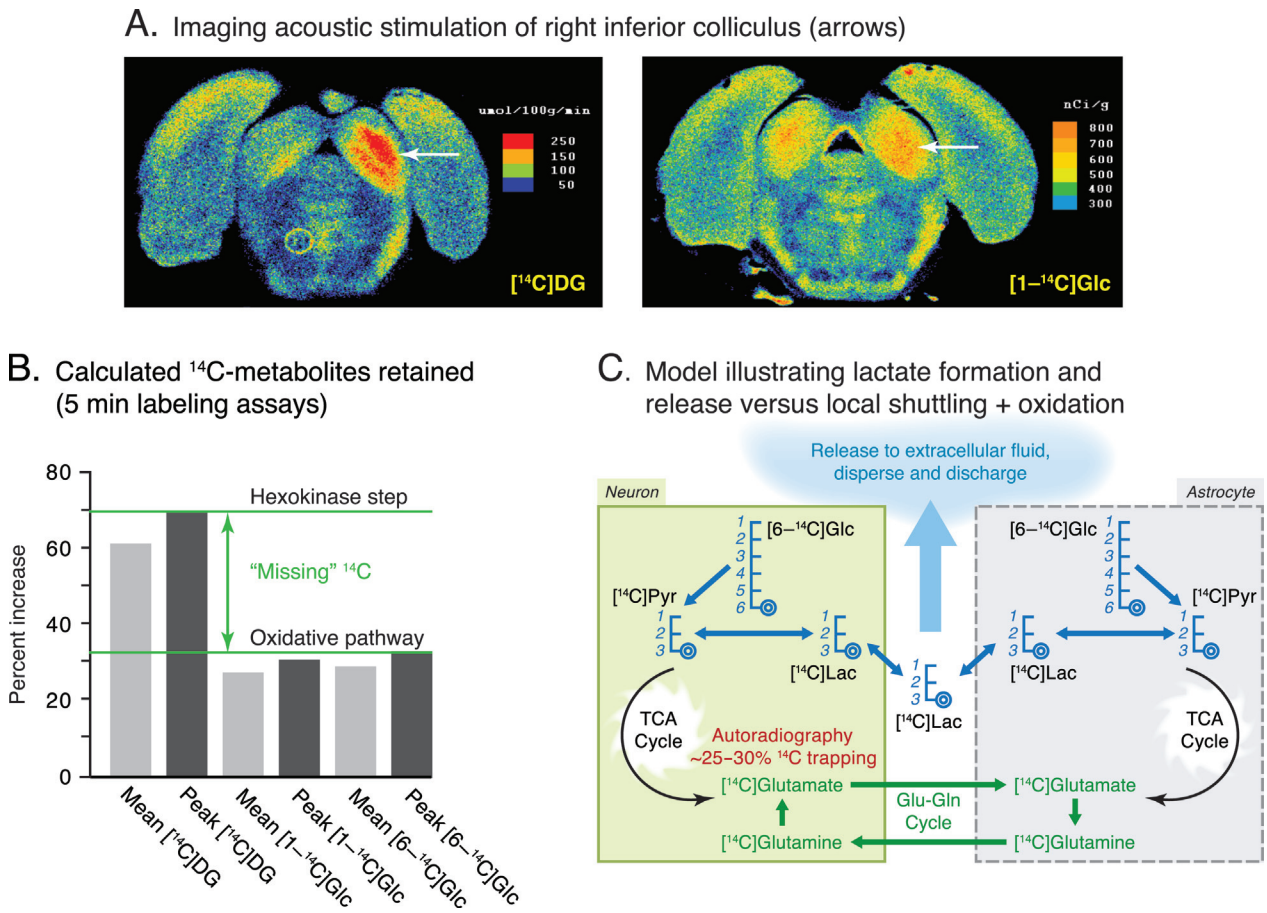

FIGURE 3.14 **Registration of focal acoustic activation with two glucose utilization tracers.** Stimulation of the auditory pathway of the rat with a single tone increases cellular activity in a tonotopic manner. Specific groups of cells in the stations of the auditory pathway respond to that tone by increasing their signaling and demand for ATP (Table 3.3). (A) Tonotopic bands of increased CMR_{glc} identify regions within the right inferior colliculus (arrows) that respond to a unilateral acoustic stimulus, and these bands are readily detected with the 45 min [^{14}C] deoxyglucose (DG) method (left panel), but not with [1-^{14}C]glucose (right panel). Note the different color-coding scales for the two tracers; rates of glucose utilization are shown for [^{14}C]DG, whereas local tissue ^{14}C concentrations are shown for [^{14}C]glucose. Reproduced from Cruz et al. (2007), with permission of Wiley-Blackwell Publishers. (B) Percent increase in quantities of metabolites of [^{14}C]DG or [1- or 6-^{14}C]glucose retained in the entire activated inferior colliculus (denoted as "mean") and in the major tonotopic band (arrows in panel A, denoted as "peak") in five min labeling assays of monotonic acoustic stimulation. The greater increases with labeled DG compared with glucose indicate that fractional increase of the hexokinase reaction is about twice that of the oxidative pathways. Thus, most of the labeled products of glucose metabolism produced by activation over and above those during rest are quickly (i.e., within 5 min) lost from the activated inferior colliculus by [^{14}C]lactate release and decarboxylation reactions (see Cruz et al., (2007), Dienel and Cruz (2008), Dienel (2012a), Dienel (2012b) for detailed discussion of these findings and their implications). Reproduced from Dienel (2012b), with permission of the author. (C) Model illustrating how shuttling of lactate from astrocytes linked to its oxidation in nearby neurons would lead to trapping of ^{14}C in activated regions. Lactate can be produced from [6-^{14}C]glucose in either or both astrocytes and neurons. Release of labeled lactate to extracellular fluid followed by its uptake and oxidation in neighboring cells would lead to incorporation of label into the large amino acid pools, mainly glutamate. However, trapping of products of glucose via the oxidative pathways does not match that of DG, indicative of rapid loss of labeled products. In contrast, release of ^{14}C-labeled lactate causes underestimation of metabolic activation, as observed during acoustic activation (panels A, B). Abbreviations: DG, deoxyglucose, Glc, glucose; Glu, glutamate; Gln, glutamine; Lac, lactate, Pyr, pyruvate; TCA, tricarboxylic acid. *Modified from Dienel and Cruz, (2004), with permission from Elsevier, and reprinted from Dienel (2012b), with permission of the author.*

different groups of cells in stations of the auditory processing pathway respond by increasing signaling and rates of glucose utilization by all cells and rates of acetate oxidation by astrocytes (Table 3.3). Focal activation of bands of cells in the inferior colliculus of the rat by a single tone stimulus is readily detectable with the routine [^{14}C]DG method using a 45-min experimental period (Fig. 3.14A). The 45-min assay duration takes advantage of the metabolic stability of [^{14}C]DG-6-P in brain tissue and minimizes the effects of uncertainties in the true values of rate constants used to estimate (i) the unmetabolized [^{14}C]DG in brain and (ii) the brain time-activity integral on the calculated CMR_{glc}. Focal activation is also detected with 5 min [^{14}C]DG assays,

but the higher proportion of unmetabolized [^{14}C]DG increases the background and blunts the relative increase. Also, calculated metabolic rates for brief assays are not as accurate as desired due to a higher impact of estimates of values for rate constants on unmetabolized precursor level and integrated specific activity in brain (Adachi et al., 1995). Tonotopic bands are registered with [^{14}C]DG in 5-min assays but they are barely detectable with [1- or 6-^{14}C]glucose (Fig. 3.14A, Cruz et al., 2007). Broadband acoustic activation is registered with [^{14}C]acetate (Table 3.3) but not with β-hydroxy[^{14}C]butyrate (Cruz et al., 2005). These findings are of considerable interest, because glucose and β-hydroxybutyrate label the "large" glutamate pool ascribed to neurons, whereas acetate labels the small glutamate pool in astrocytes. Although acetate and β-hydroxybutyrate are transported into brain from blood by the same monocarboxylic acid carrier MCT1 they have different metabolic fates in brain. The discrepant labeling patterns obtained in parallel assays with [^{14}C]DG and [1- or 6-^{14}C]glucose (Fig. 3.14A) are due to rapid spreading and release of labeled metabolites of glucose by various pathways, including decarboxylation by the pentose shunt pathway, release of labeled lactate, spreading via gap junctions, and rapid elimination of labeled products that correspond to most of the additional glucose consumed during activation compared to rest (Cruz et al., 2007). Even with 5-min assays, the rise in trapping of products of [^{14}C]DG in the entire inferior colliculus and in the peak tonotopic band (arrow, Fig. 3.14A) is 60 and 70%, respectively, greatly exceeding the corresponding values obtained with [1- or 6-^{14}C]glucose (Fig. 3.14B). Because DG assays the hexokinase step and most of the label trapping from [1- or 6-^{14}C]glucose occurs via the oxidative pathways (Fig. 3.11), the "missing" labeled carbon (Fig. 3.14B) corresponds mainly to labeled lactate that is released from activated tissue in substantial quantities (Fig. 3.14C). Lactate is quickly labeled by [^{14}C]glucose, it is the major readily diffusible metabolite of the glycolytic pathway, and its release from brain is detected within 2 min after onset of activation (Dienel, 2012a; Dienel, 2012b). Lactate release from brain is consistent with the fall in the ratio of oxygen to glucose utilization during brain activation and the small incremental rise in oxygen utilization during brain activation. Lactate oxidation requires oxygen consumption, and, because the rise in oxygen consumption ranges from 0–30% in many studies of brain activation in humans and rats, the contribution of brain-derived lactate to total oxidative fuel cannot be more than 30%. In fact, the contribution of lactate must be lower than this upper limit of the rise in CMR_{O2} because both neurons and astrocytes oxidize glucose-derived pyruvate directly. Astrocytes oxidize about 20% of the glucose under resting or anesthetized conditions (Hertz, 2011; Rothman et al., 2011), so the maximum contribution of lactate is reduced to ~24%. If neurons directly oxidize about half of the glucose, then lactate shuttling might maximally contribute ~12% to total oxidation (also see Mangia et al., 2011).

Calculated rates of glucose utilization in different brain regions during broadband acoustic stimulation of conscious rats illustrate the pathway-specific effects of a physiological stimulus on utilization of glucose by all brain cells and by oxidation of acetate by astrocytes. Structures within the auditory pathway respond to different extents whereas nonauditory pathways have stable rates of glucose utilization (Table 3.3). Note the low metabolic rates in white matter structures (corpus callosum and cerebellar white) compared to gray matter, the large range of CMR_{glc} throughout brain (5–7-fold in the resting and activated hemisphere, respectively), the more modest range (2.6–2.9-fold) of acetate oxidation, and the large stimulus-induced response of CMR_{glc} (66%) compared to astrocytic oxidative metabolism (18%) (Table 3.3). These findings illustrate the large dynamic range of responsiveness of glucose utilization during physiological activity and demonstrate that oxidative metabolism in astrocytes increases during sensory stimulation. Astrocytes are not simply glycolytic, as is sometimes assumed based on tissue culture studies; they also increase oxidative metabolism to generate ATP during activation.

Lactate shuttling is unlikely to provide much fuel during brain activation in normal subjects. In 1994, the finding that glutamate-stimulated lactate release from cultured astrocytes was incorporated into a model that proposed that lactate released from astrocytes is fuel for activated neurons (Pellerin and Magistretti, 1994). The current status of the controversial notion that excitatory neurotransmission stimulates glycolysis in astrocytes, astrocyte-to-neuron lactate shuttling, and lactate oxidation by nearby neurons has been reviewed (Jolivet et al., 2010; Pellerin and Magistretti, 2012), and this idea has persisted in the literature in spite of a paucity of direct evidence for astrocyte-to-neuron lactate shuttling. In fact, most of the limited number of studies selectively cited in support of this model of brain energetics (Jolivet et al., 2010; Pellerin and Magistretti, 2012) are not representative of the many studies carried out in similar model systems in other laboratories over many decades (Dienel, 2012a). Under activating conditions cultured neurons and synaptosomes isolated from adult animals increase their rates of glucose uptake, glycolysis, and glucose oxidation by many-fold. Furthermore, modeling based on different assumptions predicts lactate shuttling from neurons to astrocytes, along with glycogenolysis to support energy demands of activated

astrocytes, thereby freeing-up blood borne glucose for use by neurons (Mangia et al., 2009, DiNuzzo et al., 2010b, DiNuzzo et al., 2010a, Mangia et al., 2011, Dinuzzo et al., 2012). In fact, glucose phosphorylation rises markedly in neuronal nerve terminals during seizures, contradicting predictions of and directly disproving the astrocyte-to-neuron lactate shuttle model (Patel et al., 2014). As discussed above, glutamate stimulates astrocytic respiration and glutamate oxidation and probably provides some of the ATP required by activated astrocytes, but the extent of glutamate oxidation *in vivo* remains to be established (Dienel, 2013).

The lactate shuttle concept has been extensively debated because the cellular origin of lactate produced during brain activation is unknown, the direction and magnitude of lactate trafficking remain to be established, and the fraction locally oxidized and the proportion released to blood must be determined *in vivo* in conscious subjects. These are technically difficult assays, and data obtained in normal conscious subjects are not equivalent to findings in anesthetized subjects, during vigorous exercise, during lactate infusions to raise blood lactate levels and flood the brain with lactate, or during severe hypoglycemia and aglycemia. Biochemical arguments against the lactate shuttle hypothesis (Chih et al., 2001; Chih and Roberts Jr, 2003) are consistent with strong *in vivo* evidence derived from studies in many laboratories that the magnitude of any lactate shuttling coupled to local oxidation is quite small. Most lactate is released from activated tissue (Fig. 3.14), probably by avid lactate uptake into astrocytes, lactate dispersal throughout the astrocytic syncytium, and lactate discharge from endfeet for release via perivascular fluid and blood (reviewed by Dienel, 2012b). Furthermore, Caesar et al. (2008) found that electrical stimulus-induced increases in extracellular lactate level, blood flow, CMR_{glc}, and CMR_{O2} in the cerebellum of the anesthetized rat were eliminated by treatment with CNQX to block postsynaptic neuronal activation; CNQX does not block glutamate-stimulated glycolysis in cultured astrocytes (Pellerin and Magistretti, 1994) or glutamate uptake into astrocytes (Duan et al., 1999). Because glutamate would be continuously taken up into cerebellar astrocytes during CNQX treatment, the *in vivo* stimulus-induced glycolytic activity is not due to astrocytic glutamate uptake. Thus, brain activation-induced lactate generation in this intact animal preparation is dissociated from astrocytic glutamate transport, and the lactate released to extracellular fluid arose from evoked postsynaptic activity, a conclusion that is supported by studies in hippocampal slices (Brennan et al., 2006; Shuttleworth, 2010; Hall et al., 2012). Together, these findings emphasize the importance of inclusion of neuronal glucose utilization and lactate production into modeling of functional metabolism. Astrocytic glutamate uptake is not the major or the only factor governing lactate generation during brain activation *in vivo*.

In summary, current data support a minor, if any, role for lactate as fuel during brain activation in normal, physically inactive subjects, with its predominant release from brain as a glycolytic by-product, perhaps to help stimulate blood flow to activated tissue (Laptook et al., 1988; Hein et al., 2006; Lombard, 2006; Yamanishi et al., 2006; Gordon et al., 2008). However, during exercise or lactate infusion when blood lactate rises above that in brain, greater quantities of lactate enter the brain and are oxidized. Also, during severe glucose deprivation (extreme hypoglycemia or aglycemia), a condition that only occurs during insulin overdose or experimental design, endogenous substrates, including amino acids, lactate, glycolytic and TCA cycle intermediates, are known to be oxidized by brain (Siesjö, 1978). Finally, interpretation of the contribution of lactate to total oxidation in assays carried out in anesthetized subjects need to take into account the effects of anesthesia and suppression of metabolism.

Flow-metabolism "coupling." The concept of tight coupling of blood flow and metabolism arose from the correlation between local rates of blood flow and CMR_{glc} in different brain structures (Fig. 3.15A). This idea was further strengthened by demonstration that (i) GLUT1 glucose transporter density and capillary density are also highly correlated with local rates of glucose utilization (Fig. 3.15B) and that (ii) regional GLUT1 and MCT1 densities are correlated (Fig. 3.15C). Thus, the physical structure of the microvasculature, rates of blood flow, transporter capacity, and metabolic rate are coordinated at a local level so that fuel supply can satisfy local energy demand. Low activity in white matter is associated with low flow and low transport capacity whereas high-activity structures are endowed with high flow and transport capacity. Signaling activities of neurons and astrocytes generate compounds that regulate vasodilation and govern local blood flow rates (Attwell et al., 2010; Paulson et al., 2010).

Whiskers are an extremely important tactile system in many animals, and the representation of whiskers in the sensory cortex is correspondingly high, as is representation of the hands and mouth in somatosensory cortex of primates. Each whisker is represented by a specific group of cells in sensory cortex that involves all lamina from dorsal to ventral cortex and corresponds to a "barrel." Modulation of the activity of the whisker-to-barrel pathway by anesthesia during rest and sensory stimulation is illustrated in Fig. 3.15D. Note the progressive rise in CMR_{glc} reflecting increased activities of cells from the resting anesthetized, activated anesthetized, awake resting, and awake activated states. CMR_{glc} rises from anesthesia to

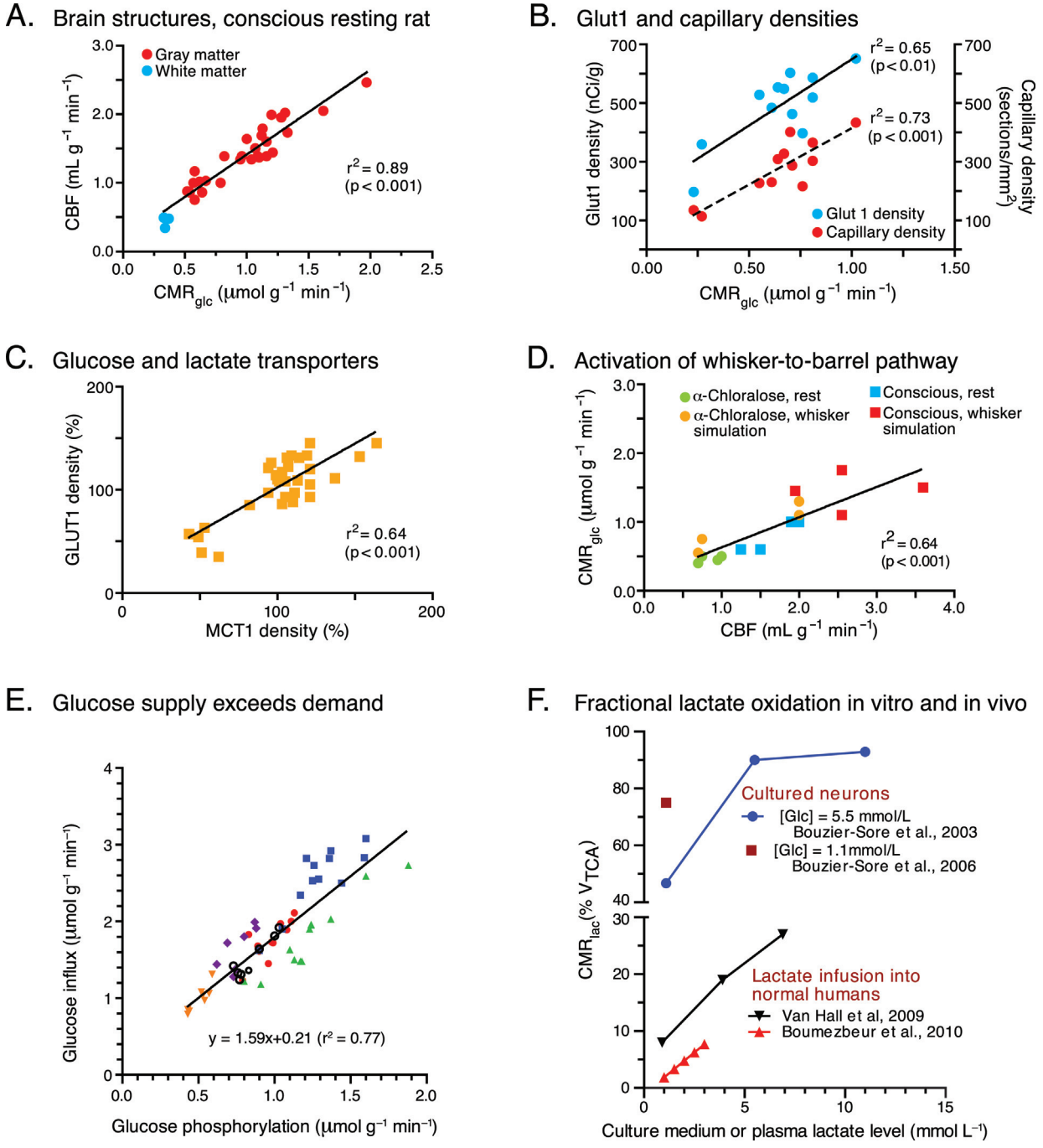

FIGURE 3.15 **Relationships among blood flow, glucose utilization, metabolite transport, and capillary density during rest and brain activation.** (A) Local rates of cerebral blood flow (CBF) correlate with rates of glucose utilization (CMR_{glc}) in the same rat brain structure (*plotted from data of Sokoloff et al. (1977), Sakurada et al. (1978)*). Note the low flow-metabolism rates in white compared to gray matter and the heterogeneity of rates in gray matter (also see Fig. 3.13). (B) Local capillary densities and glucose transporter GLUT1 densities in adult rat brain are correlated with CMR_{glc} (*plotted from data of Zeller et al. (1997)*). (C) Regional glucose (GLUT1) and lactate transport (MCT, monocarboxylic acid transporter) capacities are correlated in adult rat brain (plotted from data of Maurer et al. (2004)). (D) Flow-metabolism relationships in four stations of the whisker-to-barrel pathway of the rat during rest and whisker stimulation in α-chloralose-anesthetized and conscious rats (*plotted from data of Nakao et al. (2001)*. Note the much lower flow and metabolic rates in anesthetized rats and the lack of change in two structures in stimulated, anesthetized rats compared with resting, anesthetized rats (for details, see Nakao et al., 2001). (E) Rates of glucose influx exceed rates of glucose utilization by about 60% over a four-fold range of utilization rates and over a wide range of brain and arterial plasma glucose concentrations. *Plotted from data of Cremer et al. (1983), Hargreaves et al. (1986) and modified from Dienel (2012b), with permission of the author.* (F) Relative oxidation of lactate (CMR_{lac}) compared with glucose, expressed as percent of total oxidation rate, V_{TCA}, in cultured immature neurons is at least four-fold higher than in normal adult human brain *in vivo* during exercise or during lactate infusion to raise plasma lactate level above that in brain. Thus, lactate and glucose oxidation in cultured neurons does not correspond to mature brain. *Plotted from data of Bouzier-Sore et al. (2003), Bouzier-Sore et al. (2006), van Hall et al. (2009), Boumezbeur et al. (2010).*

awake and from rest to stimulation, but the magnitude of CMR_{glc} is much lower during anesthesia than in the awake animal. Also, the local rate of cerebral blood flow changes in proportion to metabolic rate. Because the CMR_{glc} is differentially suppressed in each structure by anesthesia during rest and activation, the data in Fig.3.15D can be used to estimate the "cost of consciousness" in stations of the auditory pathway.

During brain activation influx of glucose from blood into brain exceeds glucose utilization by about 60% over a four-fold range of metabolic activity and over a wide range of plasma and brain glucose levels (Fig. 3.15E). Thus, glucose demand is not limited by its delivery, suggesting that brain cells do not need supplementary fuel (i.e., lactate) during activation. This conclusion is supported by the very rapid hemodynamic response to stimulation illustrated by many studies in anesthetized subjects (that would have subnormal metabolic and blood flow rates due to anesthesia) demonstrating that the onset of the hemodynamic response occurs within 0.2 to 1.8 seconds, with most values being less than 0.7 s (Masamoto and Kanno, 2012). The readily detectable BOLD effect (i.e., increased oxyhemoglobin in cerebral venous blood (Kim and Ogawa, 2012)) in activated brain structures indicates that oxygen is delivered to activated tissue in excess of demand and that a lack of oxygen does not explain the manifestation of "aerobic glycolysis" during brain activation, i.e., the disproportionate increase in CMR_{glc} compared with CMR_{O2} (Fox and Raichle, 1986; Fox et al., 1988; Madsen et al., 1995; Madsen et al., 1999).

Lactate does become a significant supplementary fuel for brain when its blood level rises during exercise or lactate infusions and drives lactate into brain. Normal physically inactive rats and humans have plasma lactate levels in the range of about 0.5–1 mM and the fractional contribution of lactate to total brain oxidative rate is about 1–8% at 1 mM, whereas when plasma lactate level exceeds 3 mM plasma lactate oxidation rises to ~7–25% of the total (Fig. 3.15F). In sharp contrast to these findings in normal human brain, lactate oxidation by cultured neurons was reported by the Pellerin-Magistretti group to range from 45–90% of the total when medium lactate ranged from 1–11 mM (Fig. 3.15F). These findings indicate that metabolism in cultured immature neurons does not correspond to that in normal adult brain, and caution must be exercised when interpreting culture data in terms of normal brain *in vivo*.

Neurotransmission–Metabolism Relationships

Glucose and oxygen requirements. Oxidation of glucose is proportional to glutamate–glutamine cycling (Fig. 3.9B), providing strong evidence for tight linkage between metabolism and neurotransmission (Rothman et al., 2011). However, the TCA cycle-derived amino acid transmitters are not the only systems dependent on glycolytic and oxidative metabolism of glucose and on adequate levels of O_2. The neuromodulators D-serine and glycine are generated from the glycolytic pathway and both the catecholaminergic and cholinergic pathways are linked to tissue oxygen content and oxidative metabolism (Fig. 3.16). Catecholamine neurotransmitter synthesis and degradation is highly dependent on the activity of mixed-function oxidases (tyrosine hydroxylase, tryptophan hydroxylase, dopamine-β-hydroxylase, and monoamine oxidase) that consume molecular O_2 (Fig. 3.16). Generation of acetylcholine from mitochondrial pyruvate (Fig. 3.16) is closely coupled to oxidative metabolism of glucose even though only 1% of the glucose is used to synthesize acetylcholine (Joseph and Gibson, 2007).

Neuronal requirements for glycolysis and glycolytic ATP. During the past decade, considerable attention has been placed on astrocytic glycolysis and lactate production, but neurons also depend on the glycolytic and oxidative pathways, not only for energy, but also to sustain neurotransmission (Schousboe et al., 2011; Bak et al., 2012). For example, glycolysis provides the energy for vesicular packaging of neurotransmitters (Fig. 3.16), an integral aspect of synaptic signaling. The driving force for the vesicular glutamate transporter (VGLUT) is the proton gradient inside the vesicle that is generated by H^+-ATPase. Ueda and colleagues found high enrichment of glyceraldehyde-3-P dehydrogenase and 3-phosphoglycerate kinase on synaptic vesicles and showed that impairment of glycolysis reduces vesicular glutamate content and lowers glutamate release from synaptosomes (Ueda and Ikemoto, 2007). These studies demonstrate functional linkage of these glycolytic enzymes to the vesicular protein pump and indicate that a local pool of glycolytically derived ATP, not mitochondrially derived ATP, is preferred by the vesicular proton pump and that glutamate can be synthesized by synaptic vesicles from α-ketoglutarate and aspartate (Takeda et al., 2012).

A role for glyceraldehyde-3-phosphate dehydrogenase (GAPDH) in neurotransmission is not limited to glycolytic activation during excitatory glutamatergic activity because this enzyme can also serve as a $GABA_A$ receptor kinase. The $GABA_A$ postsynaptic receptor is a chloride channel that mediates fast synaptic inhibition by causing hyperpolarization. GAPDH co-localizes with the α1 subunit of the $GABA_A$ receptor and is proposed to become autophosphorylated by locally produced glycolytic ATP, then this phosphoryl group is transferred to the receptor thereby modulating the receptor-mediated responses to GABA; all of the glycolytic machinery to sustain this process is

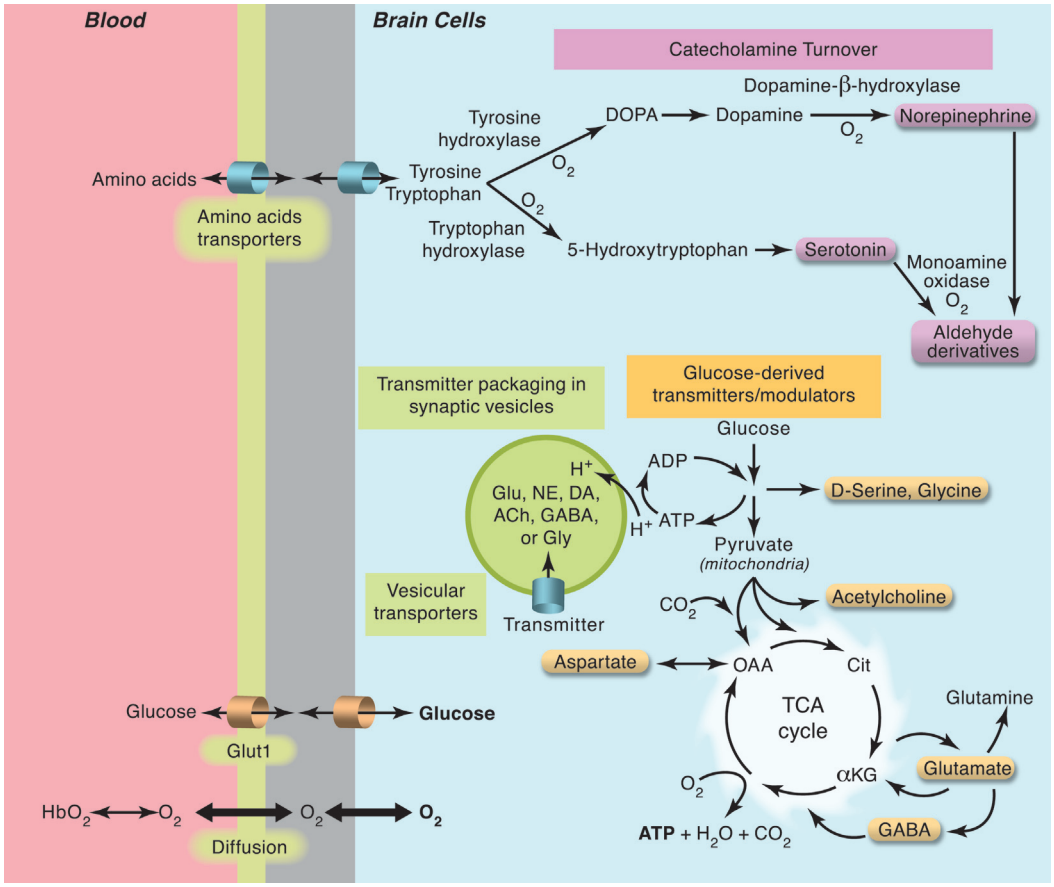

FIGURE 3.16 **Energy metabolism and neurotransmission are closely interrelated.** Oxygen and glucose have dual roles in brain, serving as fuel for generation of ATP and as substrates for enzymes that synthesize neurotransmitters and other compounds required by brain. Oxygen not only serves as the electron acceptor in the electron transport chain, it also is an important substrate for mixed-function oxidases that synthesize and degrade catecholamine neurotransmitters. Glucose derived neurotransmitters are synthesized via the glycolytic and oxidative pathways, and ATP generated from both processes is essential for critical processes involved in neurotransmission, e.g., packaging of neurotransmitters in synaptic vesicles and maintenance and restoration of transmembrane ionic gradients. Also see Figs. 3.9 and 3.12.

localized in postsynaptic densities (Laschet et al., 2004, and cited references). A deficiency in the GABAA receptor phosphorylation has been reported in human epileptogenic tissue, and abnormal GABAergic inhibition may link glycolytic metabolism and enzymes with seizure activity (Laschet et al., 2007). GAPDH may also be involved in seizure activity by generation of NADH that can modulate the binding of a transcriptional repressor complex and thereby influence neuronal excitability; inhibition of glycolysis with deoxyglucose can reduce epilepsy progression (Garriga-Canut et al., 2006) or have pro-convulsant actions (Gasior et al., 2010). Thus, glycolysis has critical roles in both pre- and postsynaptic neuronal structures, and multifunctional roles of NAD^+, NADH, and GAPDH are important emerging research areas that are discussed in later following sections (Fig. 3.22).

The ability of alternative substrates (e.g., fructose, mannose, pyruvate, lactate) to replace glucose and maintain neurotransmission has been of intense interest since the 1960s. Early studies observed that electrically evoked neuronal population spikes in hippocampal brain slices were frequently *not maintained* by alternative substrates even when the ATP concentration exceeded 80% of control, indicating that high energy level is not sufficient to sustain synaptic function (summarized in Fig. 4 of Dienel and Hertz, 2005 and its related text). A detailed series of studies by Okada and colleagues showed that the specific conditions employed during slice preparation are critical to the outcome of substrate substitution studies. For example, the speed of slice preparation and other conditions have a high impact on both the functional recovery of slices and the ability of various substrates to support neuronal function; major factors include adenosine, glutamate, and calcium homeostasis (Okada and Lipton, 2007).

More recent work in cultured cells and brain slices also supports important roles for glycolytic metabolism of glucose in neurotransmission (Allen et al., 2005; Bak et al., 2006; Bak et al., 2012). Although synaptosomes

have considerable excess glycolytic, as well as oxidative, capacity (Kauppinen and Nicholls, 1986; Choi et al., 2009), about half of the vesicle-containing presynaptic boutons in axons from CA3 to CA1 neurons in the hippocampus do not have mitochondria (Shepherd and Harris, 1998) and most dendritic spines lack mitochondria (Bourne and Harris, 2008). Postsynaptic densities contain glycolytic enzymes (Wu et al., 1997), consistent with glycolytic contribution to the functions in these neuronal structures, as well as to fuel the plasma membrane calcium pump in dendritic spines (Ivannikov et al., 2010). To sum up, alternative substrates can support neuronal energetics and evoked potentials or other functions in brain slices and cultured cells under defined conditions for a certain amount of time, but neurons do have specific requirements for glycolytic and oxidative metabolism of glucose for a number of important processes. Energy supply is an essential, but not exclusive aspect, of glucose metabolism required to support neurotransmission.

Na^+, K^+-ATPase activation. Maintenance and reestablishing ionic gradients, mainly by Na^+, K^+-ATPase, is considered to be the major energy expenditure during brain signaling (Howarth et al., 2012). Ionic pumping increases in neurons and astrocytes during activation but the metabolic reactions that provide energy for various pumps have not been definitively identified, contrasting some peripheral tissues in which the Na^+, K^+-ATPase preferentially uses ATP derived from glycolysis (e.g., Lynch and Balaban, 1987; Lynch and Paul, 1987; and references cited therein). Astrocytic Na^+, K^+-ATPase activity rises during excitatory neurotransmission because glutamate is removed from the synaptic cleft by its co-transport into astrocytes along with Na^+. However, as discussed above, the source of ATP to fuel this transporter is not resolved. Glutamate oxidation, glycolysis, glycogenolysis, and astrocytic oxidative metabolism of acetate and other substrates rise during activation *in vivo* (Dienel, 2012a; Dienel, 2012b).

Astrocytic glycogenolysis. Uptake of K^+ from extracellular fluid into astrocytes stimulates glycogenolysis in a concentration-dependent manner (Hof et al., 1988; Xu et al., 2013), and many neurotransmitters (with the striking exception of glutamate (Sorg and Magistretti, 1991)) also activate glycogenolysis, thereby linking astrocytic glycolytic activity to local and more distant neuronal signaling activities (Hertz et al., 2007). The ultimate fate of the glycogen degraded during brain activation is also unknown, but modeling predicts its use to support astrocytic K^+ clearance and at the same time inhibit astrocytic utilization of blood-borne glucose so that more is available for neurons (DiNuzzo et al., 2010b; DiNuzzo et al., 2011; Dinuzzo et al., 2012). Glycogenolysis has also been linked to memory and learning (Hertz and Gibbs, 2009; Newman et al., 2011; Suzuki et al., 2011; Duran et al., 2013), but more work is required to identify the specific roles of glycogen and glycogen-derived pyruvate/lactate under different experimental conditions.

Cellular glucose oxidation rates and turnover of excitatory and inhibitory amino acid neurotransmitters. Magnetic resonance spectroscopic (MRS) studies are particularly useful for studies of the metabolic fate of specific atoms in labeled molecules and have made major contributions to our understanding of metabolic processes and compartmentation in living brain. For example, relationships between rates of glutamate–glutamine cycling and oxidative metabolism have been established (Rothman et al., 2011), and MRS metabolomics studies are used to characterize phenotypes of diseases and drug effects (Griffin and Kauppinen, 2007; Nasrallah et al., 2010; Maher et al., 2011).

As illustrated in Fig. 3.17A, metabolism of glucose that is labeled in carbon one (i.e., [1-^{13}C]glucose, where the ^{13}C-labeled carbon atom is indicated in red) labels carbon 3 of pyruvate, carbon 2 of acetyl CoA, and, during the first turn of the TCA cycle, it labels carbon 4 of glutamate; the same labeling pattern is obtained with [6-^{13}C]glucose. Glucose metabolism labels both neurons and astrocytes, but because most of the brain tissue glutamate is located in neurons, dilution of ^{13}C into the glutamate pool mainly reflects neuronal metabolism. [2-^{13}C]Acetate (indicated in green circles) is preferentially metabolized via the astrocytic TCA cycle and it labels carbon 2 of acetyl CoA as well as carbon 4 of glutamate and glutamine (Fig. 3.17A). In contrast, entry of ^{13}C derived from [1-^{13}C]glucose into the astrocytic TCA cycle via the anaplerotic pyruvate carboxylase reaction (blue circles) labels carbon 2 of oxaloacetate and glutamate. Thus, MRS assays using differentially labeled glucose and acetate can distinguish between astrocytic and neuronal metabolism and entry of pyruvate into the TCA cycle via the pyruvate carboxylase reaction and the pyruvate dehydrogenase reaction.

Metabolic compartmentation to the TCA cycles in astrocytes and neurons in rat brain *in vivo* is illustrated by the MRS assays in Fig. 3.17B. Carbon 4 of glutamate is quickly and highly labeled by [1,6-$^{13}C_2$]glucose, whereas labeling of glutamine-C4 lags and does not attain the same extent of enrichment. In contrast, infusion of [2-^{13}C]acetate preferentially labels glutamine-C4, with much slower incorporation into glutamate-C4. Reversal of the labeling patterns with the two labeled substrates is explained by differential labeling of the large glutamate pool by glucose and the small glutamate pool by acetate. Note the long time (~50 min) required to reach *isotopic steady state* (Box 3.3). Model-dependent analysis of the temporal profiles of labeling of different carbon atoms of

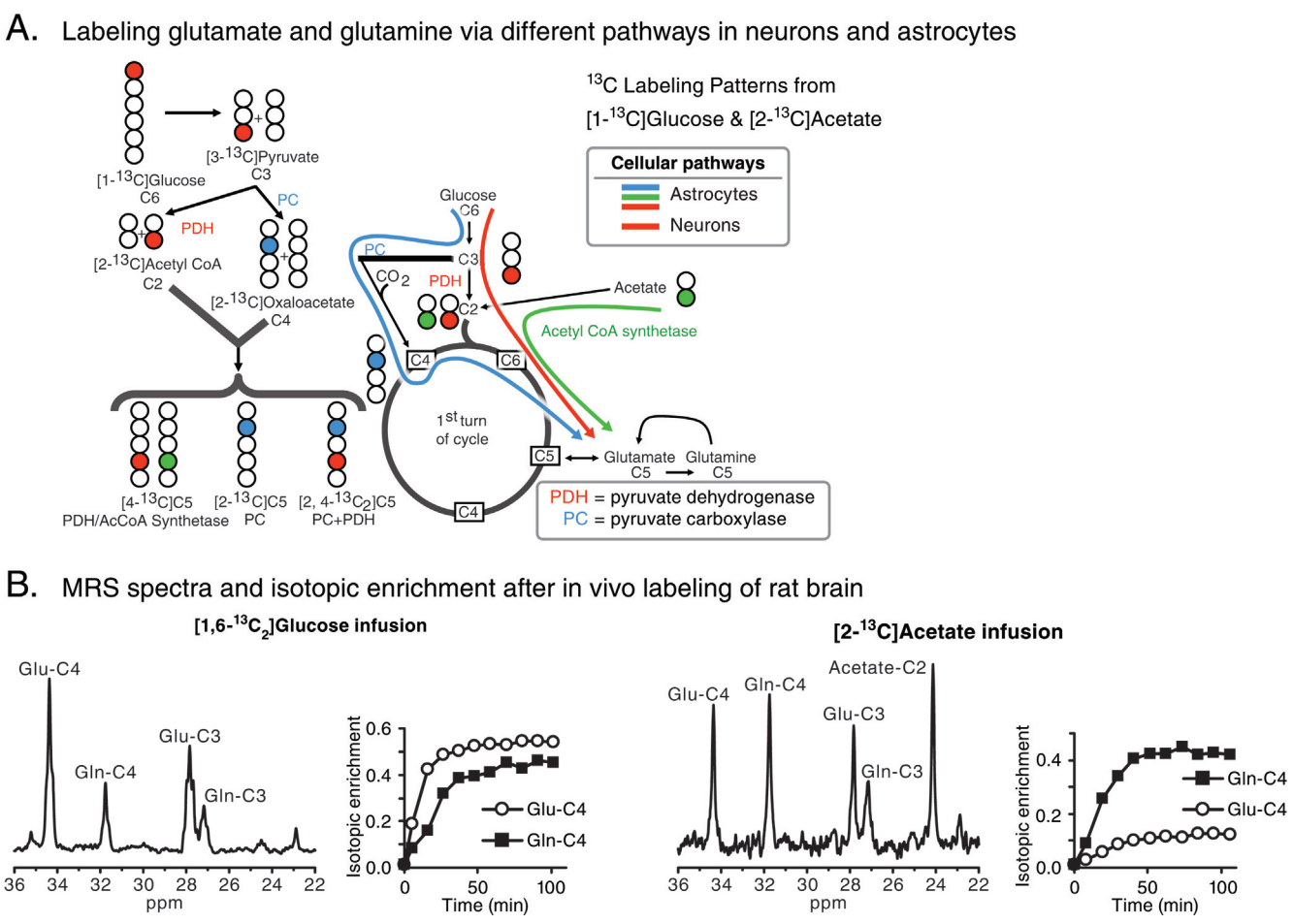

FIGURE 3.17 **Cellular compartmentation of metabolism: Labeling patterns of glutamate and glutamine.** (A) Magnetic resonance spectroscopy (MRS) has the advantage that labeled carbons can be identified and the extent of their labeling quantified in brain *in vivo*, thereby allowing real-time assessment of metabolic pathway fluxes and metabolite shuttling between astrocytes and neurons. Metabolism of a glucose molecule (Note: C6 denotes a 6-carbon molecule, C5, a 5-carbon molecule, etc.) that is labeled with ^{13}C in carbon one (red), causes labeling of (i) carbon 3 of *one* of the two pyruvate molecules generated from glucose, (ii) carbon 2 of *one* of the two molecules of acetyl Coenzyme A (CoA) generated by the pyruvate dehydrogenase reaction (PDH), and (iii) carbon 4 of glutamate (denoted as Glu-C4) during the first turn of the TCA cycle, followed by labeling of carbon 4 of glutamine (Gln-C4) by the glutamine synthetase reaction. The same labeling *patterns* are obtained with [6-^{13}C]glucose, but less label will accumulate with [1-^{13}C]glucose if the pentose phosphate shunt pathway is active due to decarboxylation of carbon one (Fig. 3.6). Labeling patterns resulting from subsequent turns of the TCA cycle are more complex and can be detected with current technology (e.g., Glu-C3, Gln-C3). When [1-^{13}C]glucose is metabolized via the pyruvate carboxylase (PC) reaction in astrocytes, carbon 2 of oxaloacetate (a 4-carbon compound, denoted by C4) becomes labeled (blue), labeling carbon 2 of glutamate (Glu-C2) and glutamine (Gln-C2). Metabolism of [2-^{13}C]acetate by astrocytes causes labeling of carbon 4 of glutamate (Glu-C4) and glutamine (Gln-C4) (green). (B) MRS measurements of metabolic labeling by [1,6-$^{13}C_2$]glucose and [2-^{13}C]acetate of metabolites in rat brain *in vivo*, determined at 9.4 Tesla in a localized volume of $9x5 \times 9$ mm^3 that encompasses most of the brain. The left panels of each pair show representative spectra at *isotopic steady-state* (see Boxes 3.2 and 3.3). Peak intensities reflect ^{13}C concentrations, which are the products of total concentration times isotopic enrichment. Note the strikingly different ratios of glutamate (Glu)-C4 to glutamine (Gln)-C4 peak intensities obtained with [1,6-$^{13}C_2$]glucose and [2-^{13}C]acetate (identified as acetate-C2 in the right-panel spectrum), which directly reflects metabolic compartmentation. The right panels in each pair show the time courses of ^{13}C label incorporation into Glu-C4 and Gln-C4 in the rat brain *in vivo* during infusion of [1,6-$^{13}C_2$]glucose (left) and [2-^{13}C]acetate (right). With ^{13}C-glucose, Glu-C4 is labeled more rapidly and reaches higher isotopic enrichment than Gln-C4, consistent with glucose being metabolized predominantly in neuronal TCA cycle, followed by glutamate−glutamine cycling and incorporation of label into glutamine in the astrocytes. Isotopic enrichment after 120 min is about 54% for Glu-C4 and 45% for Gln-C4. Assuming glutamate and glutamine concentration to be 10 mmol L^{-1} and 4 mmol L^{-1}, respectively, this corresponds to ^{13}C concentrations of 5.4 mmol L^{-1} for Glu-C4 and 1.8 mM for Gln-C4, consistent with a 3:1 peak ratio on the NMR spectrum (left). In contrast, with ^{13}C-acetate, Gln-C4 is labeled more rapidly and reaches higher isotopic enrichment than Glu-C4, consistent with acetate being metabolized predominantly in the astrocytic TCA cycle; the lower concentration of glutamate is the true precursor for glutamine, and astrocytes contain most of the glutamine. Isotopic enrichment after 120 min is ~42% for Gln-C4 and only 12% for Glu-C4. Also, glutamate labeling is heavily diluted by unlabeled glucose metabolized in neurons and glutamate−glutamine cycling of unlabeled glutamate from neurons. Assuming glutamate and glutamine concentration to be 10 mmol L^{-1} and 4 mmol L^{-1}, respectively, ^{13}C concentrations at isotopic steady state are 1.6 mmol L^{-1} for Gln-C4 and 1.2 mmol L^{-1} for Glu-C4, consistent with similar peak intensities for both signals on the MRS spectrum. *The figures in panel B were kindly provided by Dinesh Deelchand and Pierre-Gilles Henry, Center for Magnetic Resonance Research, University of Minnesota, Minneapolis.*

glutamate, glutamine, and aspartate is used to calculate glucose oxidation rates in neurons and astrocytes, glutamate–glutamine cycling, and anaplerotic rate. Current estimates of TCA cycle rates in astrocytes and neurons are about 20–30% and 70–80%, respectively, of the total glucose oxidation rate, and pyruvate carboxylase is about 10% of the oxidative flux (e.g., Hertz, 2011; Rothman et al., 2011).

Summary

Brain imaging relies mainly on metabolic fluxes that govern the levels, labeling, or redox state reporter molecules, and recent studies in many interrelated fields using different combinations of technologies have made considerable progress in understanding function-induced shifts in metabolic activity. Brain activation is a very complex process that can vary with stimulus intensity and duration, physiological state of the subject (awake or anesthetized), and the anatomical pathway. Signaling by neural cells is heterogeneously stimulated with varying temporal and spatial profiles causing changes in blood flow and metabolic rates to satisfy increased metabolic demand. Restoration of ionic gradients is considered to be the major energy-consuming process, and recent work has brought attention to the contributions of postsynaptic cells during activation. The cellular basis of increased metabolic activity and the pathway fluxes preferentially stimulated during brain activation are not fully understood due to technical limitations of *in vivo* studies. It has been argued that if (i) neurons account for most of the oxidative metabolism of glucose, (ii) similar amounts of glucose are consumed by astrocytes and neurons, and (iii) the ratio of oxygen to glucose consumption is close to six, then there may be some lactate shuttling and oxidation within brain under resting conditions. However, during activation, much more glucose is consumed compared with oxygen, labeled metabolites of glucose, including lactate, are quickly released from brain, and CMR_{glc} is greatly underestimated when measured with labeled glucose compared with DG. The physiological status of the subject, experimental conditions, and spatial–temporal limitations of currently available methodologies must be taken into account when interpreting data related to the cellular basis of brain activation.

PATHOPHYSIOLOGICAL CONDITIONS DISRUPT ENERGY METABOLISM

Derangement of brain energy metabolism arises from many causes, including inadequate nutrition, genetic diseases involving brain transporters and enzymes, neurodegenerative diseases, traumatic brain injury, mitochondrial dysfunction, diseases involving other organ systems that result in imbalances that seriously affect brain development and function, and diseases that affect fuel delivery to brain (Table 3.4). Because cardiovascular and pulmonary disease and diabetes are becoming increasingly important as midlife diseases that can have profound effects on brain function, this section will focus on some selected consequences of hypoglycemia (low glucose levels), hypoxia (low oxygen levels), and ischemia (no blood flow, therefore depriving tissue of both oxygen and glucose) on metabolite levels that reflect major shifts in overall energy status. Impairment of mitochondrial energy metabolism and its relationship to cell death are key aspects of energetics of brain injury and disease, and interested readers are referred to several reviews (Gibson et al., 2010; Brand and Nicholls, 2011; Perez-Pinzon et al., 2012).

Hypoglycemia

Compensatory regulatory mechanisms in peripheral organs involving the endocrine system, mobilization of glycogen, and use of endogenous compounds to synthesize glucose (e.g., amino acids from muscle) tightly control blood glucose levels. For this reason, overt hypoglycemia is rare under normal circumstances. However, with the increase in prevalence of diabetes and the possibility of excessive insulin administration, hypoglycemia is a potentially serious problem for diabetic patients because the supply of glucose to the brain depends on the gradient from blood to brain (Fig. 3.3A). When glucose supply cannot satisfy demand, the brain-to-plasma glucose concentration ratio falls (Fig. 3.3B), and when the brain glucose level fall below about 0.5 μmol g^{-1} (in the rat) hexokinase becomes unsaturated, causing the rate of glucose utilization to fall progressively as glucose level is reduced (Fig.3.3C). As the severity of hypoglycemia increases, the level of alertness shifts from lethargy to stupor and to coma, and these transitions are characterized by progressive changes in EEG to the point of isoelectricity (Table 3.5, top).

The energy status in brain is maintained at normal levels until a threshold is reached at which point phosphocreatine (PCr) is consumed to buffer ATP levels; PCr levels then quickly fall and creatine (Cr) levels rise (Fig. 3.18A). During this interval, brain ATP, ADP, and AMP levels are nearly constant, but once a critical point is reached energy failure is rapid and nearly complete; there is an abrupt fall in ATP concentration that is accompanied by increases in ADP and AMP

TABLE 3.4 Examples of conditions or disorders involving brain energy metabolism pathways

Category	Compound, reaction, or processes affected	Characteristics	Consequences
Nutrition	Thiamine (vitamin B_1)	Deficiency impairs transketolase and α-ketoglutarate DH activities	Impair pentose phosphate shunt and TCA cycle activities; selective regional brain damage
	Pyridoxal phosphate	Deficiency impairs transaminase and decarboxylase activities	Many reactions affected, including synthesis of neurotransmitters
	Biotin	Deficiency impairs carboxylation reactions	Anaplerotic reactions affected; developmental delay, seizures, death if not treated with supplements
Transport	Glucose	GLUT1 deficiency	Reduced glucose transport into brain; seizures, developmental delay
Anaplerosis	CO_2 fixation	Pyruvate carboxylase deficiency	Reduced anaplerosis, affecting TCA cycle-derived amino acids; severe mental retardation or death
Fuel delivery	Glucose	Hypoglycemia (low glucose)	Rate of glucose utilization (CMR_{glc}) falls; oxidative metabolism of endogenous metabolites rises; progressive decline in level of consciousness with time and severity, with risk of brain damage and death
	Oxygen	Hypoxia, anoxia (low or no oxygen)	CMR_{O2} is impaired but may be maintained by compensatory mechanisms (e.g., HIF pathway); glycolysis increases; mental capability falls with risk of brain damage and death
	Glucose and oxygen	Ischemia (severe reduction or blockade of blood flow; little or no delivery of glucose and O_2)	Unconscious within seconds; selective neuronal death or necrotic infarction of affected tissue, depending on severity, duration, and restoration of blood flow
Mitochondrial defects	Oxidative metabolism	Deficiencies in pyruvate DH and α-ketoglutarate DH	Common phenotype in many diseases that can arise for many reasons. Oxidative deficiencies are present in Alzheimer's and Huntington's diseases, stroke, motor neuron disease
		Mutations in mitochondrial or nuclear DNA have been identified for all respiratory chain complexes and ATP synthase	Deficiencies cause encephalopathy, lactic acidosis, movement disorders, death
Amino acid, fatty acid, & glycogen metabolism	Many pathways	Major effects are in peripheral pathways, causing secondary consequences in brain	Phenylketonuria, maple syrup urine disease, hepatic disease, homocystinuria, urea cycle defects, and fatty acid oxidation defects involve the central nervous system with serious consequences, including mental retardation

concentrations (Fig. 3.18B). During the hypoglycemic span when ATP levels are maintained at normal levels, endogenous substrates in brain are consumed, and the tissue contents of glycogen and the amino acids that can be oxidized via the TCA cycle are progressively depleted (Siesjö, 1978). Increased cerebral blood flow is one of the compensatory responses to severe hypoglycemia, and oxygen consumption is maintained at about 80% of normal until late stages of a hypoglycemic episode, reflecting the continuous oxidation of endogenous brain metabolites (Table 3.5, top). A particular problem with diabetic patients is that they often do not recognize the signs and symptoms of hypoglycemia, a condition called hypoglycemic unawareness that puts the patient at risk for serious accidents during cognitive impairment (Cheah and Amiel, 2012; McCall, 2012). Selective neuronal vulnerability and cell death during prolonged hypoglycemia have a variety of potential causes (Suh et al., 2007). Administration of glucose is required to bring a subject out of hypoglycemic coma, and, although consciousness may be restored relatively quickly, the time required for recovery is considerably longer than might be anticipated because endogenous compounds must be resynthesized from glucose to restore their normal levels via the anaplerotic reactions (Amaral,

TABLE 3.5 Influence of hypoglycemia and hypoxia on human physiology and brain function

Arterial plasma glucose[a] [mmol L^{-1} (mg dL^{-1})]	Physiological or mental status[a,b]	CBF[c] (mL 100 g^{-1} min^{-1})	$CMRO_2$[c] (mL O_2 100 g^{-1} min^{-1})
3.9–6 (70–110)	Normal fasting range	54	3.3
4.5 (81)	Decrease insulin secretion		
3.6–3.8 (65–68)	Counterregulatory hormone responses (increase secretion of glucagon, epinephrine, growth hormone, cortisol)		
3.0 (54)	Symptoms of hypoglycemia become manifest: anxiety, palpitations, hunger, tremor, sweaty, dizzy, weak.		
2.6 (47)	Cognitive dysfunction threshold: difficulty speaking and thinking, blurred vision		
1.7 (30)	Mild confusional state and delirium		
1.1 (20)	Cognitive failure, stupor, seizures	61	2.6
<0.6 (10)	Deep coma and ultimately death	63	1.9
$\%O_2$ IN INSPIRED AIR[b] (ESTIMATED ALTITUDE IN FEET)			
21 (Sea level)	Normal	54	3.3
18 (4,000)	Delayed dark adaptation		
16–15 (7,500–9,000)	Impaired complex learning; reading test errors		
14 (11,000)	Hyperventilation		
13 (13,000)	Short term memory impairment		
14–11% (11–17,000)	Acute mountain sickness – headache, poor concentration and test performance		
11 (17,000)	Loss of critical judgment		
10 (19,000)	Increase CBF 35% (no change in global $CMRO_2$)	73	3.3
9 (21,500)	Increase CBF 70% (no change in global $CMRO_2$)		
8–6 (24,000–31,000)	Loss of consciousness		

[a]*From data reported or compiled by Ferrendelli (1974).*
[b]*Data from Siesjö et al. (1974). Note that compensatory changes associated with acclimatization at altitude (e.g., increased red blood cell number, angiogenesis, and blood flow) help to maintain normal brain function.*
[c]*From compilation by McIlwain and Bachelard (1985).*
Note that the endocrine changes in response to reduced blood glucose levels occur well before cognitive changes. Increasing the duration of exposure to any specific level of hypoglycemia below 3 mM can lead to progressive decline in brain function. During hypoxia (10% O_2), the arteriovenous difference for oxygen decreases, but blood flow increases and CMR_{O2} remains normal even though brain function is impaired.

2012). Many factors associated with diabetes, including chronic hyperglycemia and recurrent episodes of hypoglycemia, contribute to cognitive dysfunction in diabetic patients (McCrimmon et al., 2012).

Hypoxia

Hypoxia, an inadequate level of oxygen in the inspired air, is frequently experienced by persons going to high altitude. Also, patients with chronic respiratory and cardiovascular diseases may not have sufficient oxygen levels in their blood. Reducing the oxygen level in inspired air from the normal value of 21% at sea level causes progressive deterioration of mental function, with compensatory increases in blood flow to deliver more oxygen to the brain (Table 3.5, bottom). One of the earliest changes during *acute* hypoxia is reduced neurotransmitter turnover. Mild hypoxia (i.e., reduction in inspired oxygen level from 30 to 15 or 10%) causes an increase in blood flow sufficient to maintain near-normal CMR_{O2} (Fig. 3.19A). Glucose utilization also increases during hypoxia, with greater production of lactate (Fig. 3.19B). Acetylcholine levels are stable during this interval, but acetylcholine synthesis falls by more than 50% (Fig. 3.19C). Thus, acetylcholine synthesis is closely correlated with oxidative metabolism of glucose, and acetylcholine synthesis rates fall

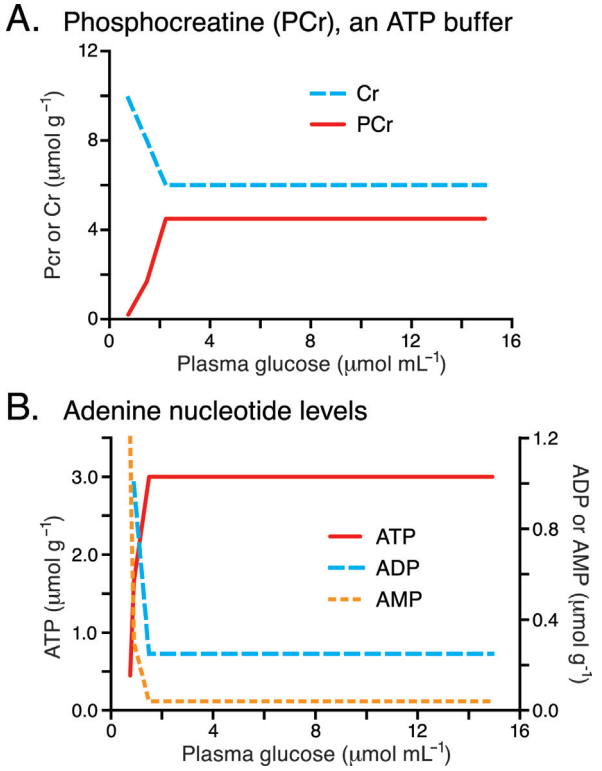

FIGURE 3.18 **Energy failure occurs during severe hypoglycemia.** (A) Phosphocreatine (PCr) is a high-energy "buffer" for ATP, and its concentration in brain is stable over a wide range of plasma glucose levels (~3–16 μmol mL^{-1}). However, when plasma glucose level is too low (2–3 μmol mL^{-1}) to maintain an adequate supply of glucose to brain (compare to Fig. 3.3), PCr level falls and creatine (Cr) concentration rises. (B) ATP concentration is maintained constant over a slightly larger range than PCr due to buffering. At a critical point, energy failure is abrupt, ATP is quickly consumed, and ADP and AMP levels rapidly rise. *Plotted from data of Lewis et al. (1974).*

proportionately as glucose oxidation is impaired (Fig. 3.19D). Biogenic amine synthesis is also very sensitive to reduced oxygen content, and hydroxylation of tryptophan (Fig. 3.16) falls by nearly half before lactate levels rise appreciably (Fig. 3.19E). During hypoxia, the supply of glucose from blood is not limiting, and brain ATP levels are preserved by buffering by PCr and by increased glycolysis to cause a large increase in tissue lactate concentration; hypoxic energy failure begins when the arterial oxygen content falls below about 35 mm Hg (Fig. 3.19F). To summarize, synthesis of specific neurotransmitters is much more sensitive to hypoxia than concentrations of these transmitters or levels of energy metabolites. Increased glycolysis compensates for deficits in oxidative metabolism over a limited range of graded hypoxia and lactate levels increase markedly. ATP concentration is buffered by PCr until a critical supply–demand energy threshold is reached and ATP levels fall. PCr level falls before ATP during hypoxia (Fig. 3.19E) and hypoglycemia (Fig. 3.18).

The brain and other body tissues have an oxygen-sensing mechanism that mediates adaptation to chronic hypoxia. The hypoxia-inducible factor-1 (HIF-1) is a transcription factor that exists in two isoforms, one of which serves as a sensor to assay tissue oxygen levels and controls the coordinated expression of genes that increase capillary density, glucose transporters, and glycolytic enzymes (LaManna et al., 2007). In brief, oxygen-dependent hydroxylation reactions result in the continuous degradation of the HIF-1α subunit by proteosomes (Fig. 3.20). Inadequate levels of oxygen cause HIF-1α to accumulate to a high enough level that it forms a heterodimer with HIF-1β. This complex binds to the hypoxia response element, thereby stimulating graded increases in mRNA and protein levels of factors that substantially increase glycolytic capacity, glucose transport, and vascular density in hypoxic tissue. To summarize, the HIF system carries out a compensatory program to adapt to hypoxia by increasing glucose delivery and metabolic capability (Fig. 3.20). The effects of this system are evident in cultured astrocytes exposed a low oxygen atmosphere for eight hours; lactate dehydrogenase and pyruvate kinase activities rise about 3- and 4-fold, respectively, and glucose utilization doubles during a metabolic challenge (Marrif and Juurlink, 1999). Thus, brain cells can adapt to the levels of essential fuel and nutrients in their environment, and glycolytic capacity of cultured cells can be up- or down-regulated by the oxygen level in the culture medium.

Ischemia

Ischemia is the blockade of blood flow to brain, thereby eliminating the supply of oxygen and glucose and preventing removal of metabolic by-products. Ischemia can be a local event, arising from a blood clot or vascular damage or it can be a global event secondary to a heart attack. Oxygen depletion prevents oxidative metabolism of amino acids and glucose depletion results in the immediate consumption of endogenous glucose and glycogen, with generation of large amounts of lactate in the brain. PCr levels fall immediately after onset of ischemia (Fig. 3.21A), followed quickly by decreases in levels of ATP, glucose, and glycogen (Fig. 3.21B); energy failure is complete within about 60 s and it results in loss of consciousness. By 2 min after decapitation, lactate levels rise to ~10 μmol g^{-1} (Fig. 3.21B), whereas during hypoxia the brain lactate level approaches twice this level (Fig. 3.19E, F) due to the continuous supply of glucose from blood, upregulation of glycolysis, and restricted efflux of lactate to blood because levels of MCT1 in adult blood–brain barrier are low and the transporter approaches saturation. Depending on the duration of ischemia, tissue damage can be selective or

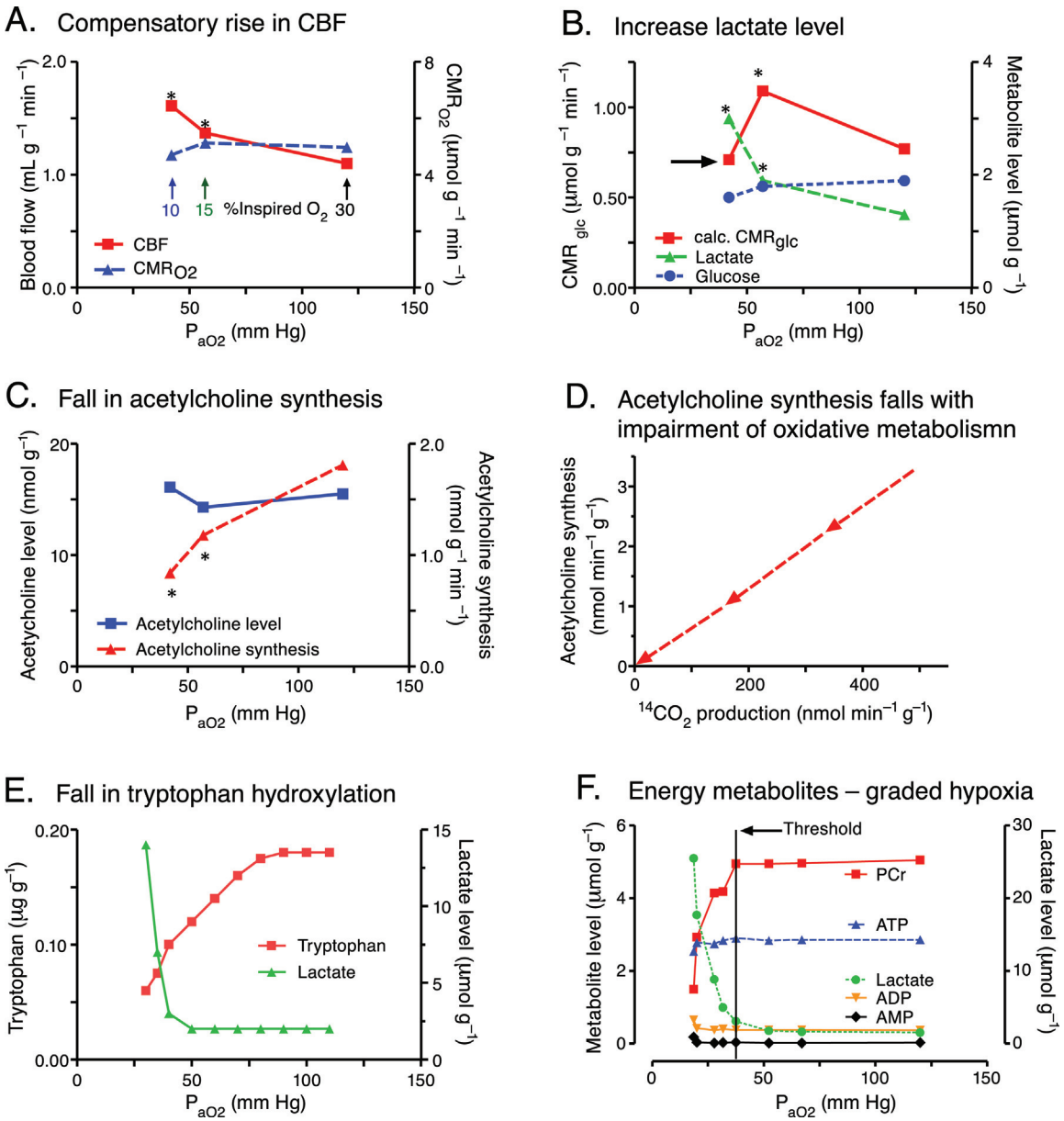

FIGURE 3.19 **Compensatory metabolic and blood flow responses and high sensitivity of neurotransmitter turnover to hypoxia.** Mild hypoxia, a 50% reduction in percent of inspired oxygen (from 21% at sea level to 10%), is associated with (A) a compensatory rise in blood flow that helps maintain the rate of oxygen consumption in brain (i.e., calculated by the Fick principle, $CMR_{O2} = CBF \times (A\text{-}V)_{O2}$), (B) an increase in glucose utilization and lactate production while brain glucose levels are stable (glucose delivery is able to match demand), and (C) a fall in the synthesis but not concentration of acetylcholine (*Panels A–C are plotted from data of Gibson and Duffy (1981)*). In panel B, glucose utilization rate was calculated by dividing the quantity of label recovered in metabolites by the specific activity of [U-^{14}C]glucose. The fall in *calculated* rate when inspired oxygen was reduced from 15 to 10% (arrow, panel B), probably reflects efflux of labeled metabolites of glucose from brain (e.g., lactate), not a fall in the true rate of glucose utilization, which should have increased in parallel with the level of lactate accumulation. (D) The rate of acetylcholine synthesis is very sensitive to hypoxia, and, under a variety of conditions, it is strongly correlated with glucose oxidation, reflected by $^{14}CO_2$ production from labeled glucose (*plotted from data of Joseph and Gibson (2007)*). (E) Tryptophan synthesis (see Fig. 3.16) is also highly sensitive to graded hypoxia, and its rate falls well before upregulation of glycolytic metabolism and increased tissue lactate levels (*plotted from data of Davis et al. (1973)*). (F) The apparent threshold for a hypoxia-induced change in energy metabolism is about P_{AO2} of 37 mm Hg, when lactate levels begin to rise and PCr levels begin to fall. Only after PCr concentration is reduced by more than 50% does ATP level begin to fall and ADP and AMP levels increase (*plotted from data of Siesjo and Nilsson (1971)*).

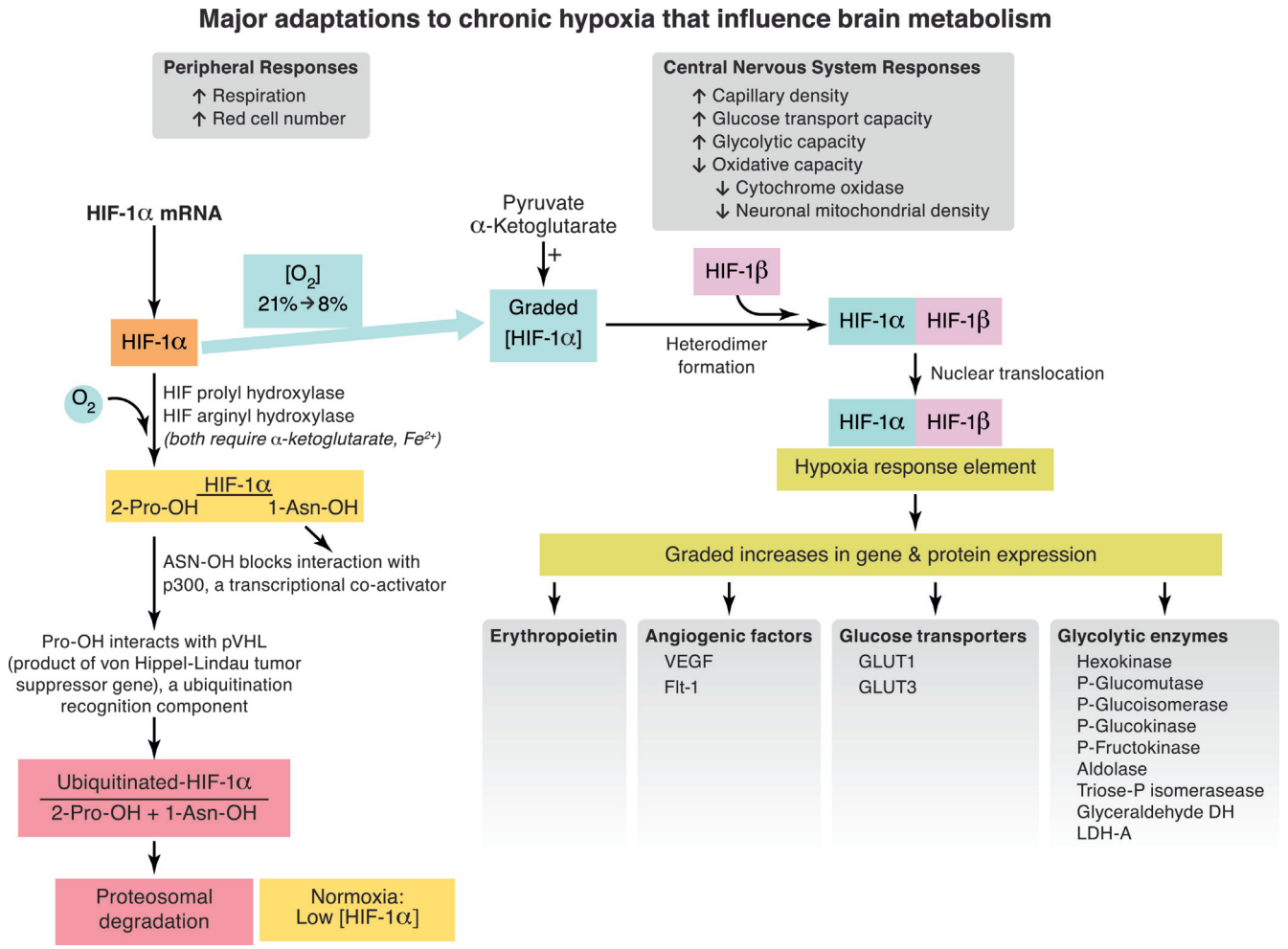

FIGURE 3.20 **An oxygen detection system regulates gene expression during chronic hypoxia.** The transcription factor, hypoxia-inducible factor-1 (HIF-1) exists in α and β isoforms and can form a heterodimer that binds to the hypoxia response element in the nucleus and induces transcription of a number of genes that enable adaptation to hypoxia. HIF-1α is hydroxylated on proline (Pro) and asparagine (Asn) moieties by enzymes that require oxygen; these posttranslational modifications influence transcriptional activity of HIF-1α and act as recognition sites for ubiquination that leads to proteosome-mediated degradation. Thus, at normal oxygen levels, HIF-1α is continuously degraded and its levels are low; with progressive reduction in oxygen level HIF-1α accumulates, forms heterodimers, and stimulates gene and protein expression, thereby increasing the brain's capacity for blood flow, transport, and carbohydrate metabolism. *Adapted from LaManna et al. (2007), with the kind permission of Springer Science and Business Media.*

severe. In the hippocampus, CA1 pyramidal neurons are most vulnerable to duration of ischemia, but the progression of cell death takes place over several days after a 30 min transient global ischemic episode in the rat; small-to medium-sized neurons in the caudate also exhibit selective vulnerability, but they die faster, within 24 h of reperfusion. Prolonged ischemia results in necrotic cell death or infarction, in which all cell types in the flow-compromised tissue are killed over a relatively short time course. Brief energy failure is not sufficient to kill brain cells, and many of the deleterious processes that irreversibly damage vulnerable neurons (excitotoxicity, oxidative damage, loss of calcium homeostasis, etc.) take place during the reperfusion interval. Abnormal NMDA receptor activation, dysregulation of calcium homeostasis, and impairment of mitochondrial ATP generation are considered to be major factors in ischemic neuronal death (Nicholls et al., 2007). Many therapeutic strategies have been tested for postischemic neuroprotection in various model systems, including the HIF-hypoxia-adaptive system (Karuppagounder and Ratan, 2012) but none have had much success in humans (Ginsberg, 2009; O'Collins et al., 2012).

Summary

Brain can compensate for inadequate supplies of oxygen and glucose over a varied range of fuel deficits, depending on severity and duration. Energy levels can

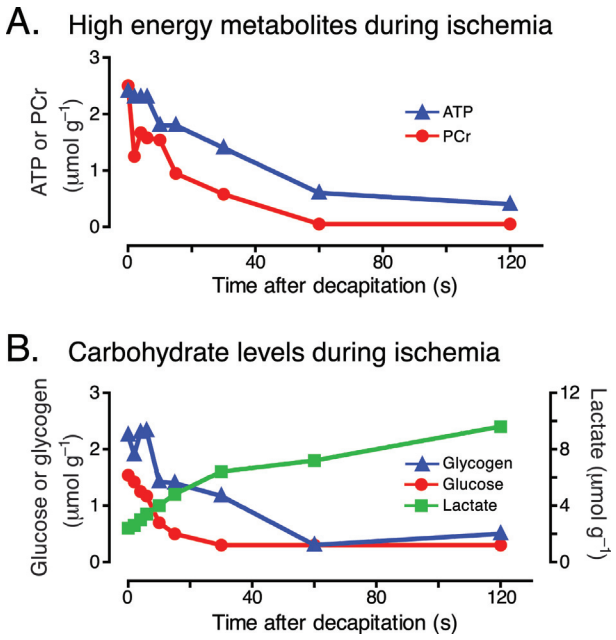

FIGURE 3.21 **Ischemia deprives brain of blood flow, blocking delivery of oxygen and glucose and removal of metabolic by-products.** (A) High energy metabolites are nearly depleted within 1 min after onset of ischemia in adult mouse brain. PCr levels fall faster than ATP levels. (B) Glucose and glycogen are quickly consumed, leading to a large increase in tissue lactate concentration. *Plotted from data of Lowry et al. (1964).*

be maintained by increased glycolysis when oxygen levels are reduced and by upregulation of glucose transporters and glycolytic enzymes via the HIF system, but it is likely that turnover of neurotransmitters dependent on oxygen supply (e.g., catecholamines) and oxidative metabolism (acetylcholine) is impaired. Low glucose levels can also be tolerated to a certain extent, but once hexokinase becomes unsaturated, glucose utilization rates will fall and when the critical threshold is reached energy failure is abrupt and complete. Ischemia causes rapid energy failure and loss of consciousness within about a minute of blood flow stoppage. Recovery from energy failure involves several stages, restoration of ionic gradients, generation of high-energy compounds, and resynthesis of compounds consumed when fuel supplies were inadequate.

ROLES OF NUTRIENTS AND METABOLITES IN REGULATION OF SPECIFIC FUNCTIONS AND OVERALL METABOLIC ECONOMY

Emphasis on local control of pathway flux by regulation of the activities of rate limiting enzymes by metabolic intermediates, second messengers, and energy-related compounds has been a hallmark of biochemistry for decades. In addition, nutrients, metabolites, and cofactors also regulate gene expression and have key roles in the integration of metabolic economy. These concepts are less developed in brain compared with peripheral organs, but are anticipated to attract more attention by neuroscientists in the future.

AMP-activated Protein Kinase (AMPK) Signaling Pathway—A Metabolic Sensor

Signaling and integration of local and global metabolic economy is the function of the AMP-activated protein kinase system (Hardie et al., 2012). Cycling of ATP and ADP takes place with biological work, and the cytoplasmic ATP pool is buffered by creatine-phosphate (P-Cr) (Fig. 3.22A). When ATP consumption exceeds its production, ADP accumulates and the myokinase (adenylate kinase) reaction converts 2 ADP to ATP + AMP. This is a very sensitive amplification system that reports the "energy charge" of a cell because the AMP/ATP ratio varies with the square of the ADP/ATP ratio (Fig. 3.22A). AMP is an allosteric regulator of phosphofructokinase and glycogen phosphorylase (Fig. 3.4), and AMP also signals *local* energy status by activating the AMPK system by three mechanisms: (i) stimulation of LKB1, a kinase that phosphorylates Thr^{172} on the alpha subunit of AMPK to form AMPK-P, (ii) allosteric activation of the AMPK gamma subunit, and (iii) inhibition of dephosphorylation of AMPK-P. On the other hand, *tissue and organism status* are integrated via receptor-mediated changes in intracellular calcium level to activate a calmodulin kinase kinase (CaMKK) to form AMPK-P. Phosphorylated AMPK is allosterically modulated by the redox cofactors, NAD^+ and NADH, and the AMP-activated protein kinase regulates anabolic/catabolic balance by enhancing ATP-generating pathways by regulating many steps, ranging from reaction fluxes to gene transcription, and by inhibiting ATP-consuming biosynthetic pathways (Fig. 3.22B). The AMPK system is a very sensitive energy sensor at a cellular and organismal level that detects metabolic stress as increased AMP concentration. The AMPK system is widely distributed in brain and has major roles in control of feeding behavior and control of body weight due to regulation of AMPK activity in hypothalamic neurons by hormones, peptides, and nutrients (Hardie et al., 2012; Ramamurthy and Ronnett, 2012). AMPK activation also increases production of fructose-2,6-P_2, a potent allosteric activator of phosphofructo-1-kinase, by stimulating a kinase (6-phosphofructo-2-kinase), thereby enhancing glycolytic flux (Fig. 3.22B). The fructose-2,6-P_2 flux-activating system is present in cultured astrocytes, not cultured neurons, and it conveys resistance to hypoxia/anoxia and is responsive to nitric oxide signaling (Bolanos et al., 2010). Because AMP levels are increased in ischemia, the

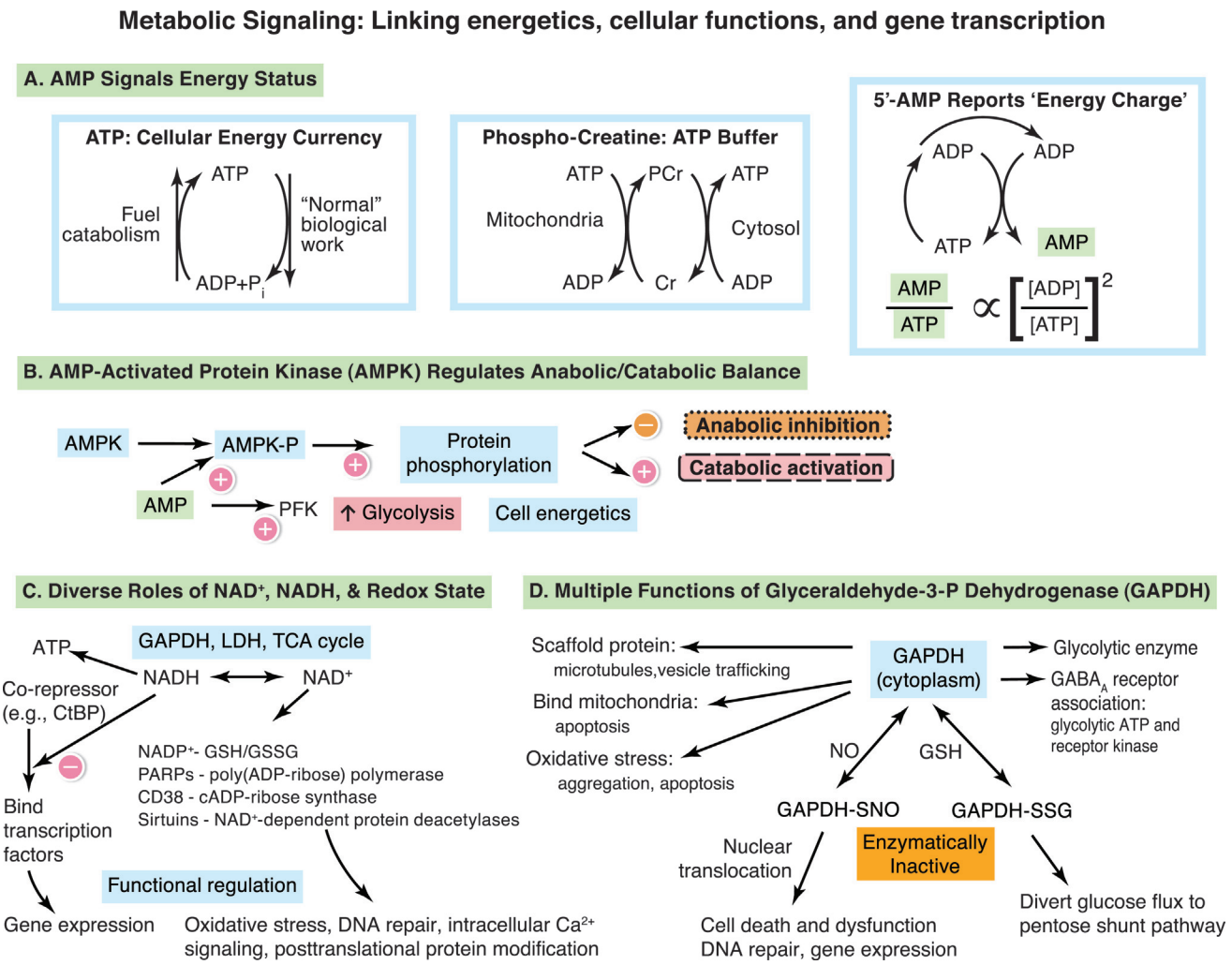

FIGURE 3.22 **Multifunctional roles of energy metabolites, redox cofactors, and enzymes coordinate metabolic signaling with cellular function and gene expression.** (A) ATP is the currency for cellular work. ATP production is highly regulated, and its concentration is buffered by phosphocreatine (PCr). When ADP accumulates, the adenylyl kinase reaction converts 2ADP into ATP + AMP, so that increased AMP level (and AMP/ATP ratio), which is normally quite low, amplifies small changes in ATP concentration. (B) AMP not only has regulatory roles in the glycolytic and glycogenolytic pathways (Fig. 3.4), it is also a signaling molecule that reports "energy charge." AMP has a key role in regulating the overall metabolic balance by anabolic (energy-requiring reactions) and catabolic (energy-producing reactions) processes by stimulating phosphorylation of AMP-activated protein kinase (AMPK). Redox cofactors also modulate the activity of AMPK-P, which acts via protein phosphorylation to inhibit anabolic and stimulate catabolic processes. In astrocytes, but not neurons, AMPK-P phosphorylates phospho-2-fructokinase to stimulate production of 2,6-bisphosphofructose, an activator of phosphofructo-1-kinase, which enhances glycolysis. (C) NAD^+ and NADH are critical cofactors in the oxidation–reduction (redox) reactions of the glycolytic pathway (Fig. 3.4), but they also have important signaling roles for regulation of diverse pathways that govern gene expression, cell survival, and intracellular signaling (see text). CtBP denotes C-terminal binding protein; LDH, lactate dehydrogenase; GSH, reduced glutathione; GSSG, oxidized glutathione. (D) Glyceraldehyde-3-phosphate dehydrogenase (GAPDH) is a multifunctional protein that has many important roles in cellular activity and survival. GAPDH is much more than a "housekeeping protein" that is used as a "loading control" for western blots. Enzymatically inactive adducts are formed in reactions involving nitric oxide (NO) and reduced glutathione (GSH) that can cause apoptosis or shift metabolic fluxes, respectively. Functions of GAPDH can be cell-type specific (e.g., when linked to GABA receptors) or be nonenzymatic (see text).

stimulation of energy-producing pathways by activated AMPK may be neuroprotective, but activation of AMPK exacerbates ischemic damage, and AMPK activation is reduced by hypothermia, conveying neuroprotection (Li and McCullough, 2010; Li et al., 2011). In summary, the AMPK system in brain has profound effects on cellular and whole-body energy homeostasis and it has important roles in pathophysiology.

Novel Roles for Nutrients in Brain Function: Signaling, Gene Expression, and Memory

Glucose is generally regarded as mainly an energy fuel, but glucose itself, its metabolites (mimicked by analogs 3-*O*-methylglucose or 2-deoxyglucose-6-phosphate), and downstream products (e.g., glucosamine) are known to regulate transcription of genes in

various tissues (e.g., glucose regulated genes) (Scott et al., 1998; Vaulont et al., 2000; Allagnat et al., 2005; Minn et al., 2006; Malhotra et al., 2013). Glucose administration can influence cognitive processes in aged rodents and humans by facilitating learning during memory task activities (Gold, 2005; Salinas and Gold, 2005). Cofactors, such as NAD^+, NADH, $NADP^+$, and NADPH are integral components of the glycolytic and pentose shunt pathways, but have many other important functions in addition to oxidation–reduction (redox) reactions (Fig. 3.22C) (Nakamura et al., 2012; Requardt et al., 2012; Wilhelm and Hirrlinger, 2012). For example, they have central nervous system roles in (i) DNA repair via PARP-1 (poly[ADP-ribose]polymerase-1), a nuclear enzyme involved in DNA repair that can cause NAD^+ depletion and inhibition of glycolysis (Alano et al., 2010; Tang et al., 2010) and (ii) in calcium signaling after NAD^+ release from a cell and its conversion by ectoenzymes to signaling molecules, nicotinic acid adenine dinucleotide phosphate (NAADP) (Heidemann et al., 2005; Pandey et al., 2009) or cyclic ADP ribose (cADPR) (Higashida et al., 2007; Young and Kirkland, 2008). NAD^+ is also required for the action of sirtuins, a family of deacetylases, that regulate activities of transcription factors and metabolic cofactors in many pathways and tissues (Chalkiadaki and Guarente, 2012; Houtkooper et al., 2012). Emerging studies identify important roles for sirtuins in brain development, aging, and neurodegenerative diseases (Harting and Knoll, 2010; Bonda et al., 2011). The transcription corepressor, C-terminal binding protein (CtBP), is a functional dehydrogenase that undergoes conformational change with binding of NAD^+ and NADH (Fig. 3.22C); NADH has a much higher affinity for CtBP, allowing it to serve as a redox sensor that destabilizes interactions with CtBP and transcription factors (Kumar et al., 2002; Fjeld et al., 2003). Glycolytic inhibition by deoxyglucose is thought to lower NADH level and increase formation of a repressor complex that acts to enhance transcription of brain-derived neurotrophic factor (BDNF) and its receptor TrkB and thereby increase neuronal excitability; the anticonvulsant properties of deoxyglucose are ascribed to blockade of seizure-induced expression of BDNF and TrkB (Garriga-Canut et al., 2006). Thus, glucose, glucose metabolites, and redox compounds are multifunctional, providing energy, interfacing with cellular damage prevention and repair, regulating genes in pathways relevant to nutritional status, improving cognition in old subjects, and generating signals that register metabolic fluxes or activities in different pathways (Fig. 3.12).

Multifunctional Metabolic Proteins

Many proteins involved in energy metabolism have functions unrelated to their enzymatic activities for which they are named. Multiple uses of a single protein is called gene sharing, and a fascinating aspect of some metabolic enzymes is their capability for multifunctional roles in which the protein fulfills specific and very different functions. For example, the crystalline proteins account for the vast majority of the water-soluble proteins in the transparent lens of the eye, and specific metabolic enzymes are major components of the crystallin lens in a species-dependent manner. In the duck, bird, and crocodile, the glycolytic enzyme lactate dehydrogenase (LDH) has a dual function as the epsilon-crystallin lens protein, whereas α-enolase is the same as tau-crystallin; in cephalopods (squid and octopus), the S-crystallin lens protein is equivalent to glutathione S-transferase (Piatigorsky, 2003). Transketolase, an enzyme in the pentose phosphate shunt pathway, is an abundant component in the mammalian cornea (Sax et al., 2000). Aldehyde dehydrogenase 3A1 is also a corneal crystallin that appears to protect against UV-induced oxidative damage by various mechanisms (Estey et al., 2007). Aldolase is a glycolytic enzyme (Fig. 3.4) that converts fructose 1,6-bisphosphate to glyceraldehyde 3-phosphate and dihydroxyacetone phosphate, and it also has noncatalytic roles as a scaffold protein that can bind to F-actin, α-tubulin, dynein, glucose transporter GLUT4, sorting nexin 9, and other proteins; these interactions are inhibited by binding of products or substrates to the enzyme, suggesting that the free pool of aldolase may act to coordinate membrane events with the cytoskeleton (Rangarajan et al., 2010). A fascinating study that examined siRNA-induced knockdown of glycolytic enzymes as a means to control cancer cell proliferation found that an 80% decrement in aldolase activity did not alter glycolytic flux or ATP level, but reduced proliferation by about 80%; proliferation was rescued by expression of enzymatically inactive aldolase, suggesting a role for aldolase interaction with the actin cytoskeleton in proliferation (Lew and Tolan, 2012). This study emphasizes the large excess capacities of glycolytic enzymes compared with *in vivo* pathway flux and unanticipated effects of enzyme knockdown.

Glyceraldehyde-3-phosphate dehydrogenase (GAPDH), a glycolytic enzyme commonly used as a "housekeeping protein" loading control for Western blots, has many important functions (Fig. 3.22D) in addition to its enzymatic activity that generates NADH during the conversion of glyceraldehyde-3-P to 1,3-diphosphoglycerate (Sirover, 2012). GAPDH enzymatic activity is inhibited

by S-nitrosylation, which leads to nuclear translocation where the enzyme acts as an NO donor and regulator of gene expression and cell death (Tristan et al., 2011). In the diabetic retina and retinal Müller cells exposed to 25 mM glucose for a few days, the ensuing oxidative-nitrosative stress causes S-nitrosylation of GAPDH, nuclear translocation of GAPDH, and subsequent apoptosis of retinal Müller cells (Yego and Mohr, 2010). S-Glutathionylation also inhibits GAPDH activity and is thought to divert glucose to the pentose phosphate shunt pathway to generate NADPH and help manage oxidative stress. GAPDH and phosphoglycerate kinase bind to the $GABA_A$ receptor, and GAPDH autophosphorylation leads to phosphorylation of the receptor that slows rundown of $GABA_A$ currents, whereas prevention of receptor phosphorylation accelerates the rundown; this behavior links postsynaptic glycolysis to inhibitory neurotransmission and suggests a role in epilepsy (Laschet et al., 2007; Pumain et al., 2008). GAPDH also functions as a scaffold protein, and its binding to mitochondria and its oxidative stress-induced aggregation are linked to apoptosis (Fig. 3.22D); these and other properties of GAPDH link the protein to various neurodegenerative diseases (Butterfield et al., 2010; Tristan et al., 2011). To sum up, examples of novel roles for metabolites, cofactors, and enzymes illustrate the interactive complexity of different systems with respect to cellular function, metabolism, gene expression, behavior, and disease.

METABOLOMICS, TRANSCRIPTOMICS, AND PROTEOMICS

Systems biology is increasingly important because it describes complex profiles of metabolites, mRNAs, and proteins in cells and tissues under different conditions. Characterization of relationships among expression of different molecular species during development and aging, under different physiological conditions, and responses to genetic manipulation is particularly useful for development of biomarkers for diseases, assessment of therapeutic efficacies of drugs, and understanding perturbations of regulatory systems after genetic engineering; these are emerging topics in brain energy metabolism.

Metabolomics

Metabolomics deals with assessment of the metabolic profile of a living cell, tissue, organism, or biological fluid to characterize and distinguish between normal and altered states (Box 3.4). Goals and applications of the field include discovery and identification of biomarkers, mechanisms of drug-induced toxicity, efficacy of drugs

BOX 3.4

METABOLOMICS

Definitions of metabolomics vary with specialty disciplines and can be confusing due to different nomenclatures in a rapidly growing field. One set of simple definitions (Fiehn, 2002; Nicholson et al., 2002; Goodacre et al., 2004; Griffin, 2004) is as follows.

Metabolome. A set of metabolites synthesized by an organism, which can be defined on all levels of complexity for organisms, tissues, cells, cell components, or fluids; the conditions of the sample need to be exactly specified.

Metabolomics. Comprehensive analysis of metabolites under a specific set of conditions in which there is a direct connection between genetic activity, protein activity, and the metabolic activity itself.

Metabolite fingerprinting. Classification of samples according to biological relevance or origin by high throughput analytical methods in which unseparated samples are analyzed and individual compounds are not identified. Fingerprinting does not aim to identify individual components; rather; it quickly classifies samples on the basis of their components.

Metabonomics. The quantitative measurement of the multivariate metabolic responses of multicellular systems to pathophysiological stimuli or genetic modification; metabonomics deals with "classifying samples, understanding biochemical mechanisms, identifying biomarkers, quantitatively analyzing concentrations and fluxes, probing molecular dynamics and interactions" (Nicholson et al., 2002).

Metabolic profiling. Analysis of a group of metabolites associated with a specific pathway.

Metabolite target analysis. Restricted assays of metabolites related to a specific enzyme system affected by a perturbation, as in pharmaceutical studies.

Metabolite biomarker. A molecular indicator of pathology or a specific "state" that might be useful for diagnostic purposes or monitoring of effects of therapeutic intervention.

at preclinical and clinical stages of development, and clinical disease diagnosis and prognosis. Because many factors influence metabolite levels and pathway fluxes (genetics, environment, temperature, nutrition and diet, age and gender, hormones, estrus stage, health status, diurnal and seasonal effects, physical fitness, stress, gut microflora), a systems approach is required. This analytical process involves successive stages: (i) *obtain raw data* for the metabolic signature via one or more technologies (e.g., high pressure liquid chromatography, gas chromatography, capillary electrophoresis, magnetic resonance spectroscopy, mass spectrometry, etc.) in which the individual peaks do not need to be identified; (ii) use *data reduction procedures* to digitize complex spectra from each sample; (iii) employ *pattern recognition techniques* (e.g., principle component analysis) to map different samples, (iv) carry out *statistical comparisons* of patterns; and (v) develop *databases*. For example, fingerprint analysis (Box 3.4) is a very powerful approach that can classify and distinguish biofluid and tissue samples. This approach is capable of distinguishing urine samples from human, rat, rabbit, and mouse, as well as distinguishing mouse strain, rodent gender, stage of estrus cycle, age, and time of urine collection (day or night) (Bollard et al., 2005).

Anatomical brain regions have specialized functions and neurotransmitter pathways, and metabolomic analysis of brain tissues is a rapidly progressing field that will make major contributions to characterization of normal brain tissue and altered brain function during pathophysiological and drug-treatment conditions (Kaddurah-Daouk et al., 2008). For example, analysis of postmortem brain from schizophrenic patients demonstrates profound changes in protein expression and metabolite levels in tissue from subjects with low-cumulative medication levels but not with medium-cumulative medication compared with controls and bipolar disorder patients, suggesting efficacy of treatment (Chan et al., 2011). $^{1}H/^{13}C$-NMR spectroscopy and metabolomic analysis of glutamate receptor subtypes and GABA receptor modulation revealed distinct patterns of metabolic change evoked by receptor agonists and antagonists (Rae et al., 2006; Rae et al., 2009). Metabolomic analysis helps characterize anesthetic effects (Makaryus et al., 2011; Jacob et al., 2012) and facilitates the search for biomarkers to characterize brain tumors (Hekmatyar et al., 2010) and Alzheimer's disease (Salek et al., 2010). Multiple "Omics" approaches are also used to better understand Parkinson's disease (Caudle et al., 2010).

Transcriptomics

Analysis of mRNA expression in cultured brain cells and tissue under different conditions provides important information regarding changes in gene expression arising from different developmental stages, physiological conditions, or genetic manipulations that influence the cell's capacity to synthesize specific proteins. For example, transcriptome analyses of acutely isolated astrocytes, neurons, oligodendrocytes, and endothelial cells during early mouse brain development generated a database comprised of more than 20,000 genes and revealed distinct differences among the major brain cell types (Cahoy et al., 2008; Daneman et al., 2010).

Extensive analysis of brain transcripts relevant to energy metabolism is rare, and findings must be accompanied by studies to verify the functional metabolic capacity suggested by the presence or absence of specific mRNAs. For example, analysis of mRNA levels in astrocytes and nonastrocytic cells acutely isolated from mature murine brain showed distinct enrichments of mRNA that were generally in accordance with established distributions of metabolic enzymes among astrocytes and neurons (Lovatt et al., 2007). Many studies have examined changes in levels of small numbers of specific mRNAs related to proteins of interest, and results from some of these studies underscore the important observation that *up- or down-regulation of mRNA need not be correlated with changes in protein levels*, implying translational regulation. Also, *mRNA and protein* levels may change *disproportionately or in different directions*, and even if there are large changes in *protein concentration, the altered capacity may, but need not, be accompanied by changes in levels of relevant metabolites or fluxes* through the pathway in which enzyme levels are altered (Box 3.2). For example, during water deprivation, the hypothalamic-neurohypophyseal system is activated by dehydration, and greater secretion of vasopressin and oxytocin increases the activity of magnocellular neurons that regulate water balance; higher rates of neuronal firing are associated with a 2.6-fold increase in glucose utilization. One aspect of the compensatory response to water deprivation is increased levels of glucose transporter protein GLUT1, which is expressed in glia and endothelial cells, and GLUT3, which is expressed in neurons. Notably, GLUT1 *mRNA levels fell* by about 43% after 3 days of water deprivation, whereas the GLUT1 *protein level increased* 28%; during rehydration, the GLUT1 *protein level fell* towards normal, and its *mRNA level increased* (Koehler-Stec et al., 2000). During water deprivation, GLUT3 mRNA increased by about 74% and the GLUT3 protein level increased 40%, and both normalized during rehydration. Prolonged seizures quickly *upregulate* GLUT1 and GLUT3 *mRNA levels* in 10–21-day-old rats *without changes* in glucose *transporter protein* levels (Nehlig et al., 2006). Thus, mRNA levels, enzymatic catalytic activities, and

pathway fluxes can be independently regulated and change in opposing directions by varying magnitude. It may be erroneous to conclude that altered mRNA levels reflect protein and functional changes.

Genetic Engineering and Metabolism

Knock-in, knock-out, or mutation. Modification, removal, or insertion of genes is a very powerful tool to evaluate regulation, signaling, and function, but the phenotype arising from genetic manipulation can arise, in part, from secondary effects in many seemingly unrelated pathways. For example, astrocytes are extensively linked together via gap junctional channels comprised of connexin (Cx) proteins (Cx43, Cx32, and Cx26), and these intercellular pores enable passage from cell to cell of many small (i.e., molecular weight less than ~1 kDalton) biological compounds, as well as various fluorescent dyes used to assay gap junctional trafficking (see also Chapter 9). Array analysis of gene expression changes in connexin-43 knockout mice revealed up- and downregulation of 252 mRNAs that encode for proteins in many pathways; 35% were downregulated and 65% were upregulated and of the altered genes 29% were related to transcription, 19% to energy and metabolism, 9% to cell junctions, adhesion and extracellular matrix, 9% to cell signaling, 9% to transport, 8% to cell cycle, 9% to organelle genetics and cytoskeletal proteins, and 7% to unknown functions (Iacobas et al., 2005; Iacobas et al., 2008). These findings demonstrate that knockdown or knockout of a single gene can elicit large, widespread compensatory changes in gene expression in many functional systems that do not appear to be directly related to the function of the deleted gene. Notably, a substantial fraction of the genes involved in compensatory responses to Cx43 knockout is related to metabolic and energetic functions, suggesting that (i) metabolite trafficking via the astrocytic syncytium has an important role in metabolic activities of the cells and (ii) the presence of other connexins (Cx32 and Cx26) in Cx43-null astrocytes cannot carry out functions of Cx43. Gene expression linkage patterns in connexin-null brain suggest that regulation of networks of transcriptome is likely to contribute to altered phenotypes when specific functions are missing (Spray and Iacobas, 2007).

Pathway modulation. Genetic engineering approaches are often used to construct microorganisms that can mass-produce biological compounds of interest. Even when genes are successfully inserted and enzymes are overproduced, a frequent observation is that metabolite levels and metabolic fluxes are unchanged. For example, increasing the activities in yeast of eight enzymes involved in glycolysis and ethanol production by about *4–14-fold had no effect* on concentrations of major metabolites or ethanol formation, in spite of enhanced levels of major rate-limiting enzymes, hexokinase, phosphofructokinase, and pyruvate kinase (Schaaff et al., 1989). Selective increases in enzyme expression of a rate-limiting enzyme such as phosphofructokinase *generally do not alter glycolytic flux* under a variety of conditions in different organisms, including mammalian cell lines (Urbano et al., 2000). Little is known about metabolic flux changes in brain cells in response to "engineered" variations in enzyme amount, but regional and cell-type differences in amounts of mRNA and enzyme protein have been reported, with the *inference* that differences in capacity are reflected by differences in flux. However, this may not be the case, and metabolic demand (e.g., brain work and ADP generation from ATP) is an important aspect of control of metabolic rates. Metabolic control is a complex process involving interactions of many compounds and pathways (Fell, 1996).

Proteomics

The entire set of proteins in a cell, organ, or organism comprises the proteome, and proteomic analysis often focuses on protein profiles or proteins related to specific functions, subcellular fractions, organelles, or cells. Proteomic analysis of brain has been reviewed by Maurer and Kuschinsky (2007), with coverage of techniques, analysis of energy metabolism proteins, and studies of diseases. Proteins are commonly separated by two-dimensional gel electrophoresis (separation by isoelectric point and molecular weight) after extraction of samples of interest, but other separation procedures are also employed. Proteins can be analyzed by image analysis after staining and identified by various procedures, including amino acid sequencing, mass spectrometry, and immunoassays. *Proteomic profiling* is similar in principle to metabolite profiling and differential levels of proteins under specific conditions are described. *Functional proteomics* has a somewhat different focus related to protein or enzyme activity, protein–protein actions, posttranslational modifications (e.g., phosphorylation, glycosylation, sulfation, proteolytic cleavage). An interesting example of proteomic analysis is the effect of 17β-estradiol on brain mitochondrial protein expression and function. Estradiol treatment altered levels of 66 proteins out of the 500 spots detected by image analysis by at least two-fold, with upregulation of 42% and downregulation of 58%; the levels and activities of key mitochondrial enzymes were increased, and these changes were associated with increases in levels of specific mRNAs and in respiratory activity assayed in isolated mitochondria,

as well as reduced free radical formation (Nilsen et al., 2007). Thus, estradiol has widespread effects on mitochondrial protein levels and function that are consistent with its neuroprotective effects.

High-throughput protein analysis is likely to be very useful in characterization of complex disorders of brain function, particularly when used in conjunction with other systems approaches. For example, an integrative study using parallel metabolomic, transcriptomic, and proteomic analyses of postmortem human brain tissue from control subjects and schizophrenic patients identified specific alterations that are related to energy metabolism and oxidative stress (Prabakaran et al., 2004). Analysis of altered proteins, mRNAs, and metabolite levels was consistent with abnormal mitochondrial function, upregulation of oxidative stress response systems, and downregulation of glycolysis and oxidative metabolism components. These attributes were sufficient to differentiate controls from about 90% of the schizophrenic patients. Integrated approaches are also used to classify glioma tumors (Riddick and Fine, 2011).

METABOLIC SCALING ACROSS SPECIES

Whole-body metabolic rate in mammals varies inversely with size, and relationships are approximately linear when plotted on log–log graphs. The smallest animals have the highest metabolic rates and the metabolic cost of carrying out various activities by small mammals is greater than that for large animals (see monographs Schmidt-Nielsen, 1972; Schmidt-Nielsen, 1984). Similarly, brain metabolic rate scales with brain size, with larger brains having lower metabolic rates (Karbowski, 2007; Karbowski, 2011). Large brains appear to reduce signaling delays and cost in various ways, including increasing axonal fiber volume to enhance conduction velocity and reduce energy expenditure; over the range of brain size from the shrew to monkey, calculated metabolic cost and measured brain glucose utilization rates fall by a factor of 10 as brain weight increases over three orders of magnitude (Wang et al., 2008). Within various primate species, the ratio of glia-to-neurons in area 9L of frontal cortex correlates with brain weight (log–log scale), and comparison of glial density to neuronal density in this brain region in humans and 18 anthropoid primate species reveals that human glial cell (astrocytes plus oligodendrocytes, excluding microglia) density is unexpectedly high (Marino, 2006, Sherwood et al., 2006). Recent analyses show that neuronal density and neuron/glial ratios do not scale universally with brain mass across species, and human brain may be considered as a "scaled-up" primate brain that has similar numbers of neurons and glia but high numbers of neurons per unit volume that confer cognitive advantages (Herculano-Houzel, 2012a; Herculano-Houzel, 2012b). Thus, cognitive function, relative densities of major brain cell types, and cellular specialization (e.g., dendritic arborization, axonal length and diameter, etc.) may be linked to the energetics of neuronal signaling. Notably, human protoplasmic astrocytes are much larger and more complex than those in rodents, and implantation of human glial progenitor cells into neonatal mice enhances synaptic plasticity and learning in adult mice (Han et al., 2013), consistent with the important role of astrocytic glycogen in cognitive performance (Duran et al., 2013). Species differences in scaling of metabolism, structure, and function raise the interesting possibility that similar genetic manipulations in small (mice) compared to large (primates) subjects may have a different, size-dependent impact on functional metabolism.

SUMMARY

Brain energy metabolism is a very complex process involving specialized functions of neurons, astrocytes, the vasculature, and other cells. Glucose and oxygen are the primary and obligatory fuels for brain, but minor substrates are also consumed to varying extents under different developmental, physiological, and pathophysiological states. The physical structure of the brain and many regulatory systems ensure that local capacities for fuel delivery, energy generation, and functional activity are closely matched under normal and activated conditions. Ion pumping is the major energy-consuming process in brain, and neuronal activity governs ATP demand and glucose utilization at a local level. Because functional activity and metabolic rates are closely correlated, pathways and compounds involved in metabolism are commonly used for brain imaging or spectroscopic studies using different technologies and a wide range of experimental approaches and systems. Metabolic fluxes can be measured in real time *in vivo*, and they are heterogeneous throughout the brain at a regional, cellular, and subcellular level. The cellular contributions to brain energetics and brain images are not firmly established, but specific neurons in the brainstem can control the overall metabolic economy of the body and feeding behavior. Glucose utilization is integrated with pathways of glucose-derived neurotransmitter turnover, which is much more sensitive to metabolic disruption than metabolite or transmitter concentrations. The brain has no significant energy reserves except glycogen, and progressive decrements in cognitive activity occur when oxygen and glucose levels are inadequate.

During abnormal states, brain ATP levels are maintained within the normal range until a critical threshold is reached. Subsequent energy failure is abrupt and complete, with loss of consciousness. Recovery from transient energy failure requires restoration of ionic gradients and levels of high-energy compounds, resynthesis of endogenous compounds consumed during the episode, and repair of damage. Evaluation of disease states and pharmacological treatment paradigms is often monitored by metabolic brain imaging. Emerging systems biology approaches are powerful procedures to characterize and identify tissue and biofluid samples. Major advances in brain energetics are technology-driven, and multimodal approaches are making important contributions to understanding functional metabolism in brain.

References

Reference monographs

Balázs, R., Cremer, J.E. (Eds.), 1972. Metabolic Compartmentation in the Brain. John Wiley & Sons, New York.

Berl, S., Clarke, D.D., Schneider, D. (Eds.), 1975. Metabolic Compartmentation and Neurotransmission: Relation to Brain Structure and Function. Plenum Press, New York.

Davson, H., Segal, M.B., 1996. Physiology of the CSF and Blood–Brain Barriers. CRC Press, Boca Raton.

Fell, D. (Ed.), 1996. Understanding the Control of Metabolism. Portland Press, Colchester.

Gibson, G.E., Dienel, G.A., 2007. Brain energetics: Integration of molecular and cellular processes. In: Lajtha, A. (Ed.), Handbook of Neurochemistry and Molecular Biology, third ed. Springer-Verlag, Berlin.

McIlwain, H., Bachelard, H.S., 1985. Biochemistry and the Central Nervous System, fifth ed. Churchill Livingstone, Edinburgh.

Passonneau, J.V., Lowry, O.H., 1993. Enzymatic Analysis: A Practical Guide. Humana Press, Totowa, NJ.

Phelps, M.E., 2004. PET. Molecular Imaging and Its Biological Applications. Springer, New York.

Phelps, M.E., Mazziotta, J.C., Schelbert, H.R. (Eds.), 1986. Positron Emission Tomography and Autoradiography: Principles and Applications for the Brain and Heart. Raven Press, New York.

Riggs, D.S., 1970. The Mathematical Approach to Physiological Problems. The MIT Press, Cambridge, MA.

Schmidt-Nielsen, K., 1972. How Animals Work. Cambridge University Press, New York.

Schmidt-Nielsen, K., 1984. Scaling. Why Is Animal Size So Important? Cambridge University Press, New York.

Siesjö, B.K., 1978. Brain Energy Metabolism. Wiley-Interscience, John Wiley & Sons, Chichester.

Literature references

Abe, T., Takahashi, S., Suzuki, N., 2006. Oxidative metabolism in cultured rat astroglia: effects of reducing the glucose concentration in the culture medium and of D-aspartate or potassium stimulation. J. Cereb. Blood. Flow. Metab. 26, 153–160.

Adachi, K., Cruz, N.F., Sokoloff, L., Dienel, G.A., 1995. Labeling of metabolic pools by [6-^{14}C]glucose during K^+-induced stimulation of glucose utilization in rat brain. J. Cereb. Blood. Flow. Metab. 15, 97–110.

Alano, C.C., Garnier, P., Ying, W., Higashi, Y., Kauppinen, T.M., Swanson, R.A., 2010. NAD^+ depletion is necessary and sufficient for poly(ADP-ribose) polymerase-1-mediated neuronal death. J. Neurosci. 30, 2967–2978.

Allagnat, F., Martin, D., Condorelli, D.F., Waeber, G., Haefliger, J.A., 2005. Glucose represses connexin36 in insulin-secreting cells. J. Cell. Sci. 118, 5335–5344.

Allen, N.J., Karadottir, R., Attwell, D., 2005. A preferential role for glycolysis in preventing the anoxic depolarization of rat hippocampal area CA1 pyramidal cells. J. Neurosci. 25, 848–859.

Amaral, A.I., 2012. Effects of hypoglycaemia on neuronal metabolism in the adult brain: role of alternative substrates to glucose. J. Inherit. Metab. Dis. 36 (4), 621–634.

Attwell, D., Buchan, A.M., Charpak, S., Lauritzen, M., Macvicar, B. A., Newman, E.A., 2010. Glial and neuronal control of brain blood flow. Nature. 468 (7321), 232–243.

Bachelard, H., Badar-Goffer, R., 1993. NMR spectroscopy in neurochemistry. J. Neurochem. 61, 412–429.

Badar-Goffer, R.S., Bachelard, H.S., Morris, P.G., 1990. Cerebral metabolism of acetate and glucose studied by ^{13}C-n.m.r. spectroscopy. A technique for investigating metabolic compartmentation in the brain. Biochem. J. 266, 133–139.

Bak, L.K., Schousboe, A., Sonnewald, U., Waagepetersen, H.S., 2006. Glucose is necessary to maintain neurotransmitter homeostasis during synaptic activity in cultured glutamatergic neurons. J. Cereb. Blood. Flow. Metab. 26, 1285–1297.

Bak, L.K., Obel, L.F., Walls, A.B., Schousboe, A., Faek, S.A., Jajo, F.S., et al., 2012. Novel model of neuronal bioenergetics: Post-synaptic utilization of glucose but not lactate correlates positively with Ca^{2+} signaling in cultured mouse glutamatergic neurons. ASN Neuro. 4 (3), 151–160. Available from: http://dx.doi.org/10.1042/AN20120004, Apr 5; pii: e00083.

Ball, K.K., Gandhi, G.K., Thrash, J., Cruz, N.F., Dienel, G.A., 2007. Astrocytic connexin distributions and rapid, extensive dye transfer via gap junctions in the inferior colliculus: implications for [^{14}C]glucose metabolite trafficking. J. Neurosci. Res. 85, 3267–3283.

Bauer, D.E., Jackson, J.G., Genda, E.N., Montoya, M.M., Yudkoff, M., Robinson, M.B., 2012. The glutamate transporter, GLAST, participates in a macromolecular complex that supports glutamate metabolism. Neurochem. Int. 61, 566–574.

Bergles, D.E., Diamond, J.S., Jahr, C.E., 1999. Clearance of glutamate inside the synapse and beyond. Curr. Opin. Neurobiol. 9, 293–298.

Bolanos, J.P., Almeida, A., Moncada, S., 2010. Glycolysis: a bioenergetic or a survival pathway? Trends. Biochem. Sci. 35, 145–149.

Bollard, M.E., Stanley, E.G., Lindon, J.C., Nicholson, J.K., Holmes, E., 2005. NMR-based metabonomic approaches for evaluating physiological influences on biofluid composition. NMR. Biomed. 18, 143–162.

Bonda, D.J., Lee, H.G., Camins, A., Pallas, M., Casadesus, G., Smith, M.A., et al., 2011. The sirtuin pathway in ageing and Alzheimer disease: mechanistic and therapeutic considerations. Lancet. Neurol. 10, 275–279.

Boumezbeur, F., Petersen, K.F., Cline, G.W., Mason, G.F., Behar, K.L., Shulman, G.I., et al., 2010. The contribution of blood lactate to brain energy metabolism in humans measured by dynamic ^{13}C nuclear magnetic resonance spectroscopy. J. Neurosci. 30, 13983–13991.

Bourne, J.N., Harris, K.M., 2008. Balancing structure and function at hippocampal dendritic spines. Annu. Rev. Neurosci. 31, 47–67.

Bouzier-Sore, A.K., Voisin, P., Canioni, P., Magistretti, P.J., Pellerin, L., 2003. Lactate is a preferential oxidative energy substrate over glucose for neurons in culture. J. Cereb. Blood. Flow. Metab. 23, 1298–1306.

Bouzier-Sore, A.K., Voisin, P., Bouchaud, V., Bezancon, E., Franconi, J.M., Pellerin, L., 2006. Competition between glucose and lactate as oxidative energy substrates in both neurons and astrocytes: a comparative NMR study. Europ. J. Neurosci. 24, 1687–1694.

Brand, A., Engelmann, J., Leibfritz, D., 1992. A ^{13}C NMR study on fluxes into the TCA cycle of neuronal and glial tumor cell lines and primary cells. Biochimie. 74, 941–948.
Brand, M.D., Nicholls, D.G., 2011. Assessing mitochondrial dysfunction in cells. Biochem. J. 435, 297–312.
Brennan, A.M., Connor, J.A., Shuttleworth, C.W., 2006. NAD(P)H fluorescence transients after synaptic activity in brain slices: predominant role of mitochondrial function. J. Cereb. Blood. Flow. Metab. 26, 1389–1406.
Butterfield, D.A., Hardas, S.S., Lange, M.L., 2010. Oxidatively modified glyceraldehyde-3-phosphate dehydrogenase (GAPDH) and Alzheimer's disease: many pathways to neurodegeneration. J. Alzheimers Dis. 20, 369–393.
Butterworth, R.F., 2006. Metabolic encephalopathies. In: Siegel, G.J., Albers, R.W., Brady, S.T., Price, D.L. (Eds.), Basic Neurochemistry: Molecular, Cellular, and Medical Aspects, seventh ed. Academic Press, San Diego, pp. 593–602.
Buxton, R.B., 2010. Interpreting oxygenation-based neuroimaging signals: the importance and the challenge of understanding brain oxygen metabolism. Front. Neuroenerg. 2, 8.
Buxton, R.B., 2012. Dynamic models of BOLD contrast. NeuroImage. 62 (2), 953–961.
Caesar, K., Hashemi, P., Douhou, A., Bonvento, G., Boutelle, M.G., Walls, A.B., et al., 2008. Glutamate receptor-dependent increments in lactate, glucose and oxygen metabolism evoked in rat cerebellum in vivo. J. Physiol. 586, 1337–1349.
Cahoy, J.D., Emery, B., Kaushal, A., Foo, L.C., Zamanian, J.L., Christopherson, K.S., et al., 2008. A transcriptome database for astrocytes, neurons, and oligodendrocytes: a new resource for understanding brain development and function. J. Neurosci. 28, 264–278.
Caudle, W.M., Bammler, T.K., Lin, Y., Pan, S., Zhang, J., 2010. Using 'omics' to define pathogenesis and biomarkers of Parkinson's disease. Expert. Rev. Neurother. 10, 925–942.
Cerdan, S., Kunnecke, B., Seelig, J., 1990. Cerebral metabolism of [1,2-^{13}C2]acetate as detected by in vivo and in vitro ^{13}C NMR. J. Biol. Chem. 265, 12916–12926.
Cerdan, S., Rodrigues, T.B., Sierra, A., Benito, M., Fonseca, L.L., Fonseca, C.P., et al., 2006. The redox switch/redox coupling hypothesis. Neurochem. Int. 48, 523–530.
Cetin, N., Ball, K., Gokden, M., Cruz, N.F., Dienel, G.A., 2003. Effect of reactive cell density on net [2-^{14}C]acetate uptake into rat brain: labeling of clusters containing GFAP + - and lectin + -immunoreactive cells. Neurochem. Int. 42, 359–374.
Chalkiadaki, A., Guarente, L., 2012. Sirtuins mediate mammalian metabolic responses to nutrient availability. Nat. Rev. Endocrinol. 8, 287–296.
Chan, M.K., Tsang, T.M., Harris, L.W., Guest, P.C., Holmes, E., Bahn, S., 2011. Evidence for disease and antipsychotic medication effects in post-mortem brain from schizophrenia patients. Mol. Psych. 16, 1189–1202.
Chance, B., Thorell, B., 1959. Localization and kinetics of reduced pyridine nucleotide in living cells by microfluorometry. J. Biol. Chem. 234, 3044–3050.
Chance, B., Cohen, P., Jobsis, F., Schoener, B., 1962. Intracellular oxidation-reduction states in vivo. Science. 137, 499–508.
Cheah, Y.S., Amiel, S.A., 2012. Metabolic neuroimaging of the brain in diabetes mellitus and hypoglycaemia. Nat. Rev. Endocrinol. 8, 588–597.
Chih, C.P., Roberts Jr, E.L., 2003. Energy substrates for neurons during neural activity: a critical review of the astrocyte-neuron lactate shuttle hypothesis. J. Cereb. Blood. Flow. Metab. 23, 1263–1281.
Chih, C.P., Lipton, P., Roberts Jr., E.L., 2001. Do active cerebral neurons really use lactate rather than glucose? Trends. Neurosci. 24, 573–578.
Choi, S.W., Gerencser, A.A., Nicholls, D.G., 2009. Bioenergetic analysis of isolated cerebrocortical nerve terminals on a microgram scale: spare respiratory capacity and stochastic mitochondrial failure. J. Neurochem. 109, 1179–1191.
Choi, S.W., Gerencser, A.A., Lee, D.W., Rajagopalan, S., Nicholls, D. G., Andersen, J.K., et al., 2011. Intrinsic bioenergetic properties and stress sensitivity of dopaminergic synaptosomes. J. Neurosci. 31, 4524–4534.
Clark, J.B., Lai, J.C.K., 1989. Glycolytic, tricarboxylic acid and related enzymes in brain. In: Boulton, A.A., Baker, G.B., Butterworth, R. F. (Eds.), Neuromethods 11. Carbohydrates and Energy Metabolism. Humana Press, Clifton, NJ, pp. 233–281.
Clarke, D.D., Lajtha, A.L., Maker, H.S., 1989. Intermediary metabolism. In: Siegel, G.J., Agranoff, B.W., Albers, R.W., Fisher, S.K., Uhler, M. D. (Eds.), Basic Neurochemistry. Molecular, Cellular, and Medical Aspects, fourth ed. Raven Press, New York, pp. 541–564.
Cooper, A.J., 2012. The role of glutamine synthetase and glutamate dehydrogenase in cerebral ammonia homeostasis. Neurochem. Res. 37, 2439–2455.
Cooper, A.J., Plum, F., 1987. Biochemistry and physiology of brain ammonia. Physiol. Rev. 67, 440–519.
Cremer, J.E., 1982. Substrate utilization and brain development. J. Cereb. Blood. Flow. Metab. 2, 394–407.
Cremer, J.E., Cunningham, V.J., Seville, M.P., 1983. Relationships between extraction and metabolism of glucose, blood flow, and tissue blood volume in regions of rat brain. J. Cereb. Blood. Flow. Metab. 3, 291–302.
Cruz, N.F., Dienel, G.A., 2002. High glycogen levels in brains of rats with minimal environmental stimuli: implications for metabolic contributions of working astrocytes. J. Cereb. Blood. Flow. Metab. 22, 1476–1489.
Cruz, N.F., Lasater, A., Zielke, H.R., Dienel, G.A., 2005. Activation of astrocytes in brain of conscious rats during acoustic stimulation: acetate utilization in working brain. J. Neurochem. 92, 934–947.
Cruz, N.F., Ball, K.K., Dienel, G.A., 2007. Functional imaging of focal brain activation in conscious rats: impact of [^{14}C]glucose metabolite spreading and release. J. Neurosci. Res. 85, 3254–3266.
Dalsgaard, M.K., 2006. Fueling cerebral activity in exercising man. J. Cereb. Blood. Flow. Metab. 26, 731–750.
Daneman, R., Zhou, L., Agalliu, D., Cahoy, J.D., Kaushal, A., Barres, B.A., 2010. The mouse blood-brain barrier transcriptome: a new resource for understanding the development and function of brain endothelial cells. PloS one. 5, e13741.
Davis, J.N., Carlsson, A., Macmillan, V., Siesjo, B.K., 1973. Brain tryptophan hydroxylation: dependence on arterial oxygen tension. Science. 182, 72–74.
DiNuzzo, M., Mangia, S., Maraviglia, B., Giove, F., 2010a. Changes in glucose uptake rather than lactate shuttle take center stage in subserving neuroenergetics: evidence from mathematical modeling. J. Cereb. Blood. Flow. Metab. 30, 586–602.
DiNuzzo, M., Mangia, S., Maraviglia, B., Giove, F., 2010b. Glycogenolysis in astrocytes supports blood-borne glucose channeling not glycogen-derived lactate shuttling to neurons: evidence from mathematical modeling. J. Cereb. Blood. Flow. Metab. 30, 1895–1904.
DiNuzzo, M., Maraviglia, B., Giove, F., 2011. Why does the brain (not) have glycogen? Bioessays. 33, 319–326.
Dienel, G.A., 2002. Energy generation in the central nervous system. In: Edvinsson, L., Krause, D.N. (Eds.), Cerebral Blood flow and Metabolism, second ed. Lippincott Williams & Wilkins, Philadelphia, pp. 140–161.
Dienel, G.A., 2006. Functional brain imaging. In: Dermietzel, R., Spray, D.C., Nedergaard, M. (Eds.), Blood-Brain Barriers. From Ontogeny to Artificial Interfaces, vol. 2. Wiley-VCH Verlag, Weinheim, pp. 551–599.

Dienel, G.A., 2012a. Brain lactate metabolism: the discoveries and the controversies. J. Cereb. Blood. Flow. Metab. 32, 1107–1138.

Dienel, G.A., 2012b. Fueling and imaging brain activation. ASN Neuro. 4 (5), 267–321. Available from: http://dx.doi.org/10.01042/AN20120021.

Dienel, G.A., 2013. Astrocytic energetics during excitatory neurotransmission: What are contributions of glutamate oxidation and glycolysis? Neurochem. Int. 63, 244–258.

Dienel, G.A., Cruz, N.F., 2004. Nutrition during brain activation: does cell-to-cell lactate shuttling contribute significantly to sweet and sour food for thought?. Neurochem. Int. 45, 321–351.

Dienel, G.A., Cruz, N.F., 2006. Astrocyte activation in working brain: energy supplied by minor substrates. Neurochem. Int. 48, 586–595.

Dienel, G.A., Cruz, N.F., 2008. Imaging brain activation: simple pictures of complex biology. Ann. N. Y. Acad. Sci. 1147, 139–170.

Dienel, G.A., Hertz, L., 2005. Astrocytic contributions to bioenergetics of cerebral ischemia. Glia. 50, 362–388.

Dienel, G.A., Cruz, N.F., Mori, K., Holden, J.E., Sokoloff, L., 1991. Direct measurement of the lambda of the lumped constant of the deoxyglucose method in rat brain: determination of lambda and lumped constant from tissue glucose concentration or equilibrium brain/plasma distribution ratio for methylglucose. J. Cereb. Blood. Flow. Metab. 11, 25–34.

Dienel, G.A., Liu, K., Cruz, N.F., 2001a. Local uptake of ^{14}C-labeled acetate and butyrate in rat brain in vivo during spreading cortical depression. J. Neurosci. Res. 66, 812–820.

Dienel, G.A., Popp, D., Drew, P.D., Ball, K., Krisht, A., Cruz, N.F., 2001b. Preferential labeling of glial and meningial brain tumors with [2-(14)C]acetate. J. Nucl. Med. 42, 1243–1250.

Dienel, G.A., Wang, R.Y., Cruz, N.F., 2002. Generalized sensory stimulation of conscious rats increases labeling of oxidative pathways of glucose metabolism when the brain glucose-oxygen uptake ratio rises. J. Cereb. Blood. Flow. Metab. 22, 1490–1502.

Dienel, G.A., Ball, K.K., Cruz, N.F., 2007a. A glycogen phosphorylase inhibitor selectively enhances local rates of glucose utilization in brain during sensory stimulation of conscious rats: implications for glycogen turnover. J. Neurochem. 102, 466–478.

Dienel, G.A., Schmidt, K.C., Cruz, N.F., 2007b. Astrocyte activation in vivo during graded photic stimulation. J. Neurochem. 103, 1506–1522.

Dinuzzo, M., Mangia, S., Maraviglia, B., Giove, F., 2012. The role of astrocytic glycogen in supporting the energetics of neuronal activity. Neurochem. Res. 37, 2432–2438.

Dringen, R., Hoepken, H.H., Minich, T., Ruedig, C., 2007. Pentose phosphate pathway and NADPH metabolism. In: Gibson, G.E., Dienel, G.A. (Eds.), Brain Energetics. Integration of Molecular and Cellular Processes, third ed. Springer-Verlag, Berlin, pp. 41–62.

Duan, S., Anderson, C.M., Stein, B.A., Swanson, R.A., 1999. Glutamate induces rapid upregulation of astrocyte glutamate transport and cell-surface expression of GLAST. J. Neurosci. 19, 10193–10200.

Dubinsky, J.M., 2009. Heterogeneity of nervous system mitochondria: location, location, location!. Exp. Neurol. 218, 293–307.

Duffy, T.E., Howse, D.C., Plum, F., 1975. Cerebral energy metabolism during experimental status epilepticus. J. Neurochem. 24, 925–934.

Duncan, G.E., Stumpf, W.E., Pilgrim, C., 1987a. Cerebral metabolic mapping at the cellular level with dry-mount autoradiography of [^{3}H]2-deoxyglucose. Brain. Res. 401, 43–49.

Duncan, G.E., Stumpf, W.E., Pilgrim, C., Breese, G.R., 1987b. High resolution autoradiography at the regional topographic level with [^{14}C]2-deoxyglucose and [^{3}H]2-deoxyglucose. J. Neuros. Meth. 20, 105–113.

Duncan, G.E., Kaldas, R.G., Mitra, K.E., Breese, G.R., Stumpf, W.E., 1990. High activity neurons in the reticular formation of the medulla oblongata: a high-resolution autoradiographic 2-deoxyglucose study. Neuroscience. 35, 593–600.

Duran, J., Saez, I., Gruart, A., Guinovart, J.J., Delgado-García, J.M., 2013. Impairment in long-term memory formation and learning-dependent synaptic plasticity in mice lacking glycogen synthase in the brain. J. Cereb. Blood Flow Metab. 33, 550–556.

Edmond, J., 1992. Energy metabolism in developing brain cells. Can. J. Physiol. Pharmacol. 70 (Suppl.), S118–S129.

Eriksson, G., Peterson, A., Iverfeldt, K., Walum, E., 1995. Sodium-dependent glutamate uptake as an activator of oxidative metabolism in primary astrocyte cultures from newborn rat. Glia. 15, 152–156.

Estey, T., Piatigorsky, J., Lassen, N., Vasiliou, V., 2007. ALDH3A1: a corneal crystallin with diverse functions. Exp. Eye. Res. 84, 3–12.

Ferrendelli, J.A., 1974. Cerebral utilization of nonglucose substrates and their effect in hypoglycemia. Res. Publ. Assoc. Res. Nerv. Ment. Dis. 53, 113–123.

Fiehn, O., 2002. Metabolomics—the link between genotypes and phenotypes. Plant. Mol. Biol. 48, 155–171.

Fjeld, C.C., Birdsong, W.T., Goodman, R.H., 2003. Differential binding of NAD^{+} and NADH allows the transcriptional corepressor carboxyl-terminal binding protein to serve as a metabolic sensor. Proc. Natl. Acad. Sci. U.S.A. 100, 9202–9207.

Fonnum, F., Johnsen, A., Hassel, B., 1997. Use of fluorocitrate and fluoroacetate in the study of brain metabolism. Glia. 21, 106–113.

Fox, P.T., Raichle, M.E., 1986. Focal physiological uncoupling of cerebral blood flow and oxidative metabolism during somatosensory stimulation in human subjects. Proc. Natl. Acad. Sci. U.S.A. 83, 1140–1144.

Fox, P.T., Raichle, M.E., Mintun, M.A., Dence, C., 1988. Nonoxidative glucose consumption during focal physiologic neural activity. Science. 241, 462–464.

Gandhi, G.K., Cruz, N.F., Ball, K.K., Dienel, G.A., 2009. Astrocytes are poised for lactate trafficking and release from activated brain and for supply of glucose to neurons. J. Neurochem. 111, 522–536.

Garriga-Canut, M., Schoenike, B., Qazi, R., Bergendahl, K., Daley, T. J., Pfender, R.M., et al., 2006. 2-Deoxy-D-glucose reduces epilepsy progression by NRSF-CtBP-dependent metabolic regulation of chromatin structure. Nat. Neurosci. 9, 1382–1387.

Gasior, M., Yankura, J., Hartman, A.L., French, A., Rogawski, M.A., 2010. Anticonvulsant and proconvulsant actions of 2-deoxy-D-glucose. Epilepsia. 51, 1385–1394.

Genda, E.N., Jackson, J.G., Sheldon, A.L., Locke, S.F., Greco, T.M., O'Donnell, J.C., et al., 2011. Co-compartmentalization of the astroglial glutamate transporter, GLT-1, with glycolytic enzymes and mitochondria. J. Neurosci. 31, 18275–18288.

Gibson, G.E., Duffy, T.E., 1981. Impaired synthesis of acetylcholine by mild hypoxic hypoxia or nitrous oxide. J. Neurochem. 36, 28–33.

Gibson, G.E., Shi, Q., 2010. A mitocentric view of Alzheimer's disease suggests multi-faceted treatments. J. Alzheimers Dis. 20 (Suppl. 2), S591–S607.

Gibson, G.E., Starkov, A., Blass, J.P., Ratan, R.R., Beal, M.F., 2010. Cause and consequence: mitochondrial dysfunction initiates and propagates neuronal dysfunction, neuronal death and behavioral abnormalities in age-associated neurodegenerative diseases. Biochim. Biophys. Acta. 1802, 122–134.

Ginsberg, M.D., 2009. Current status of neuroprotection for cerebral ischemia: synoptic overview. Stroke. 40, S111–S114.

Gold, P.E., 2005. Glucose and age-related changes in memory. Neurobiol. Aging. 26 (Suppl. 1), 60–64.

Goodacre, R., Vaidyanathan, S., Dunn, W.B., Harrigan, G.G., Kell, D. B., 2004. Metabolomics by numbers: acquiring and understanding global metabolite data. Trends. Biotechnol. 22, 245–252.

Gordon, G.R., Choi, H.B., Rungta, R.L., Ellis-Davies, G.C., Macvicar, B.A., 2008. Brain metabolism dictates the polarity of astrocyte control over arterioles. Nature. 456, 745–749.

Griffin, J.L., 2004. Metabolic profiles to define the genome: can we hear the phenotypes? Philos. Trans. R. Soc. Lond. B. Biol. Sci. 359, 857–871.

Griffin, J.L., Kauppinen, R.A., 2007. A metabolomics perspective of human brain tumours. FEBS J. 274, 1132–1139.

Gruetter, R., Novotny, E.J., Boulware, S.D., Rothman, D.L., Mason, G. F., Shulman, G.I., et al., 1992. Direct measurement of brain glucose concentrations in humans by 13C NMR spectroscopy. Proc. Natl. Acad. Sci. U.S.A. 89, 1109–1112.

Halestrap, A.P., Price, N.T., 1999. The proton-linked monocarboxylate transporter (MCT) family: structure, function and regulation. Biochem. J. 343 (Pt 2), 281–299.

Hall, C.N., Klein-Flugge, M.C., Howarth, C., Attwell, D., 2012. Oxidative phosphorylation, not glycolysis, powers presynaptic and postsynaptic mechanisms underlying brain information processing. J. Neurosci. 32, 8940–8951.

Hamprecht, B., Dringen, R., 1995. Energy metabolism. In: Kettenmann, H., Ransom, B.R. (Eds.), Neuroglia. Oxford University Press, New York, pp. 473–487.

Hamprecht, B., Verleysdonk, S., Wiesinger, H., 2004. Enzymes of carbohydrate and energy metabolism. In: Kettenmann, H., Ransom, B.R. (Eds.), Neuroglia, second ed. Oxford University Press, New York, pp. 202–215.

Han, X., Chen, M., Wang, F., Windrem, M., Wang, S., Shanz, S., et al., 2013. Forebrain engraftment by human glial progenitor cells enhances synaptic plasticity and learning in adult mice. Cell Stem Cell. 12, 342–353.

Hardie, D.G., Ross, F.A., Hawley, S.A., 2012. AMPK: a nutrient and energy sensor that maintains energy homeostasis. Nat. Rev. Mol. Cell. Biol. 13, 251–262.

Hargreaves, R.J., Planas, A.M., Cremer, J.E., Cunningham, V.J., 1986. Studies on the relationship between cerebral glucose transport and phosphorylation using 2-deoxyglucose. J. Cereb. Blood. Flow. Metab. 6, 708–716.

Harris, J.J., Attwell, D., 2012. The energetics of CNS white matter. J. Neurosci. 32, 356–371.

Harting, K., Knoll, B., 2010. SIRT2-mediated protein deacetylation: an emerging key regulator in brain physiology and pathology. Eur. J. Cell. Biol. 89, 262–269.

Heidemann, A.C., Schipke, C.G., Kettenmann, H., 2005. Extracellular application of nicotinic acid adenine dinucleotide phosphate induces Ca^{2+} signaling in astrocytes in situ. J. Biol. Chem. 280, 35630–35640.

Hein, T.W., Xu, W., Kuo, L., 2006. Dilation of retinal arterioles in response to lactate: role of nitric oxide, guanylyl cyclase, and ATP-sensitive potassium channels. Invest. Ophthalmol. Vis. Sci. 47, 693–699.

Hekmatyar, S.K., Wilson, M., Jerome, N., Salek, R.M., Griffin, J.L., Peet, A., et al., 2010. 1)H nuclear magnetic resonance spectroscopy characterisation of metabolic phenotypes in the medulloblastoma of the SMO transgenic mice. Brit. J. Cancer. 103, 1297–1304.

Herculano-Houzel, S., 2012a. Neuronal scaling rules for primate brains: the primate advantage. Prog. Brain. Res. 195, 325–340.

Herculano-Houzel, S., 2012b. The remarkable, yet not extraordinary, human brain as a scaled-up primate brain and its associated cost. Proc. Natl. Acad. Sci. U.S.A. 109 (Suppl. 1), 10661–10668.

Hertz, L., 2011. Astrocytic energy metabolism and glutamate formation—relevance for 13C-NMR spectroscopy and importance of cytosolic/mitochondrial trafficking. Magn. Reson. Imaging. 29, 1319–1329.

Hertz, L., Dienel, G.A., 2005. Lactate transport and transporters: general principles and functional roles in brain cells. J. Neurosci. Res. 79, 11–18.

Hertz, L., Gibbs, M.E., 2009. What learning in day-old chickens can teach a neurochemist: focus on astrocyte metabolism. J. Neurochem. 109 (Suppl. 1), 10–16.

Hertz, L., Peng, L., Dienel, G.A., 2007. Energy metabolism in astrocytes: high rate of oxidative metabolism and spatiotemporal dependence on glycolysis/glycogenolysis. J. Cereb. Blood. Flow. Metab. 27, 219–249.

Higashida, H., Salmina, A.B., Olovyannikova, R.Y., Hashii, M., Yokoyama, S., Koizumi, K., et al., 2007. Cyclic ADP-ribose as a universal calcium signal molecule in the nervous system. Neurochem. Int. 51, 192–199.

Hof, P.R., Pascale, E., Magistretti, P.J., 1988. K^+ at concentrations reached in the extracellular space during neuronal activity promotes a Ca^{2+}-dependent glycogen hydrolysis in mouse cerebral cortex. J. Neurosci. 8, 1922–1928.

Holden, J.E., Mori, K., Dienel, G.A., Cruz, N.F., Nelson, T., Sokoloff, L., 1991. Modeling the dependence of hexose distribution volumes in brain on plasma glucose concentration: implications for estimation of the local 2-deoxyglucose lumped constant. J. Cereb. Blood. Flow. Metab. 11, 171–182.

Houtkooper, R.H., Pirinen, E., Auwerx, J., 2012. Sirtuins as regulators of metabolism and healthspan. Nat. Rev. Mol. Cell. Biol. 13, 225–238.

Howarth, C., Gleeson, P., Attwell, D., 2012. Updated energy budgets for neural computation in the neocortex and cerebellum. J. Cereb. Blood. Flow. Metab. 32, 1222–1232.

Hyder, F., Rothman, D.L., 2012. Quantitative fMRI and oxidative neuroenergetics. NeuroImage. 62, 985–994.

Hyder, F., Sanganahalli, B.G., Herman, P., Coman, D., Maandag, N. J., Behar, K.L., et al., 2010. Neurovascular and neurometabolic couplings in dynamic calibrated fMRI: transient oxidative neuroenergetics for block-design and event-related paradigms. Front. Neuroenerg. 2 (18). Available from: http://dx.doi.org/10.3389/fnene.2010.00018.

Iacobas, D.A., Iacobas, S., Urban-Maldonado, M., Spray, D.C., 2005. Sensitivity of the brain transcriptome to connexin ablation. Biochim. Biophys. Acta. 1711, 183–196.

Iacobas, D.A., Iacobas, S., Urban-Maldonado, M., Scemes, E., Spray, D.C., 2008. Similar transcriptomic alterations in Cx43 knockdown and knockout astrocytes. Cell. Commun. Adhes. 15, 195–206.

Ivannikov, M.V., Sugimori, M., Llinas, R.R., 2010. Calcium clearance and its energy requirements in cerebellar neurons. Cell Calcium. 47, 507–513.

Jacob, Z., Li, H., Makaryus, R., Zhang, S., Reinsel, R., Lee, H., et al., 2012. Metabolomic profiling of children's brains undergoing general anesthesia with sevoflurane and propofol. Anesthesiology. 117, 1062–1071.

Jöbsis, F.F., O'Connor, M., Vitale, A., Vreman, H., 1971. Intracellular redox changes in functioning cerebral cortex. I. Metabolic effects of epileptiform activity. J. Neurophysiol. 34, 735–749.

Jolivet, R., Allaman, I., Pellerin, L., Magistretti, P.J., Weber, B., 2010. Comment on recent modeling studies of astrocyte-neuron metabolic interactions. J. Cereb. Blood. Flow. Metab. 30, 1982–1986.

Joseph, J., Gibson, G.E., 2007. Coupling of neuronal function to oxygen and glucose metabolism through changes in neurotransmitter dynamics as revealed with aging, hypoglycemia, and hypoxia. In: Gibson, G.E., Dienel, G.A. (Eds.), Brain Energetics. Integration of Molecular and Cellular Processes, third ed. Springer-Verlag, Berlin, pp. 297–320.

Kaddurah-Daouk, R., Kristal, B.S., Weinshilboum, R.M., 2008. Metabolomics: a global biochemical approach to drug response and disease. Annu. Rev. Pharmacol. Toxicol. 48, 653–683.

Kanamori, K., Ross, B.D., Farrow, N.A., Parivar, F., 1991. A 15N-NMR study of isolated brain in portacaval-shunted rats after acute hyperammonemia. Biochim. Biophys. Acta. 1096, 270–276.
Karbowski, J., 2007. Global and regional brain metabolic scaling and its functional consequences. BMC. Biol. 5, 18.
Karbowski, J., 2011. Scaling of brain metabolism and blood flow in relation to capillary and neural scaling. PloS one. 6, e26709.
Karuppagounder, S.S., Ratan, R.R., 2012. Hypoxia-inducible factor prolyl hydroxylase inhibition: robust new target or another big bust for stroke therapeutics? J. Cereb. Blood. Flow. Metab. 32, 1347–1361.
Kaufman, E.E., Driscoll, B.F., 1992. Carbon dioxide fixation in neuronal and astroglial cells in culture. J. Neurochem. 58, 258–262.
Kauppinen, R.A., Nicholls, D.G., 1986. Synaptosomal bioenergetics. The role of glycolysis, pyruvate oxidation and responses to hypoglycaemia. Eur. J. Biochem/FEBS. 158, 159–165.
Keil, V.C., Funke, F., Zeug, A., Schild, D., Muller, M., 2011. Ratiometric high-resolution imaging of JC-1 fluorescence reveals the subcellular heterogeneity of astrocytic mitochondria. Pflugers Archiv: Eur. J. Physiol. 462, 693–708.
Kety, S.S., 1996. Seymour S. Kety. In: Squire, L.R. (Ed.), The History of Neuroscience in Autobiography, vol. 1. Society for Neuroscience, Washington, D. C., pp. 382–413.
Kety, S.S., Schmidt, C.F., 1948. The nitrous oxide method for the quantitative determination of cerebral blood flow in man: Theory, procedure and normal values. J. Clinical Invest. 27, 476–483.
Keyser, D.O., Pellmar, T.C., 1994. Synaptic transmission in the hippocampus: critical role for glial cells. Glia. 10, 237–243.
Keyser, D.O., Pellmar, T.C., 1997. Regional differences in glial cell modulation of synaptic transmission. Hippocampus. 7, 73–77.
Kim, S.G., Ogawa, S., 2012. Biophysical and physiological origins of blood oxygenation level-dependent fMRI signals. J. Cereb. Blood. Flow. Metab. 32, 1188–1206.
Koehler-Stec, E.M., Li, K., Maher, F., Vannucci, S.J., Smith, C.B., Simpson, I.A., 2000. Cerebral glucose utilization and glucose transporter expression: response to water deprivation and restoration. J. Cereb. Blood. Flow. Metab. 20, 192–200.
Korf, J., Gramsbergen, J.B., 2007. Timing of potential and metabolic brain energy. J. Neurochem. 103, 1697–1708.
Kumar, V., Carlson, J.E., Ohgi, K.A., Edwards, T.A., Rose, D.W., Escalante, C.R., et al., 2002. Transcription corepressor CtBP is an NAD(+)-regulated dehydrogenase. Mol. Cell. 10, 857–869.
Lai, J.C.K., Clark, J.B., 1989. Isolation and characterization of synaptic and nonsynaptic mitochondria from mammalian brain. In: Boulton, A.A., Baker, G.B., Butterworth, R.F. (Eds.), Neuromethods 11. Carbohydrates and Energy Metabolism. Humana Press, Clifton, NJ, pp. 43–98.
Lamanna, J.C., Pichiule, P., Chavez, J.C., 2007. 7.2 Genetics and gene expression of glycolysis. In: Gibson, G.E., Dienel, G.A. (Eds.), Brain Energetics. Integration of Molecular and Cellular Processes, third ed, Springer-Verlag, Berlin, pp. 771–778.
Landau, W.M., Freygang Jr., W.H., Roland, L.P., Sokoloff, L., Kety, S. S., 1955. The local circulation of the living brain; values in the unanesthetized and anesthetized cat. Trans. Am. Neurol. Assoc.125–129.
Lanoue, K.F., Carson, V., Berkich, D.A., 2007. Mitochondrial/cytosolic interactions via metabolite shuttles and transporters. In: Gibson, G.E., Dienel, G.A. (Eds.), Brain Energetics. Integration of Molecular and Cellular Processes, third ed. Springer-Verlag, Berlin, pp. 589–616.
Laptook, A.R., Peterson, J., Porter, A.M., 1988. Effects of lactic acid infusions and pH on cerebral blood flow and metabolism. J. Cereb. Blood. Flow. Metab. 8, 193–200.
Laschet, J.J., Minier, F., Kurcewicz, I., Bureau, M.H., Trottier, S., Jeanneteau, F., et al., 2004. Glyceraldehyde-3-phosphate dehydrogenase is a GABAA receptor kinase linking glycolysis to neuronal inhibition. J. Neurosci. 24, 7614–7622.
Laschet, J.J., Kurcewicz, I., Minier, F., Trottier, S., Khallou-Laschet, J., Louvel, J., et al., 2007. Dysfunction of GABAA receptor glycolysis-dependent modulation in human partial epilepsy. Proc. Natl. Acad. Sci. U.S.A. 104, 3472–3477.
Lavialle, M., Aumann, G., Anlauf, E., Prols, F., Arpin, M., Derouiche, A., 2011. Structural plasticity of perisynaptic astrocyte processes involves ezrin and metabotropic glutamate receptors. Proc. Natl. Acad. Sci. U.S.A. 108, 12915–12919.
Lebon, V., Petersen, K.F., Cline, G.W., Shen, J., Mason, G.F., Dufour, S., et al., 2002. Astroglial contribution to brain energy metabolism in humans revealed by 13C nuclear magnetic resonance spectroscopy: elucidation of the dominant pathway for neurotransmitter glutamate repletion and measurement of astrocytic oxidative metabolism. J. Neurosci. 22, 1523–1531.
Leong, S.F., Clark, J.B., 1984a. Regional enzyme development in rat brain. Enzymes associated with glucose utilization. Biochem. J. 218, 131–138.
Leong, S.F., Clark, J.B., 1984b. Regional enzyme development in rat brain. Enzymes of energy metabolism. Biochem. J. 218, 139–145.
Lew, C.R., Tolan, D.R., 2012. Targeting of several glycolytic enzymes using RNA interference reveals Aldolase affects cancer cell proliferation through a non-glycolytic mechanism. J. Biolog. Chem. 287, 42554–42563.
Lewis, L.D., Ljunggren, B., Ratcheson, R.A., Siesjo, B.K., 1974. Cerebral energy state in insulin-induced hypoglycemia, related to blood glucose and to EEG. J. Neurochem. 23, 673–679.
Li, B., Hertz, L., Peng, L., 2012. Aralar mRNA and protein levels in neurons and astrocytes freshly isolated from young and adult mouse brain and in maturing cultured astrocytes. Neurochem. Int. 61, 1325–1332.
Li, J., Mccullough, L.D., 2010. Effects of AMP-activated protein kinase in cerebral ischemia. J. Cereb. Blood. Flow. Metab. 30, 480–492.
Li, J., Benashski, S., Mccullough, L.D., 2011. Post-stroke hypothermia provides neuroprotection through inhibition of AMP-activated protein kinase. J. Neurotrauma. 28, 1281–1288.
Lin, Y., Stephenson, M.C., Xin, L., Napolitano, A., Morris, P.G., 2012. Investigating the metabolic changes due to visual stimulation using functional proton magnetic resonance spectroscopy at 7 T. J. Cereb. Blood. Flow. Metab. 32, 1484–1495.
Lipton, P., 1973. Effects of membrane depolarization on nicotinamide nucleotide fluorescence in brain slices. Biochem. J. 136, 999–1009.
Lombard, J.H., 2006. A novel mechanism for regulation of retinal blood flow by lactate: gap junctions, hypoxia, and pericytes. American journal of physiology. Heart Circ. Physiol. 290, H921–H922.
Lovatt, D., Sonnewald, U., Waagepetersen, H.S., Schousboe, A., He, W., Lin, J.H., et al., 2007. The transcriptome and metabolic gene signature of protoplasmic astrocytes in the adult murine cortex. J. Neurosci. 27, 12255–12266.
Lowry, O.H., 1990. How to succeed in research without being a genius. Annu. Rev. Biochem. 59, 1–27.
Lowry, O.H., Passonneau, J.V., 1964. The relationships between substrates and enzymes of glycolysis in brain. J. Biol. Chem. 239, 31–42.
Lowry, O.H., Passonneau, J.V., Hasselberger, F.X., Schulz, D.W., 1964. Effect of ischemia on known substrates and cofactors of the glycolytic pathway in brain. J. Biol. Chem. 239, 18–30.
Lynch, R.M., Balaban, R.S., 1987. Coupling of aerobic glycolysis and Na + -K + -ATPase in renal cell line MDCK. Am. J. Physiol. 253, C269–C276.
Lynch, R.M., Paul, R.J., 1987. Compartmentation of carbohydrate metabolism in vascular smooth muscle. Am. J. Physiol. 252, C328–C334.

Madsen, P.L., Hasselbalch, S.G., Hagemann, L.P., Olsen, K.S., Bulow, J., Holm, S., et al., 1995. Persistent resetting of the cerebral oxygen/glucose uptake ratio by brain activation: evidence obtained with the Kety-Schmidt technique. J. Cereb. Blood. Flow. Metab. 15, 485–491.

Madsen, P.L., Cruz, N.F., Sokoloff, L., Dienel, G.A., 1999. Cerebral oxygen/glucose ratio is low during sensory stimulation and rises above normal during recovery: excess glucose consumption during stimulation is not accounted for by lactate efflux from or accumulation in brain tissue. J. Cereb. Blood. Flow. Metab. 19, 393–400.

Maher, A.D., Cysique, L.A., Brew, B.J., Rae, C.D., 2011. Statistical integration of 1H NMR and MRS data from different biofluids and tissues enhances recovery of biological information from individuals with HIV-1 infection. J. Proteome. Res. 10, 1737–1745.

Makaryus, R., Lee, H., Yu, M., Zhang, S., Smith, S.D., Rebecchi, M., et al., 2011. The metabolomic profile during isoflurane anesthesia differs from propofol anesthesia in the live rodent brain. J. Cereb. Blood. Flow. Metab. 31, 1432–1442.

Malhotra, P., Boddy, C.S., Soni, V., Saksena, S., Dudeja, P.K., Gill, R. K., et al., 2013. D-Glucose modulates intestinal Niemann-Pick C1 Like 1 (NPC1L1) gene expression via transcriptional regulation. Am. J. Physiol. Gastrointest Liver Physiol. 304, G203–G210.

Mangia, S., Tkac, I., Gruetter, R., Van De Moortele, P.F., Maraviglia, B., Ugurbil, K., 2007. Sustained neuronal activation raises oxidative metabolism to a new steady-state level: evidence from 1H NMR spectroscopy in the human visual cortex. J. Cereb. Blood. Flow. Metab. 27, 1055–1063.

Mangia, S., Simpson, I.A., Vannucci, S.J., Carruthers, A., 2009. The in vivo neuron-to-astrocyte lactate shuttle in human brain: evidence from modeling of measured lactate levels during visual stimulation. J. Neurochem. 109 (Suppl. 1), 55–62.

Mangia, S., Dinuzzo, M., Giove, F., Carruthers, A., Simpson, I.A., Vannucci, S.J., 2011. Response to 'comment on recent modeling studies of astrocyte-neuron metabolic interactions': much ado about nothing. J. Cereb. Blood. Flow. Metab. 31, 1346–1353.

Marino, L., 2006. Absolute brain size: did we throw the baby out with the bathwater? Proc. Natl. Acad. Sci. U.S.A. 103, 13563–13564.

Marrif, H., Juurlink, B.H., 1999. Astrocytes respond to hypoxia by increasing glycolytic capacity. J. Neurosci. Res. 57, 255–260.

Martinez-Hernandez, A., Bell, K.P., Norenberg, M.D., 1977. Glutamine synthetase: glial localization in brain. Science. 195, 1356–1358.

Masamoto, K., Kanno, I., 2012. Anesthesia and the quantitative evaluation of neurovascular coupling. J. Cereb. Blood. Flow. Metab. 32, 1233–1247.

Maurer, M.H., Kuschinsky, W., 2007. Proteomics. In: Gibson, G.E., Dienel, G.A. (Eds.), Brain Energetics. Integration of Molecular and Cellular Processes, third ed. Springer-Verlag, Berlin, pp. 738–769.

Maurer, M.H., Canis, M., Kuschinsky, W., Duelli, R., 2004. Correlation between local monocarboxylate transporter 1 (MCT1) and glucose transporter 1 (GLUT1) densities in the adult rat brain. Neurosci. Lett. 355, 105–108.

McCall, A.L., 2012. Insulin therapy and hypoglycemia. Endocrinol. Metab. Clin. North. Am. 41, 57–87.

McCrimmon, R.J., Ryan, C.M., Frier, B.M., 2012. Diabetes and cognitive dysfunction. Lancet. 379, 2291–2299.

McKenna, M.C., Sonnewald, U., Huang, X., Stevenson, J., Zielke, H. R., 1996. Exogenous glutamate concentration regulates the metabolic fate of glutamate in astrocytes. J. Neurochem. 66, 386–393.

McKenna, M.C., Waagepetersen, H.S., Schousboe, A., Sonnewald, U., 2006. Neuronal and astrocytic shuttle mechanisms for cytosolic-mitochondrial transfer of reducing equivalents: current evidence and pharmacological tools. Biochem. Pharmacol. 71, 399–407.

Medina, M.A., Jones, D.J., Stavinoha, W.B., Ross, D.H., 1975. The levels of labile intermediary metabolites in mouse brain following rapid tissue fixation with microwave irradiation. J. Neurochem. 24, 223–227.

Minn, A.H., Couto, F.M., Shalev, A., 2006. Metabolism-independent sugar effects on gene transcription: the role of 3-O-methylglucose. Biochemistry. 45, 11047–11051.

Nakamura, M., Bhatnagar, A., Sadoshima, J., 2012. Overview of pyridine nucleotides review series. Circulation Res. 111, 604–610.

Nakanishi, H., Cruz, N.F., Adachi, K., Sokoloff, L., Dienel, G.A., 1996. Influence of glucose supply and demand on determination of brain glucose content with labeled methylglucose. J. Cereb. Blood. Flow. Metab. 16, 439–449.

Nakao, Y., Itoh, Y., Kuang, T.Y., Cook, M., Jehle, J., Sokoloff, L., 2001. Effects of anesthesia on functional activation of cerebral blood flow and metabolism. Proc. Natl. Acad. Sci. U.S.A. 98, 7593–7598.

Nasrallah, F.A., Maher, A.D., Hanrahan, J.R., Balcar, V.J., Rae, C.D., 2010. gamma-Hydroxybutyrate and the GABAergic footprint: a metabolomic approach to unpicking the actions of GHB. J. Neurochem. 115, 58–67.

Nehlig, A., 1996. Respective roles of glucose and ketone bodies as substrates for cerebral energy metabolism in the suckling rat. Dev. Neurosci. 18, 426–433.

Nehlig, A., 2004. Brain uptake and metabolism of ketone bodies in animal models. Prostaglandins. Leukot. Essent. Fatty. Acids. 70, 265–275.

Nehlig, A., Wittendorp-Rechenmann, E., Lam, C.D., 2004. Selective uptake of [^{14}C]2-deoxyglucose by neurons and astrocytes: high-resolution microautoradiographic imaging by cellular ^{14}C-trajectography combined with immunohistochemistry. J. Cereb. Blood. Flow. Metab. 24, 1004–1014.

Nehlig, A., Rudolf, G., Leroy, C., Rigoulot, M.A., Simpson, I.A., Vannucci, S.J., 2006. Pentylenetetrazol-induced status epilepticus up-regulates the expression of glucose transporter mRNAs but not proteins in the immature rat brain. Brain. Res. 1082, 32–42.

Newman, L.A., Korol, D.L., Gold, P.E., 2011. Lactate produced by glycogenolysis in astrocytes regulates memory processing. PloS one. 6, e28427.

Nicholls, D.G., Johnson-Cadwell, L., Vesce, S., Jekabsons, M., Yadava, N., 2007. Bioenergetics of mitochondria in cultured neurons and their role in glutamate excitotoxicity. J. Neurosci. Res. 85, 3206–3212.

Nicholson, J.K., Connelly, J., Lindon, J.C., Holmes, E., 2002. Metabonomics: a platform for studying drug toxicity and gene function. Nat. Rev. Drug. Discov. 1, 153–161.

Nilsen, J., Irwin, R.W., Gallaher, T.K., Brinton, R.D., 2007. Estradiol in vivo regulation of brain mitochondrial proteome. J. Neurosci. 27, 14069–14077.

Norenberg, M.D., Martinez-Hernandez, A., 1979. Fine structural localization of glutamine synthetase in astrocytes of rat brain. Brain. Res. 161, 303–310.

O'Collins, V.E., Macleod, M.R., Donnan, G.A., Howells, D.W., 2012. Evaluation of combination therapy in animal models of cerebral ischemia. J. Cereb. Blood. Flow. Metab. 32, 585–597.

Obel, L.F., Muller, M.S., Walls, A.B., Sickmann, H.M., Bak, L.K., Waagepetersen, H.S., et al., 2012. Brain glycogen—new perspectives on its metabolic function and regulation at the subcellular level. Front. Neuroenerg. 4 (3). Available from: http://dx.doi.org/10.3389/fnene.2012.00003.

Ogawa, S., Lee, T.M., Kay, A.R., Tank, D.W., 1990. Brain magnetic resonance imaging with contrast dependent on blood oxygenation. Proc. Natl. Acad. Sci. U.S.A. 87, 9868–9872.

Okada, Y., Lipton, P., 2007. 1.2 Glucose, oxidative energy metabolism, and neural function in brain slices—glycolysis plays a key role in neural activity. In: Gibson, G.E., Dienel, G.A. (Eds.), Brain Energetics. Integration of Molecular and Cellular Processes, third ed, Springer-Verlag, Berlin, pp. 17–39.

Oldendorf, W.H., 1981. Clearance of ratiolabeled substrates by brain after arterial injection using a diffusible internal standard. In: Marks, N., Rodnight, R. (Eds.), Research Methods in Neurochemistry, vol. 5. Plenum Publishing Corp, New York, pp. 91–112.

Oldendorf, W.H., Szabo, J., 1976. Amino acid assignment to one of three blood-brain barrier amino acid carriers. Am. J. Physiol. 230, 94–98.

Öz, G., Berkich, D.A., Henry, P.G., Xu, Y., Lanoue, K., Hutson, S.M., et al., 2004. Neuroglial metabolism in the awake rat brain: CO2 fixation increases with brain activity. J. Neurosci. 24, 11273–11279.

Pandey, V., Chuang, C.C., Lewis, A.M., Aley, P.K., Brailoiu, E., Dun, N.J., et al., 2009. Recruitment of NAADP-sensitive acidic Ca^{2+} stores by glutamate. Biochem. J. 422, 503–512.

Papa, S., Petruzzella, V., Scacco, S., 2007. Electron transport. Structure, redox-coupled protonmotive activity, and pathological disorders of respiratory chain complexes. In: Gibson, G.E., Dienel, G.A. (Eds.), Brain Energetics. Integration of Molecular and Cellular Processes, third ed. Springer-Verlag, Berlin, pp. 93–118.

Pardo, B., Rodrigues, T.B., Contreras, L., Garzon, M., Llorente-Folch, I., Kobayashi, K., et al., 2011. Brain glutamine synthesis requires neuronal-born aspartate as amino donor for glial glutamate formation. J. Cereb. Blood. Flow. Metab. 31, 90–101.

Passonneau, J.V., Lowry, O.H., 1964. The role of phosphofructokinase in metabolic regulation. Adv. Enzyme. Regul. 2, 265–274.

Patel, A.B., Lai, J.C.K., Chowdhury, G.M.I., Hyder, F., Rothman, D.L., Shulman, R.G., et al., 2014. Direct evidence for activity-dependent glucose phosphorylation in neurons: Implications for the astrocyte-to-neuron lactate shuttle. Proc. Natl. Acad. Sci. 111, 5385–5390.

Paulson, O.B., Hasselbalch, S.G., Rostrup, E., Knudsen, G.M., Pelligrino, D., 2010. Cerebral blood flow response to functional activation. J. Cereb. Blood. Flow. Metab. 30, 2–14.

Pellerin, L., Magistretti, P.J., 1994. Glutamate uptake into astrocytes stimulates aerobic glycolysis: a mechanism coupling neuronal activity to glucose utilization. Proc. Natl. Acad. Sci. U.S.A. 91, 10625–10629.

Pellerin, L., Magistretti, P.J., 2012. Sweet sixteen for ANLS. J. Cereb. Blood. Flow. Metab. 32, 1152–1166.

Peng, L., Swanson, R.A., Hertz, L., 2001. Effects of L-glutamate, D-aspartate, and monensin on glycolytic and oxidative glucose metabolism in mouse astrocyte cultures: further evidence that glutamate uptake is metabolically driven by oxidative metabolism. Neurochem. Int. 38, 437–443.

Perez-Pinzon, M.A., Stetler, R.A., Fiskum, G., 2012. Novel mitochondrial targets for neuroprotection. J. Cereb. Blood. Flow. Metab. 32, 1362–1376.

Perkins, G., Ellisman, M.H., 2007. Mitochondrial architecture and heterogeneity. In: Gibson, G.E., Dienel, G.A. (Eds.), Brain Energetics. Integration of Molecular and Cellular Processes, 3 ed. Springer-Verlag, Berlin, pp. 261–295.

Perkins, G.A., Tjong, J., Brown, J.M., Poquiz, P.H., Scott, R.T., Kolson, D.R., et al., 2010. The micro-architecture of mitochondria at active zones: electron tomography reveals novel anchoring scaffolds and cristae structured for high-rate metabolism. J. Neurosci. 30, 1015–1026.

Phelps, M.E., Huang, S.C., Hoffman, E.J., Selin, C., Sokoloff, L., Kuhl, D.E., 1979. Tomographic measurement of local cerebral glucose metabolic rate in humans with (F-18)2-fluoro-2-deoxy-D-glucose: validation of method. Ann. Neurol. 6, 371–388.

Piatigorsky, J., 2003. Crystallin genes: specialization by changes in gene regulation may precede gene duplication. J. Struct. Funct. Genomics. 3, 131–137.

Ponten, U., Ratcheson, R.A., Salford, L.G., Siesjo, B.K., 1973. Optimal freezing conditions for cerebral metabolites in rats. J. Neurochem. 21, 1127–1138.

Prabakaran, S., Swatton, J.E., Ryan, M.M., Huffaker, S.J., Huang, J.T., Griffin, J.L., et al., 2004. Mitochondrial dysfunction in schizophrenia: evidence for compromised brain metabolism and oxidative stress. Mol. Psychiat. 9, 684–697, 643.

Prichard, J.W., Shulman, R.G., 1986. NMR spectroscopy of brain metabolism in vivo. Annu. Rev. Neurosci. 9, 61–85.

Prins, M.L., 2008. Cerebral metabolic adaptation and ketone metabolism after brain injury. J. Cereb. Blood. Flow. Metab. 28, 1–16.

Pumain, R., Ahmed, M.S., Kurcewicz, I., Trottier, S., Louvel, J., Turak, B., et al., 2008. Lability of GABAA receptor function in human partial epilepsy: possible relationship to hypometabolism. Epilepsia. 49 (Suppl. 8), 87–90.

Qu, H., Eloqayli, H., Unsgard, G., Sonnewald, U., 2001. Glutamate decreases pyruvate carboxylase activity and spares glucose as energy substrate in cultured cerebellar astrocytes. J. Neurosci. Res. 66, 1127–1132.

Quistorff, B., Secher, N.H., Van Lieshout, J.J., 2008. Lactate fuels the human brain during exercise. FASEB. 22, 3443–3449.

Rae, C., Moussa Cel, H., Griffin, J.L., Parekh, S.B., Bubb, W.A., Hunt, N.H., et al., 2006. A metabolomic approach to ionotropic glutamate receptor subtype function: a nuclear magnetic resonance in vitro investigation. J. Cereb. Blood. Flow. Metab. 26, 1005–1017.

Rae, C., Nasrallah, F.A., Griffin, J.L., Balcar, V.J., 2009. Now I know my ABC. A systems neurochemistry and functional metabolomic approach to understanding the GABAergic system. J. Neurochem. 109 (Suppl. 1), 109–116.

Ramamurthy, S., Ronnett, G., 2012. AMP-Activated Protein Kinase (AMPK) and energy-sensing in the brain. Exp. Neurobiol. 21, 52–60.

Ramos, M., Del Arco, A., Pardo, B., Martinez-Serrano, A., Martinez-Morales, J.R., Kobayashi, K., et al., 2003. Developmental changes in the Ca^{2+}-regulated mitochondrial aspartate-glutamate carrier aralar1 in brain and prominent expression in the spinal cord. Brain. Res. Dev. Brain. Res. 143, 33–46.

Rangarajan, E.S., Park, H., Fortin, E., Sygusch, J., Izard, T., 2010. Mechanism of aldolase control of sorting nexin 9 function in endocytosis. J. Biol. Chem. 285, 11983–11990.

Rennels, M.L., Gregory, T.F., Blaumanis, O.R., Fujimoto, K., Grady, P.A., 1985. Evidence for a 'paravascular' fluid circulation in the mammalian central nervous system, provided by the rapid distribution of tracer protein throughout the brain from the subarachnoid space. Brain. Res. 326, 47–63.

Requardt, R.P., Hirrlinger, P.G., Wilhelm, F., Winkler, U., Besser, S., Hirrlinger, J., 2012. Ca^{2+} signals of astrocytes are modulated by the NAD + /NADH redox state. J. Neurochem. 120, 1014–1025.

Riddick, G., Fine, H.A., 2011. Integration and analysis of genome-scale data from gliomas. Nat. Rev. Neurol. 7, 439–450.

Roberts Jr, E.L., 2007. The support of energy metabolism in the central nervous system with substrates other than glucose. In: Gibson, G.E., Dienel, G.A. (Eds.), Brain Energetics. Integration of Molecular and Cellular Porcesses, third ed. Springer-Verlag, Berlin, pp. 137–179.

Rodrigues, T.B., Cerdan, S., 2007. The cerebral tricarboxylic acid cycles. In: Gibson, G.E., Dienel, G.A. (Eds.), Brain Energetics. Integration of Molecular and Cellular Porcesses, third ed. Springer-Verlag, Berlin, pp. 63–91.

Rothman, D., De Feyter, H., Maciejewski, P., Behar, K., 2012. Is there in vivo evidence for amino acid shuttles carrying ammonia from neurons to astrocytes? Neurochem. Res. 37, 2597–2612.

Rothman, D.L., Novotny, E.J., Shulman, G.I., Howseman, A.M., Petroff, O.A., Mason, G., et al., 1992. 1H-[13C] NMR measurements of [4-13C]glutamate turnover in human brain. Proc. Natl. Acad. Sci. U.S.A. 89, 9603–9606.

Rothman, D.L., De Feyter, H.M., De Graaf, R.A., Mason, G.F., Behar, K.L., 2011. 13C MRS studies of neuroenergetics and neurotransmitter cycling in humans. NMR. Biomed. 24, 943–957.

Sakurada, O., Kennedy, C., Jehle, J., Brown, J.D., Carbin, G.L., Sokoloff, L., 1978. Measurement of local cerebral blood flow with iodo ^{14}C antipyrine. Am. J. Physiol. 234, H59–H66.

Salek, R.M., Xia, J., Innes, A., Sweatman, B.C., Adalbert, R., Randle, S., et al., 2010. A metabolomic study of the CRND8 transgenic mouse model of Alzheimer's disease. Neurochem. Int. 56, 937–947.

Salinas, J.A., Gold, P.E., 2005. Glucose regulation of memory for reward reduction in young and aged rats. Neurobiol. Aging. 26, 45–52.

Savaki, H.E., Davidsen, L., Smith, C., Sokoloff, L., 1980. Measurement of free glucose turnover in brain. J. Neurochem. 35, 495–502.

Sax, C.M., Kays, W.T., Salamon, C., Chervenak, M.M., Xu, Y.S., Piatigorsky, J., 2000. Transketolase gene expression in the cornea is influenced by environmental factors and developmentally controlled events. Cornea. 19, 833–841.

Schaaff, I., Heinisch, J., Zimmermann, F.K., 1989. Overproduction of glycolytic enzymes in yeast. Yeast. 5, 285–290.

Schousboe, A., Sickmann, H.M., Bak, L.K., Schousboe, I., Jajo, F.S., Faek, S.A., et al., 2011. Neuron-glia interactions in glutamatergic neurotransmission: roles of oxidative and glycolytic adenosine triphosphate as energy source. J. Neurosci. Res. 89, 1926–1934.

Scott, D.K., O'doherty, R.M., Stafford, J.M., Newgard, C.B., Granner, D.K., 1998. The repression of hormone-activated PEPCK gene expression by glucose is insulin-independent but requires glucose metabolism. J. Biol. Chem. 273, 24145–24151.

Shank, R.P., Bennett, G.S., Freytag, S.O., Campbell, G.L., 1985. Pyruvate carboxylase: an astrocyte-specific enzyme implicated in the replenishment of amino acid neurotransmitter pools. Brain. Res. 329, 364–367.

Sharp, F.R., 1976a. Relative cerebral glucose uptake of neuronal perikarya and neuropil determined with 2-deoxyglucose in resting and swimming rat. Brain. Res. 110, 127–139.

Sharp, F.R., 1976b. Rotation induced increases of glucose uptake in rat vestibular nuclei and vestibulocerebellum. Brain. Res. 110, 141–151.

Shepherd, G.M., Harris, K.M., 1998. Three-dimensional structure and composition of CA3-->CA1 axons in rat hippocampal slices: implications for presynaptic connectivity and compartmentalization. J. Neurosci. 18, 8300–8310.

Sherwood, C.C., Stimpson, C.D., Raghanti, M.A., Wildman, D.E., Uddin, M., Grossman, L.I., et al., 2006. Evolution of increased glia-neuron ratios in the human frontal cortex. Proc. Natl. Acad. Sci. U.S.A. 103, 13606–13611.

Shibuki, K., Hishida, R., Kitaura, H., Takahashi, K., Tohmi, M., 2007. Coupling of brain function and metabolism: endogenous flavoprotein fluorescence imaging of neruonal activities by local changes in energy metabolism. In: Gibson, G.E., Dienel, G.A. (Eds.), Brain Energetics. Integration of Molecular and Cellular Processes, third ed. Springer-Verlag, Berlin, pp. 321–342.

Shuttleworth, C.W., 2010. Use of NAD(P)H and flavoprotein autofluorescence transients to probe neuron and astrocyte responses to synaptic activation. Neurochem. Int. 56, 379–386.

Siesjö, B.K., Nilsson, L., 1971. The influence of arterial hypoxemia upon labile phosphates and upon extracellular and intracellular lactate and pyruvate concentrations in the rat brain. Scand. J. Clin. Lab. Invest. 27, 83–96.

Siesjö, B.K., Johannsson, H., Ljunggren, B., Norberg, K., 1974. Brain dysfunction in cerebral hypoxia and ischemia. Res. Publ. Assoc. Res. Nerv. Ment. Dis. 53, 75–112.

Simpson, I.A., Carruthers, A., Vannucci, S.J., 2007. Supply and demand in cerebral energy metabolism: the role of nutrient transporters. J. Cereb. Blood. Flow. Metab. 27, 1766–1791.

Sirover, M.A., 2012. Subcellular dynamics of multifunctional protein regulation: mechanisms of GAPDH intracellular translocation. J. Cell. Biochem. 113, 2193–2200.

Sokoloff, L., 1986. Cerebral circulation, energy metabolism, and protein synthesis: General characteristics and principles of measurement. In: Phelps, M., Mazziotta, J., Schelbert, H. (Eds.), Positron Emission Tomography and Autoradiography: Principles and Applications for the Brain and Heart. Raven Press, New York, pp. 1–71.

Sokoloff, L., 1996a. Cerebral metabolism and visualization of cerebral activity. In: Gregor, R., Windhorst, U. (Eds.), Comprehensive Human Physiology, vol. 1. Springer-Verlag, Berlin, pp. 579–602.

Sokoloff, L., 1996b. Louis Sokoloff. In: Squire, L.R. (Ed.), The History of Neuroscience in Autobiobraphy, Society for Neuroscience, vol. 1. Washington, D. C. pp. 454–497.

Sokoloff, L., Reivich, M., Kennedy, C., Des Rosiers, M.H., Patlak, C. S., Pettigrew, K.D., et al., 1977. The [^{14}C]deoxyglucose method for the measurement of local cerebral glucose utilization: theory, procedure, and normal values in the conscious and anesthetized albino rat. J. Neurochem. 28, 897–916.

Sonnewald, U., Syversen, T., Schousboe, A., Waagepetersen, H.S., Aschner, M., 2007. Actions of toxins on cerebral metabolism at the cellular level. In: Gibson, G.E., Dienel, G.A. (Eds.), Brain Energetics. Integration of Molecular and Cellular Processes, third ed. Springer-Verlag, Berlin, pp. 569–585.

Sorg, O., Magistretti, P.J., 1991. Characterization of the glycogenolysis elicited by vasoactive intestinal peptide, noradrenaline and adenosine in primary cultures of mouse cerebral cortical astrocytes. Brain. Res. 563, 227–233.

Spray, D.C., Iacobas, D.A., 2007. Organizational principles of the connexin-related brain transcriptome. J. Mem. Biol. 218, 39–47.

Stavinoha, W.B., Weintraub, S.T., Modak, A.T., 1973. The use of microwave heating to inactivate cholinesterase in the rat brain prior to analysis for acetylcholine. J. Neurochem. 20, 361–371.

Suh, S.W., Hamby, A.M., Swanson, R.A., 2007. Hypoglycemia, brain energetics, and hypoglycemic neuronal death. Glia. 55, 1280–1286.

Suzuki, A., Stern, S.A., Bozdagi, O., Huntley, G.W., Walker, R.H., Magistretti, P.J., et al., 2011. Astrocyte-neuron lactate transport is required for long-term memory formation. Cell. 144, 810–823.

Swanson, R.A., Yu, A.C., Chan, P.H., Sharp, F.R., 1990. Glutamate increases glycogen content and reduces glucose utilization in primary astrocyte culture. J. Neurochem. 54, 490–496.

Swanson, R.A., Morton, M.M., Sagar, S.M., Sharp, F.R., 1992. Sensory stimulation induces local cerebral glycogenolysis: demonstration by autoradiography. Neuroscience. 51, 451–461.

Takahashi, S., Driscoll, B.F., Law, M.J., Sokoloff, L., 1995. Role of sodium and potassium ions in regulation of glucose metabolism in cultured astroglia. Proc. Natl. Acad. Sci. U.S.A. 92, 4616–4620.

Takahashi, S., Izawa, Y., Suzuki, N., 2012. Astroglial pentose phosphate pathway rates in response to high-glucose environments. ASN Neuro. 4 (2), Available from: http://dx.doi.org/10.1042/AN20120002, art:e00078.

Takeda, K., Ishida, A., Takahashi, K., Ueda, T., 2012. Synaptic vesicles are capable of synthesizing the VGLUT substrate glutamate from alpha-ketoglutarate for vesicular loading. J. Neurochem. 121, 184–196.

Tang, K.S., Suh, S.W., Alano, C.C., Shao, Z., Hunt, W.T., Swanson, R. A., et al., 2010. Astrocytic poly(ADP-ribose) polymerase-1 activation leads to bioenergetic depletion and inhibition of glutamate uptake capacity. Glia. 58, 446–457.

Tristan, C., Shahani, N., Sedlak, T.W., Sawa, A., 2011. The diverse functions of GAPDH: Views from different subcellular compartments. Cell. Sig. 23, 317–323.

Ueda, T., Ikemoto, A., 2007. Cytoplasmic glycolytic enzymes. Synaptic vesicle-associated glycolytic ATP-generating enzymes: coupling to neurotransmitter accumulation. In: Gibson, G.E., Dienel, G.A. (Eds.), Brain Energetics. Integration of Molecular and Cellular Processes, third ed. Springer-Verlag, Berlin, pp. 241–259.

Urbano, A.M., Gillham, H., Groner, Y., Brindle, K.M., 2000. Effects of overexpression of the liver subunit of 6-phosphofructo-1-kinase on the metabolism of a cultured mammalian cell line. Biochem. J. 352 (Pt 3), 921–927.

Van Hall, G., Stromstad, M., Rasmussen, P., Jans, O., Zaar, M., Gam, C., et al., 2009. Blood lactate is an important energy source for the human brain. J. Cereb. Blood. Flow. Metab. 29, 1121–1129.

Vaulont, S., Vasseur-Cognet, M., Kahn, A., 2000. Glucose regulation of gene transcription. J. Biol. Chem. 275, 31555–31558.

Veech, R.L., 1980. Freeze-blowing of the brain and the interpretation of the meaning of certain metabolite levels. In: Passonneau, J.V., Hawkins, R.A., Lust, W.D., Welsh, F.A. (Eds.), Cerebral Metabolism and Neural Function. Williams & Wilkins, Baltimore, pp. 34–41.

Veech, R.L., 2004. The therapeutic implications of ketone bodies: the effects of ketone bodies in pathological conditions: ketosis, ketogenic diet, redox states, insulin resistance, and mitochondrial metabolism. Prostaglandins. Leukot. Essent. Fatty. Acids. 70, 309–319.

Veech, R.L., Harris, R.L., Veloso, D., Veech, E.H., 1973. Freeze-blowing: a new technique for the study of brain in vivo. J. Neurochem. 20, 183–188.

Villringer, A., Chance, B., 1997. Non-invasive optical spectroscopy and imaging of human brain function. Trends. Neurosci. 20, 435–442.

Wang, S.S., Shultz, J.R., Burish, M.J., Harrison, K.H., Hof, P.R., Towns, L.C., et al., 2008. Functional trade-offs in white matter axonal scaling. J. Neurosci. 28, 4047–4056.

Waniewski, R.A., Martin, D.L., 1998. Preferential utilization of acetate by astrocytes is attributable to transport. J. Neurosci. 18, 5225–5233.

Wiesinger, H., 1995. Glia-specific enzyme systems. In: Kettenman, H., Ransom, B.R. (Eds.), Neuroglia. Oxford University Press, New York, pp. 488–499.

Wilhelm, F., Hirrlinger, J., 2012. Multifunctional roles of NAD(+) and NADH in astrocytes. Neurochem. Res. 37, 2317–2325.

Wu, K., Aoki, C., Elste, A., Rogalski-Wilk, A.A., Siekevitz, P., 1997. The synthesis of ATP by glycolytic enzymes in the postsynaptic density and the effect of endogenously generated nitric oxide. Proc. Natl. Acad. Sci. U.S.A. 94, 13273–13278.

Xu, J., Song, D., Xue, Z., Gu, L., Hertz, L., Peng, L., 2013. Requirement of glycogenolysis for uptake of increased extracellular K + in astrocytes: potential implications for K + homeostasis and glycogen usage in brain. Neurochem. Res. 38, 472–485.

Yamanishi, S., Katsumura, K., Kobayashi, T., Puro, D.G., 2006. Extracellular lactate as a dynamic vasoactive signal in the rat retinal microvasculature. Am. J. Physiol. 290, H925–H934.

Yego, E.C., Mohr, S., 2010. siah-1 Protein is necessary for high glucose-induced glyceraldehyde-3-phosphate dehydrogenase nuclear accumulation and cell death in Müller cells. J. Biol. Chem. 285, 3181–3190.

Young, G.S., Kirkland, J.B., 2008. The role of dietary niacin intake and the adenosine-5′-diphosphate-ribosyl cyclase enzyme CD38 in spatial learning ability: is cyclic adenosine diphosphate ribose the link between diet and behaviour? Nutr. Res. Rev. 21, 42–55.

Yu, A.C., Drejer, J., Hertz, L., Schousboe, A., 1983. Pyruvate carboxylase activity in primary cultures of astrocytes and neurons. J. Neurochem. 41, 1484–1487.

Yudkoff, M., Daikhin, Y., Melo, T.M., Nissim, I., Sonnewald, U., 2007. The ketogenic diet and brain metabolism of amino acids: relationship to the anticonvulsant effect. Annu. Rev. Nutr. 27, 415–430.

Zeller, K., Rahner-Welsch, S., Kuschinsky, W., 1997. Distribution of Glut1 glucose transporters in different brain structures compared to glucose utilization and capillary density of adult rat brains. J. Cereb. Blood. Flow. Metab. 17, 204–209.

Zielke, H.R., Zielke, C.L., Baab, P.J., 2009. Direct measurement of oxidative metabolism in the living brain by microdialysis: a review. J. Neurochem. 109 (Suppl. 1), 24–29.

Zwingman, C., Leibfritz, D., 2007. Glial-neuronal shuttle systems. In: Gibson, G.E., Dienel, G.A. (Eds.), Brain Energetics. Integration of Molecular and Cellular Processes, third ed. Springer-Verlag, Berlin, pp. 197–238.

Further References

Blass, J.P., McDowell, F.H., (Eds.), 1999. Oxidative/energy metabolism in neurodegenerative disorders. Annals of the New York Academy of Sciences, 893.

Boulton, A.A., Baker, G.B., Butterworth, R.F. (Eds.), 1989. Neuromethods 11. Carbohydrates and Energy Metabolism. Humans Press, Clifton, NJ.

Brady, S.T., Siegel, G.J., Albers, R.W., Price, D.L. (Eds.), 2012. Basic Neurochemistry. Principles of Molecular, Cellular, and Medical Neurobiology. eighth ed. Academic Press, San Diego.

Dermietzel, R., Spray, D.C., Nedergaard, M. (Eds.), 2006. Blood–Brain Barriers. From Ontogeny to Artificial Interfaces, vols. 1 and 2. Wiley-VCH, Verlag, Weinheim.

Dwyer, D., 2002. Glucose metabolism in the brain, International Review of Neurobiology, vol. 51. Academic Press, Amsterdam.

Edvinsson, L., Krause, D.N. (Eds.), 2002. Cerebral Blood Flow and Metabolism. second ed. Lippincott Williams & Wilkins, Philadelphia.

Ferguson, S.J., Nicholls, D.G., 2002. Bioenergetics, vol. 3. Academic Press, London.

Gibson, G.E., Ratan, R.R., Beal, M.F., (Eds.), 2008. Mitochondria and oxidative stress in neurodegenerative disorders. Annals of the New York Academy of Sciences, 1147, 1–414.

Hertz, L. (Ed.), 2003. Non-Neuronal Cells of the Nervous System: Function and Dysfunction. Advances in Molecular and Cell Biology. Vol. 31-1 Part I: Structure, Organization, Development and Regeneration, Vol. 31-2, Part II: Biochemistry, Physiology and Pharmacology; Vol. 31-3. Part III: Pathological Conditions. Elsevier, Amsterdam.

Passonneau, J.V., Hawkins, R.A., Lust, W.D., Welsh, F.A. (Eds.), 1980. Cerebral Metabolism and Neural Function. Williams & Wilkins, Baltimore.

Segel, I.H., 1976. Biochemical Calculations: How to Solve Mathematical Problems in General Biochemistry, second ed. John Wiley & Sons, New York.